Final Report

IMPROVING THE GEOLOGICAL INTERPRETATION OF MAGNETIC AND GRAVITY SATELLITE ANOMALIES
(4/1/85 - 11/31/86)

Grant No. NAGW-736 (Basic)

Submitted to

National Aeronautics & Space Administration
Code EE1
NASA Headquarters
Washington, DC 20546

January, 1987

William J. Hinze and Lawrence W. Braile
Department of Earth &
Atmospheric Sciences
Purdue University
West Lafayette, IN 47907

Ralph R.B. von Frese
Dept. of Geology &
Mineralogy
Ohio State University
Columbus, OH 43210

IMPROVING THE GEOLOGICAL INTERPRETATION OF MAGNETIC AND GRAVITY SATELLITE ANOMALIES

Abstract

Quantitative analysis of the geologic component of observed satellite magnetic and gravity fields requires accurate isolation of the geologic component of the observations, theoretically sound and viable inversion techniques, and integration of collateral, constraining geologic and geophysical data. A number of significant contributions have been made in this study which make quantitative analysis more accurate. These include procedures for 1) screening and processing orbital data for lithospheric signals based on signal repeatability and wavelength analysis; 2) producing accurate gridded anomaly values at constant elevations from the orbital data by three-dimensional least squares collocation; 3) increasing the stability of equivalent point source inversion and criteria for the selection of the optimum damping parameter; 4) enhancing inversion techniques through an iterative procedure based on the superposition theorem of potential fields; and 5) modeling efficiently regional-scale lithospheric sources of satellite magnetic anomalies. In addition, these techniques have been utilized to investigate regional anomaly sources of North and South America and India and to provide constraints to continental reconstruction. Since the inception of this research study, eleven papers have been presented with associated published abstracts, three theses have been completed, four papers have been published or accepted for publication and an additional manuscript has been submitted for publication.

Introduction

A major objective of the geopotential satellite program is the quantitative analysis of the geologic component of observed magnetic and gravity fields. To achieve this goal requires accurate isolation of the geologic component of the observed fields, theoretically sound and viable inversion techniques, and integration of collateral, constraining geologic and geophysical data with the satellite anomalies. During the period of Grant No. NAGW-736, considerable progress has been made toward improving quantitative interpretation by minimizing the adulterating influences of temporal variations in the magnetic field and operational characteristics of the satellite and by improved forward and inverse geologic modeling of the potential fields. These techniques have been illustrated by their application to satellite geopotential anomalies of North and South America and India using surface geologic and geophysical information to reduce the ambiguity of the quantitative interpretations. These improvements have been largely directed toward and illustrated with MAGSAT data, but most of these have direct application to geopotential data from future satellite missions.

Since the inception of this grant (4/1/85), a total of eleven papers have been presented with associated published abstracts, one M.S. thesis was completed at Purdue University and two at Ohio State University, four papers have been published or accepted for publication, and an additional manuscript has been submitted for publication. In addition, several seminars have been presented on the results to-date at U.S., European, and Indian universities and research establishments.

Discussion of Results

The precise isolation of the crustal geological component in satellite magnetic data is a difficult process, but it is a particularly troublesome problem in magnetic polar and equatorial regions where significant external temporal variations have much the same wavelength characteristics as anomalies derived from crustal sources. Preliminary satellite scalar magnetic anomaly maps prepared of South America from 2 degree averaged data (Langel et al., 1982; Hinze et al., 1982) are subject to errors caused by the medium-wavelength equatorial electrojet and other long- and short-wavelength external field effects. These effects have been minimized as discussed in Citation 1

1) Ridgway, J.R. and W.J. Hinze, 1986, MAGSAT scalar anomaly map of South America, Geophysics, v. 51, 1472-1479.

by selecting orbital profiles from quiet periods ($K_p \leq 2+$) and by using only dawn profiles which have minimum contamination from the equatorial electrojet. The ring current was corrected through the use of a standard ring current empirical equation augmented by wavelength filtering. Previous studies have used either a best-fitting linear or quadratic function to each individual profile to remove the longer wavelength components which are not removed by the standard equation.

In this case we showed how an optimum filter could be designed by a statistical regression technique to isolate the common, static (geologic) component of replicate orbital profiles. This procedure has an improved, constrained physical basis over linear or quadratic function removal. The optimum filter cutoff level was determined to be approximately 50 degrees wavelength. When wavelengths longer than this are rejected, resultant profiles from redundant satellite orbits correlate well with differences due primarily to satellite altitude. These differences are eliminated by normalizing the data to a constant altitude by the equivalent-point-source (EPS) inversion technique. The resultant map differs significantly from the original 2 degree averaged version, most notably in geomagnetic equatorial latitudes. A version of this map reduced-to-pole shows significant correlations with regional South American and Carribean tectonic features as discussed by Ridgway and Hinze (1986).

The reduced-to-pole MAGSAT anomaly map of South America has been quantitatively interpreted using our spherical-earth forward modeling technique to obtain a crustal magnetization model for eastern South America and adjacent marine areas. These results have been documented in a M.S. thesis under the citation:

2) Parrott, M.H., 1985, Interpretation of MAGSAT anomalies over South America, Unpubl. M.S. Thesis, Purdue University, 95 pp.

Modeling shows that failed rifts correspond to regions of deficient lower crustal magnetization, whereas Precambrian shields and foldbelts correspond to regions of higher magnetization. Forward modeling of marine anomalies adjacent to the east coast of South America shows that positive anomalies can result from increased thickness of uniformly magnetized crust associated with positive ocean bottom topography. Negative anomalies correlate well with oceanic basins, and may result from a thinned magnetized layer.

An important preliminary step in the presentation and analysis of satellite potential-field data is the preparation of a gridded anomaly data set normalized to a specific elevation. Numerical averaging (Regan et al., 1975) and EPS inversion (Ridgway and Hinze, 1986) have both been employed in the gridding of MAGSAT data observed over a range of elevations and irregularly distributed over the surface of the earth. The EPS method involves solving for the magnetization of a grid of magnetic dipoles which will in a least squares sense best duplicate the observed magnetic values at their specified position over the global surface. The computed magnetic dipoles are then used to determine the magnetic values on a spatial grid at a normalized elevation above the surface of the earth. In the numerical averaging technique, selected satellite magnetometer observations of orbital profiles within equal-angle or equal-area and specified elevation range parallelepipeds or bins are averaged to determine the grid value at the center of the bin. In an attempt to minimize the computational efforts involved in the EPS method and the potential error of the simplistic "binning" technique, the method of least squares collocation was extended to three dimensions and tested on simulated as well as actual data over South America. Collocation (Moritz, 1972) is a statistical estimation

technique which is widely applied to problems in physical geodesy wherein the statistical behavior of the observations are assessed through appropriate covariance functions.

The collocation method and its application to satellite data are documented in the following citations:

3) Goyal, H.K., R.R.B. von Frese and W.J. Hinze, 1985, Statistical magnetic anomalies for geologic analysis, EOS, v. 66, p. 255.

4) Goyal, H.K., R.R.B. von Frese and W.J. Hinze, 1986, Statistical prediction of satellite magnetic anomalies, EOS, v. 67, p. 264.

5) Goyal, H.K., 1986, Statistical prediction of satellite magnetic anomalies for geologic interpretation, Unpubl. M.S. Thesis, Ohio State University, 116 pp.

6) Goyal, H.K., R.R.B. von Frese, and W.J. Hinze, 1986, Statistical prediction of satellite magnetic anomalies, submitted for publication in Geophysics.

The entire preprint of Citation 6 is included in Appendix B. Orbital magnetic anomaly simulations of lithospheric sources over a spherical earth show that numerical averaging errors contribute in only a minor way to the entire error-budget over orbital elevations of MAGSAT (~ 400 km), whereas for lower orbital estimates the error of averaging may increase substantially. The computationally efficient three-dimensional least squares collocation method results in more accurate anomaly estimates than simple averaging as the prediction elevation is decreased. Statistical predictions of MAGSAT observations over South America show that, in general, three-dimensional collocation is the most efficient and cost-effective method for obtaining accurate, altitude-normalized anomaly grids from orbital or arbitrarily distributed data.

Once the orbital data are registered on a grid at constant elevation, transformation of the gridded data set into reduced-to-pole format and subsequent enhancement by continuation and gradient techniques can be readily achieved through EPS inversion. However, instabilities and large scale inversions commonly complicate the use of efficient least-squares matrix procedures. Unstable solutions are the result of errors in anomaly observations and the integrated effects of observation spacing, source spacing, elevation differences between sources and observations, geographic coordinate attributes, geomagnetic field parameters, and other factors which influence the singularity conditions of inversion. Solution instabilities caused by these singularity parameters can be efficiently minimized by the application of ridge regression. An appropriate damping factor large enough to stabilize the inversion, but small enough to produce an analytically useful solution can be chosen by comparing a range of damping factors with solution variances or the residuals between predicted anomaly maps which represent the processing objective (e.g., downward continuation, differential reduction-to-pole, etc.).

A further improvement in the accuracy and efficiency of EPS inversions, especially those involving very large data sets, can be effected by a procedure based on the superposition principle of potential fields. This so-called "bootstrap" technique involves inversions of residuals between the observations and successive stable model fields which can be readily accommodated by available computer memory. Summation of the model fields yields a well-defined representation of the observed anomalies corresponding to an integrated model which would be difficult to achieve because of excessive memory requirements and instability in the solutions. Application of these techniques to model studies and MAGSAT data over South America and the Indian subcontinent verify the utility of these methods in obtaining not only improved maps, but meaningful lithospheric magnetic polarization contrasts. Detailed discussions of the improved EPS inversion are documented in the following citations:

7) McGue, C.A. and R.R.B. von Frese, 1986, Crustal analysis of MAGSAT magnetic anomalies over India, EOS, v. 67, p. 264.

8) Ravat, D.N., W.J. Hinze, L.W. Braile and R.R.B. von Frese, 1986, Improvements in large scale inversion of the MAGSAT data, EOS, v. 67, p. 263.

9) von Frese, R.R.B., D.N. Ravat, W.J. Hinze and C.A. McGue, 1986, Improved inversion of geopotential field anomalies for lithospheric investigations, Geophysics (in press).

The entire preprint of Citation 9 is included in Appendix B. An additional manuscript applying these improved inversion techniques to simulated and South American data is nearing completion.

Significant progress has been made in improving the efficiency of the geopotential anomaly modeling algorithm (von Frese et al., 1981). Affine transformations have been identified and tested which decompose arbitrary source volumes into a series of elemental unit volumes for accurate and efficient modeling of anomaly fields by Gaussian quadrature integration. Aspects of this procedure and its application to modeling the magnetic and gravity effects of digital terrain models on a spherical earth were presented at the International Meeting on Potential Fields in Rugged Topography at Lausanne, Switzerland (Citation 10) and in a M.S. thesis at Ohio State University (Citation 11):

10) Mateskon, S.R. and R.R.B. von Frese, 1985, Gravity and magnetic terrain modeling by Gaussian quadrature integration, International Meeting on Potential Fields in Rugged Topography, (Institut de Geophysique, Universite de Lausanne, CH), IGL-Bulletin No. 7, p. 30-33.

11) Mateskon, S.R., 1985, Gravity and magnetic terrain effects computed by Gaussian quadrature integration, Unpubl. M.S. Thesis, Ohio State University, 147 p.

Considerable effort has been placed on problems of illustrating the geologic utility of satellite potential-field data, particuarly MAGSAT data. In addition to the illustrative data presented in the previous citations, the magnetic anomaly data of North and South America, Eurasia, Africa, Australia and Antarctica have been processed and reduced-to-pole. These data have been used in constraining paleocontinental reconstruction under the following citations:

12) von Frese, R.R.B., W.J. Hinze, R. Oliver, and C.R. Bentley, 1985, Continental magnetic anomaly constraints on continental reconstruction, EOS, v. 66, p. 255.

13) von Frese, R.R.B., W.J. Hinze, R. Oliver, and C.R. Bentley, 1985, Regional magnetic anomalies of rifted continental margins, IAGA, 5th General Assembly (Prague, CS), v. 2, p. 77.

14) von Frese, R.R.B., W.J. Hinze, R. Oliver, and C.R. Bentley, 1985, Satellite magnetic anomalies and continental reconstructions, 6th Gondwana Symposium (Ohio State University, Columbus, OH), Abstracts, p. 104.

15) von Frese, R.R.B., W.J. Hinze, R. Oliver, and C.R. Bentley, 1986, Regional magnetic anomaly constraints on continental breakup, Geology, v. 14, p. 68-71.

16) von Frese, R.R.B., W.J. Hinze, R. Oliver, and C.R. Bentley, 1986, Satellite magnetic anomalies of Gondwana, AGU Monograph (in press).

The entire preprint of Citation 16 is included in Appdenix B. An additional paper was presented in 1985 relating the south-central U.S. magnetic anomaly to other geophysical and geologic data. This anomaly is shown to be associated with the lower crust of the 1500 m.y. felsic anorogenic province that makes up the Central Province of the basement rocks of the midcontinent. The thermal event which caused the widespread melting of the more felsic components of the lower crust during this event apparently enhanced the magnetization of the lower crust. This paper is documented in Citation 17:

17) Starich, P.J., W.J. Hinze and L.W. Braile, 1985, The South-Central U.S. magnetic anomaly, SEG 55th Annual International Meeting and Exposition, Technical Program, p. 204-206.

Finally, two review papers have been prepared concerning the applications of satellite geopotential data. They are referenced in the following citations:

18) von Frese, R.R.B. and W.J. Hinze, 1984, Continental and oceanic magnetic anomalies: Enhancement through GRM, Proceedings of the GRM Meeting, University of Maryland, College Park, MD, 4 pp.

19) von Frese, R.R.B., 1987, Crustal applications of GASP, Geomagnetic Automonous Shuttle-Launched Probe (GASP) Workshop, Naval Ocean Research and Development Activity (NORDA), (12-14 March 1986, National Space Technology Laboratories (NSTL), Bay St. Louis, MS), Proceedings (in press).

REFERENCES

Hinze, W.J., R.R.B. von Frese, M.B. Longacre and L.W. Braile, 1982, Regional magnetic and gravity anomalies of South America, Geophys. Res. Lett., v. 9, p. 314-317.

Langel, R.A., J.D. Phillips and R.J. Horner, 1982, Initial scalar magnetic anomaly map from MAGSAT, Geophys. Res. Lett., v. 9, p. 269-272.

Moritz, H., 1980, Advanced Physical Geology, Herbert Wickmann Verlag, West Germany.

Regan, R.D., J.C. Cain and W.M. Davis, 1975, A global magnetic anomaly map, J. Geophys. Res., v. 80, p. 794-802.

Ridgway, J.R. and W.J. Hinze, 1986, MAGSAT scalar anomaly map of South America, Geophysics, v. 51, p. 1472-1479.

von Frese, R.R.B., W.J. Hinze, L.W. Braile and A.J. Luca, 1981, Spherical earth gravity and magnetic modeling by Gauss-Legendre quadrature integration, J. Geophys., v. 49, p. 234-242.

APPENDIX A

Literature Citations

CITATION # 1

MAGSAT SCALAR ANOMALY MAP OF SOUTH AMERICA

J.R. Ridgway and W.J. Hinze
Geophysics, v. 51, 1472-1479, 1986

A scalar magnetic anomaly map has been prepared for South America and adjacent marine areas from MAGSAT data. The preparation of the map poses problems, notably in the separation of external field and crustal anomalies, and in the reduction of data to a common altitude. External fields are manifested in a long-wavelength ring current effect, a medium-wavelength equatorial electrojet, and short-wavelength noise. The noise is reduced by selecting profiles from "quiet" periods ($K_p \leq 2^+$), and because the electrojet is confined primarily to dusk profiles, its effect is minimized by drawing the data set from dawn profiles only. The ring current is corrected through the use of a standard ring current equation, augmented by further wavelength filtering. The optimum filter cutoff level is determined by a statistical regression technique to be approximately 50° wavelength. When wavelengths longer than this are rejected, resultant profiles from redundant satellite orbits correlate well, with differences due primarily to satellite altitude. These differences are eliminated by normalizing the data to a constant altitude by the equivalent point source inversion technique. The resultant map differs significantly from the original 2° averaged version, most notably in low geomagnetic latitudes. A reduced-to-pole version of this map shows correlations to several regional South American and Caribbean tectonic features.

CITATION # 2

INTERPRETATION OF MAGSAT ANOMALIES OVER SOUTH AMERICA

M.H. Parrott
M.S. Thesis, Purdue University, 1985

The reduced-to-pole MAGSAT magnetic anomaly map of South America has been quantitatively interpreted using spherical-earth forward modeling techniques in order to yield a crustal magnetization model for eastern South America. This model assumes a uniform, weakly magnetized upper crust and a laterally heterogeneous, highly magnetized lower crust. Negative anomalies are modeled assuming crustal thinning or partial to complete lower crustal demagnetization. Positive anomalies are attributed to increased crustal thickness or enhanced lower crustal magnetization due to metamorphism. The model is generally consistent with regional tectonic and geologic features. Failed rifts correspond to regions of deficient lower crustal magnetization, whereas Precambrian shields and fold belts correspond to regions of high magnetization. Forward modeling of oceanic anomalies shows that positive anomalies can result from an increased thickness of uniformly magnetized crust, as in the case of oceanic topography. Negative anomalies correlate well with oceanic basins, and may result from a thinned magnetized layer. Anomalies showing poor correlation with geologic and tectonic provinces indicate either crustal magnetization contrasts without a surficial expression or a non-geologic origin related to the observation and processing of the data.

Although the magnetization model is reasonable, it is non-unique. The interpretation of MAGSAT anomalies is inherently limited by poor resolution resulting from the satellite elevation of the observations combined with the limited accuracy of the data. Therefore, forward modeling cannot completely resolve the location, thickness, or magnetization contrast of the source within the magnetized layer.

CITATION # 3

STATISTICAL MAGNETIC ANOMALIES FOR GEOLOGIC ANALYSIS

H.K. Goyal, R.R.B. von Frese and W.J. Hinze
EOS, v. 66, 255, 1985

The errors of numerically averaging satellite magnetic anomaly data for geologic analysis are investigated using orbital anomaly simulations of crustal magnetic sources by Gauss-Legendre quadrature integration. These simulations suggest that numerical averaging errors constitute small and relatively minor contributions to the total error-budget of higher orbital estimates ($\geq$ 400 km), whereas for lower orbital estimates the error of averaging may increase substantially. Least-squares collocation is also investigated as an alternative to numerical averaging and found to produce substantially more accurate anomaly estimates as the elevation of prediction is decreased towards the crustal sources.

CITATION # 4

STATISTICAL PREDICTION OF SATELLITE MAGNETIC ANOMALIES

H.K. Goyal, R.R.B. von Frese and W.J. Hinze
EOS, v. 67, 264, 1986

The geologic utility of satellite magnetic observations is limited by orbital altitude variations which may range to a few hundred kilometers. Common methods including numerical averaging and equivalent point source inversion, together with least-squares collocation were investigated for producing gridded anomaly values at constant elevation from orbital magnetic data. Once in gridded format, the anomaly data are particularly amenable to geophysical modeling and representation by point dipole sources of high order spherical harmonic expansions for enhanced geologic interpretation. In general, three-dimensional collocation is the most efficient approach to obtaining accurate anomaly values at arbitrary spatial coordinates from the orbital data. Application of the various methods to MAGSAT observations over South America demonstrates the capacity of collocation for enhancing the resolution of anomaly-tectonic correlations. In particular, the resolution of anomalies is improved with trailing plate anomalies distinctly separated into continental and oceanic components at the continental margin.

CITATION # 5

STATISTICAL PREDICTION OF SATELLITE MAGNETIC ANOMALIES FOR GEOLOGIC INTERPRETATION

H.K. Goyal
M.S. Thesis, Ohio State University, 1986

Statistical methods including numerical averaging and least-squares collocation are investigated and compared with equivalent point source (EPS) inversion for producing gridded anomaly values at constant elevation from orbital magnetic data. In general, three-dimensional collocation is the most efficient approach to obtaining accurate anomaly values at arbitrary spatial coordinates from the orbital data. Application of the various methods to MAGSAT observations over South America demonstrate the capacity of collocation for enhancing the resolution of anomaly-tectonic correlations. In particular, the resolution of anomalies is improved with trailing plate anomalies distinctly separated into continental and oceanic components at the continental margin.

CITATION # 6

STATISTICAL PREDICTION OF SATELLITE MAGNETIC ANOMALIES

H.K. Goyal, R.R.B. von Frese and W.J. Hinze
Submitted to Geophysics

The errors of numerically averaging satellite magnetic anomaly data for geologic analysis are investigated using orbital anomaly simulations of lithospheric magnetic sources over a spherical earth. These simulations suggest that numerical averaging errors constitute small and relatively minor contributions to the total error-budget of higher orbital estimates ($\gtrsim$ 400 km), whereas for lower orbital estimates the error of averaging may increase substantially. Least-squares collocation in three dimensions is also investigated as an alternative to numerical averaging and found to produce substantially more accurate anomaly estimates as the elevation of prediction is decreased towards the lithospheric sources. Three-dimensional collocation is applied to MAGSAT magnetic observations of South America to demonstrate the utility of this statistical procedure for producing accurately gridded magnetic anomalies at constant elevation for geologic analysis.

CITATION # 7

CRUSTAL ANALYSIS OF MAGSAT MAGNETIC ANOMALIES OVER INDIA

C.A. McGue and R.R.B. von Frese
EOS, v. 67, 264, 1986

As part of an investigation of crustal structures along the once-connected margins of India and Antartica, we reduced MAGSAT anomalies over India and adjacent marine areas differentially to the pole. Because of the attributes of the geomagnetic field in the study area, special procedures were required to produce a stable and detailed map of the radially polarized anomalies. These efforts included ridge regression in combination with bootstrap inversion involving successive inversions of residuals between the observations and various stable point dipole model fields. Integration of the dipole model fields produced a well-resolved map of radially polarized anomalies with enhanced details concerning the correlation of the anomalies with crustal features. Prominent positive magnetic anomalies characterize the Indian shield and West Pakistan depression and negative anomalies overly grabens and a series of basins along the northern flank of the Himalayas.

CITATION # 8

IMPROVEMENTS IN LARGE SCALE INVERSION OF THE MAGSAT DATA

D.N. Ravat, W.J. Hinze, L.W. Braile and R.R.B. von Frese
EOS, v. 67, 263, 1986

Large scale equivalent point source inversion (EPS) of MAGSAT data has been stabilized using sequential damping parameters in the ridge regression. The parameter that decreases the solutions to a physically meaningful range while maintaining the sum of squared error between the observed and the calculated anomaly values at near minimum, is selected as the optimum damping parameter. The appropriately damped solution vector shows a marked improvement over the undamped case. Magnetic anomaly and reduced-to-pole maps of South America computed by stabilized EPS inversion compare favorably with maps of the same area prepared by laborious compositing of data subsets. Moreover, stabilized (damped) EPS inversion can be achieved with closer dipole spacing than used in undamped inversion. The result is that the "birds-eye" pattern of localized anomalies coincident with the positions of wisely spaced dipoles is avoided on reduced-to-pole maps computed at a relatively low satellite elevation (350 km).

CITATION # 9

IMPROVED INVERSION OF GEOPOTENTIAL FIELD ANOMALIES FOR LITHOSPHERIC INVESTIGATIONS

R.R.B. von Frese, D.N. Ravat, W.J. Hinze and C.A. McGue
Submitted to Geophysics

Instabilities and the large scales of inversions which are common to geologic analyses of regional magnetic and gravity anomalies often complicate the use of efficient least-squares matrix procedures. Inversion stability profoundly affects anomaly analysis and hence it must be considered in any application. Wildly varying or unstable solutions are the products of errors in the anomaly observations and the integrated effects of observation spacing, source spacing, elevation differences between sources and observations, geographic coordinate attributes, geomagnetic field attitudes, and other factors which influence the singularity conditions of inversion. Solution instabilities caused by these singularity parameters can be efficiently minimized by the application of ridge regression. An effective damping factor large enough to stabilize the inversion, but small enough to produce an analytically useful solution can be chosen by comparing the curves where damping factors are plotted, respectively, against the residuals between observed and modeled anomalies and against the solution variance or the residuals between predicted anomaly maps which represent the processing objective (e.g., downward continuation, differential reduction to the radial pole, etc.).

To obtain accurate and efficient mega-scale inversions of anomaly data, a procedure based on the superposition principle of potential fields may be used. This method involves successive inversions of residuals between the observations and various stable model fields which can be readily accommodated by available computer memory. Integration of the model fields yields a well-resolved representation of the observed anomalies corresponding to an integrated model which normally could not be obtained by direct inversion due to excessive memory requirements.

MAGSAT magnetic anomaly inversions over India demonstrate the utility of these procedures for improving the geologic analysis of potential field anomalies.

CITATION # 10

GRAVITY AND MAGNETIC TERRAIN MODELING BY GAUSSIAN QUADRATURE INTEGRATION

S.R. Mateskon and R.R.B. von Frese
IGL-Bulletin No. 7, 30-33, 1985

An efficient procedure has been developed to determine the effects of gridded terrain models for accurate reduction of gravity and magnetic anomaly data. The method involves transformation of the topographic data into simple geometric forms which give the terrain effects by Gauss-Legendre quadrature integration. The procedure effectively yields an equivalent point source model of the topography where the point sources correspond to the zero nodes of the Legendre polynomials used to perform the Gaussian quadrature integration. Because point source effects involve relatively simple mathematical formulation, the procedure readily accomodates arbitrary physical property variations, geomagnetic field characteristics and coordinate transformations in the terrain anomaly computations. Anomaly attributes such as the potential and the anomaly gradients and vector components are also easily computed from the equivalent point source terrain model. To demonstrate the procedure, terrain effects are computed in spherical coordinates from a regional terrain model of the Transantarctic Mountains which includes rugged relief in excess of 4,500 m.

Preliminary results include a gravity analysis for a portion of the Transantarctic Mountains shown in Figure 1, where the topography is gridded at a spacing of 0.02^{o} latitude and 0.20^{o} longitude. Two stations were selected to demonstrate the effect of terrain on surface gravity measurements. Station A (z = 2,287 m), near the head of Keltie glacier and 10-15 km from any severe topography, involves a terrain correction of 3.15 mgals. On the other hand, station B (z = 740 m), near the grid-eastern edge of the Breadmore glacier, is within 5 km of elevations rising to over 2,000 m and requires a correction of 7.03 mgals. To emphasize the significant terrain elements for these gravity corrections, Figure 2 shows the percent contribution which each gridded terrain cell makes to the terrain corrections of stations A and B. Figures 3A and 3B show the gravitational effect of the terrain computed at elevations of 4.5 km and 7.5 km, respectively. The effect is for all mass between the lowest point (z = 71 m) and the highest point (z = 4,278 m) of the topographic grid.

All calculations were made for a density of 2.67 gm/cc and no attempt was made in this preliminary study to account for the lower density of ice. Future work will model rock density variations and ice separately and also consider the magnetic effects of the topography of the Transantarctic Mountains.

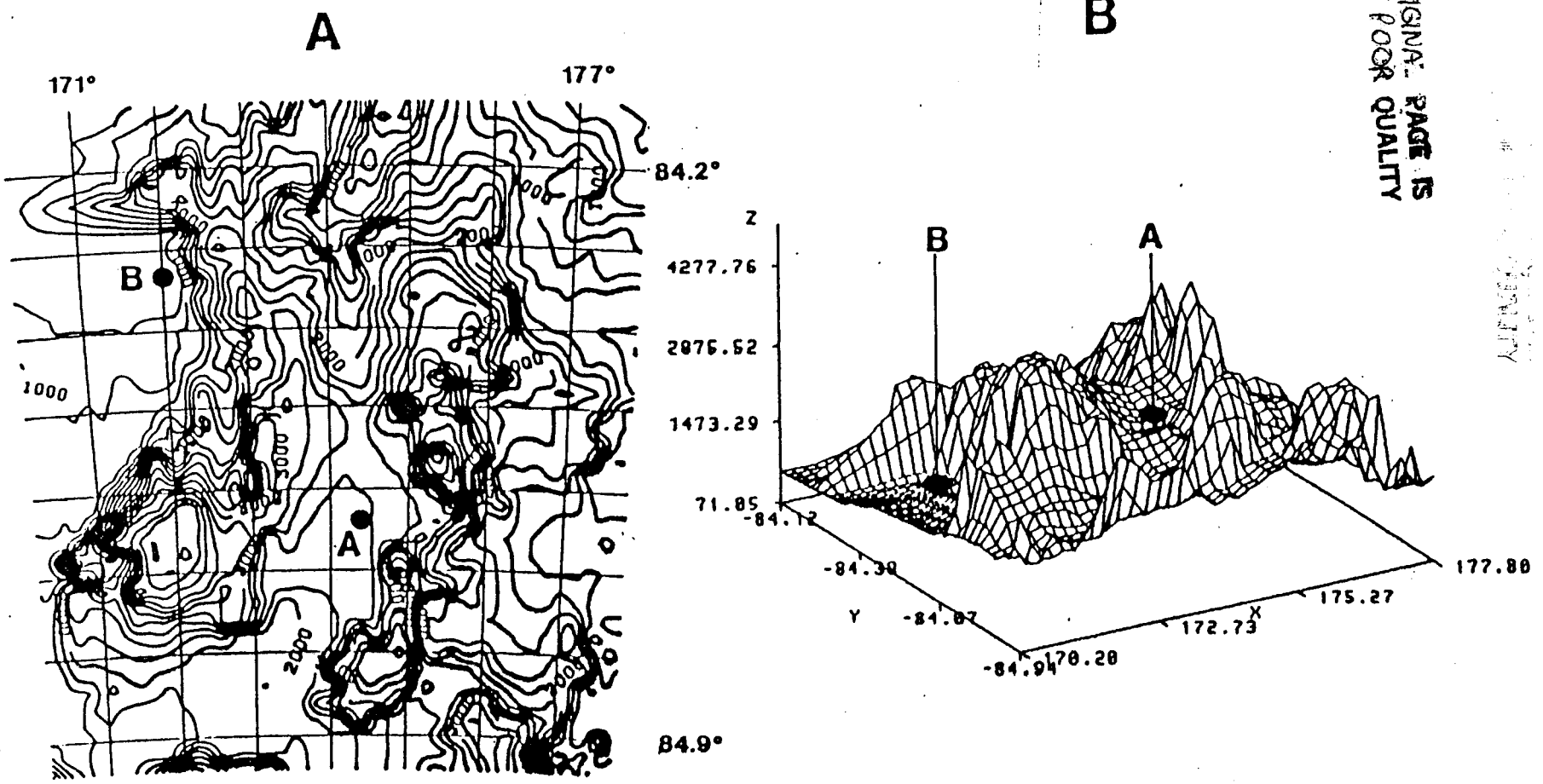

FIGURE 1. Topography of the study area in the Transantarctic Mountains. A) Presents a map of the study area contoured at 200 meter intervals, and B) a perspective plot of this region.

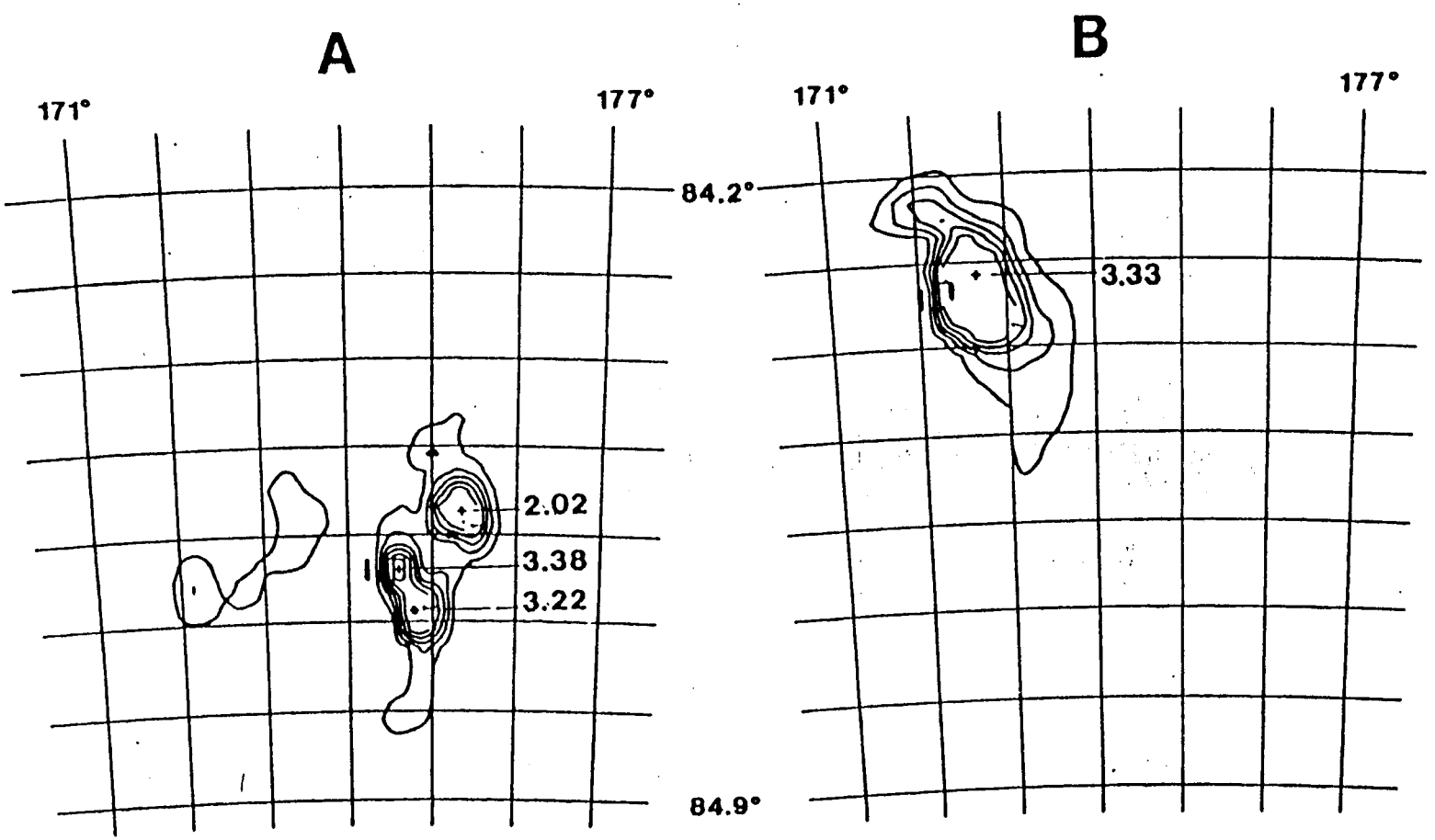

Figure 2. Percent contribution of terrain grid cells to the terrain corrections at stations A and B. Contour interval is 0.2%.

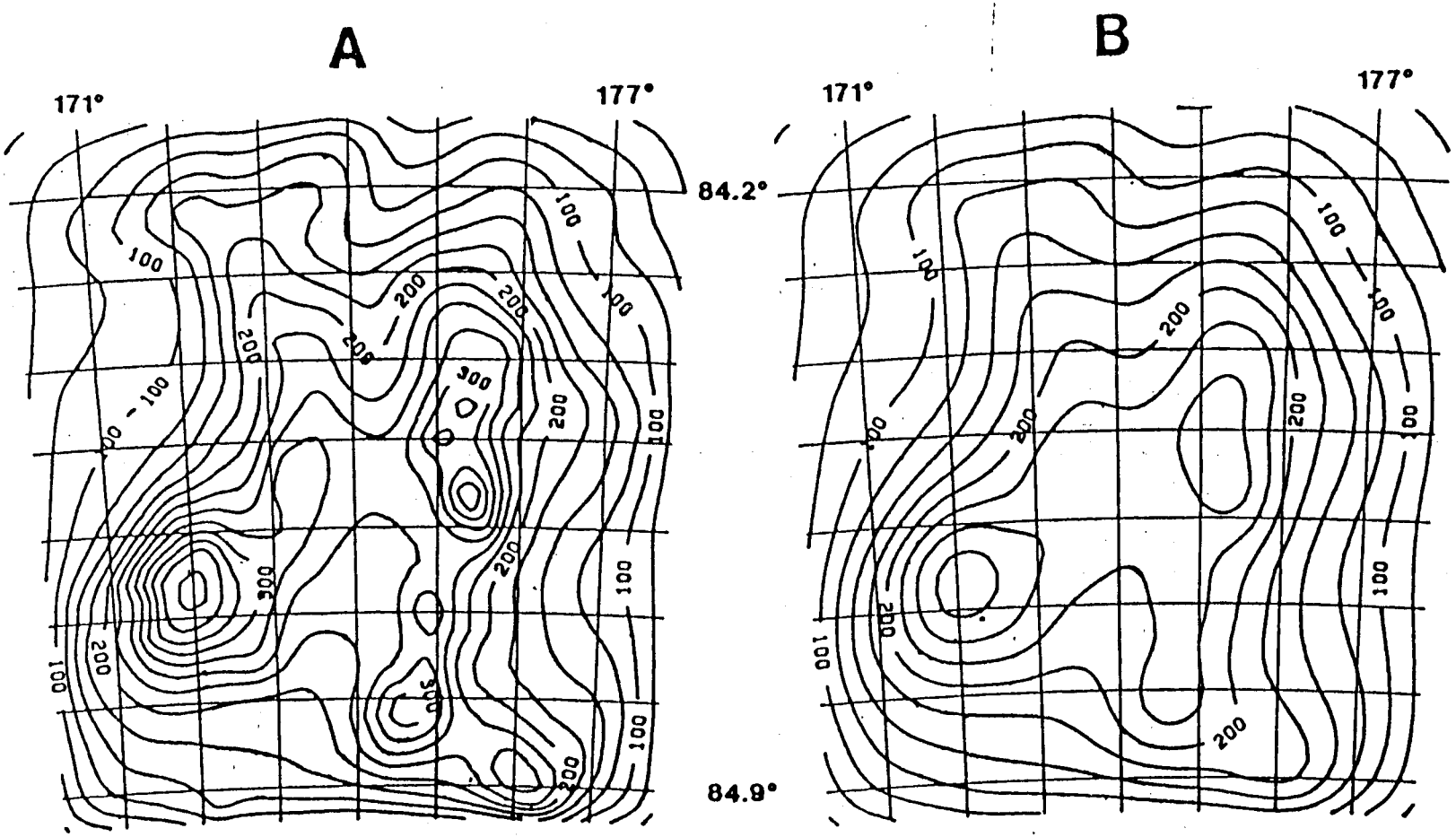

FIGURE 3. The gravitational effect of the terrain calculated at A) 4,500 meters and at B) 7,500 meters. Contour interval is 25 mgals.

CITATION # 11

GRAVITY AND MAGNETIC TERRAIN EFFECTS COMPUTED BY GAUSSIAN QUADRATURE INTEGRATION

S.R. Mateskon
M.S. Thesis, Ohio State University, 1985

Gravity and magnetic data provide important constraints for determining the structure of the crust and upper mantle. In areas of rugged topography, terrain effects can severely mask gravity and magnetic signals from deeper sources. The effects of gridded terrain models are considered for the accurate reduction of gravity and magnetic anomaly data. The gravimetric and magnetic effects due to terrain can be effectively modeled in spherical coordinates by the use of Gauss-Legendre quadrature distributed point sources. To develop criteria for the application of the method, an area of extremely rugged topography in the Transantarctic Mountains is investigated.

CITATION # 12

CONTINENTAL MAGNETIC ANOMALY CONSTRAINTS ON CONTINENTAL RECONSTRUCTION

R.R.B. von Frese, W.J. Hinze, R. Olivier and C.R. Bentley
EOS, v. 66, 255, 1985

Crustal magnetic anomalies mapped by the MAGSAT satellite for North and South America, Europe, Africa, India, Australia, and Antarctica and adjacent marine areas have been adjusted to a common elevation of 400 km and differentially reduced to the radial pole of intensity 60,000 nT. These radially polarized anomalies are normalized for differential inclination, declination and intensity effects of the geomagnetic field, so that in principle they directly reflect the geometric and magnetic polarization attributes of sources which include regional petrologic variations of the crust and upper mantle, and crustal thickness and thermal perturbations. Continental anomalies demonstrate remarkably detailed correlation of regional magnetic sources across rifted margins when plotted on a reconstruction of Pangea. Accordingly, they suggest further fundamental constraints on the geologic evolution of the continents and their reconstructions.

CITATION # 13

REGIONAL MAGNETIC ANOMALIES OF RIFTED CONTINENTAL MARGINS

R.R.B. von Frese, W.J. Hinze, R. Olivier and C.R. Bentley
IAGA, 5th General Assembly, Abstracts & Index of Authors, v. 2, 77, 1985

MAGSAT magnetic anomalies for North and South America, Europe, Africa, India, Australia and Antarctica have been adjusted to a constant elevation and differentially reduced to the pole to reflect directly the geometric and magnetic polarization attributes of crustal courses. The detailed correlations of these radially polarized anomalies across rifted margins when plotted on a reconstruction of Pangea provide further significant constraints on the evolution and dynamics of the continents and oceans.

CITATION # 14

SATELLITE MAGNETIC ANOMALIES AND CONTINENTAL RECONSTRUCTIONS

R.R.B. von Frese, W.J. Hinze, R. Olivier and C.R. Bentley
Sixth Gondwana Symposium (Ohio State Univ., Columbus, OH)
Abstracts, 104, 1985

Regional magnetic anomalies observed by NASA's magnetic satellite program (MAGSAT) for the eastern Pacific Ocean, North and South America, the Atlantic Ocean, Europe, Africa, India, Australia and Antarctica have been adjusted to a common elevation of 400 km and differentially reduced to the radial pole of intensity 60,000 nT. In principle, these radially polarized anomalies directly reflect the geometric and magnetic polarization attributes of regional lithospheric magnetic sources, as they have been normalized for differential inclination, declination and intensity effects of the geomagnetic field. Continental satellite magnetic data show an apparent sharp truncation and even parallelism of anomalies along the leading edges of the North and South American plates, whereas across trailing plate continental margins, prominent anomalies tend to continue into the ocean, reflecting perhaps subsided continental crust or the tracks of hotspots. Continental anomalies have prominent affiliations with ancient features and demonstrate remarkably detailed correlation of regional lithospheric magnetic sources across rifted margins when plotted on a reconstruction of Pangea. Accordingly, these anomalies describe geologic conditions of considerable age and provide new and fundamental constraints on the geologic evolution of the continents and their reconstructions.

CITATION # 15

REGIONAL MAGNETIC ANOMALY CONSTRAINTS ON CONTINENTAL BREAKUP

R.R.B. von Frese, W.J. Hinze, R. Olivier and C.R. Bentley
Geology, 14, 68-71, 1986

Continental lithosphere magnetic anomalies mapped by the MAGSAT satellite are related to tectonic features associated with regional compositional variations of the crust and upper mantle and crustal thickness and thermal perturbations. These continental-scale anomaly patterns when corrected for varying observation elevation and the global change in the direction and intensity of the geomagnetic field show remarkable correlation of regional lithospheric magnetic sources across rifted continental margins when plotted on a reconstruction of Pangea. Accordingly, these anomalies provide new and fundamental constraints on the geologic evolution and dynamics of the continents and oceans.

CITATION # 16

SATELLITE MAGNETIC ANOMALIES OF GONDWANA

R.R.B. von Frese, W.J. Hinze, R. Olivier and C.R. Bentley
AGU Monograph (in press)

Regional magnetic anomalies observed by NASA's recent magnetic satellite mission (MAGSAT) for the eastern Pacific Ocean, North and South America, the Atlantic Ocean, Europe, Africa, India, Australia, and Antarctica are adjusted to a fixed elevation of 400 km and differentially reduced to the radial pole of intensity 60,000 nT. Having been normalized for differential inclination, declination and intensity effects of the core field, these radially polarized anomalies in principle directly map the geometric and magnetic property variations of sources within the lithosphere. Continental satellite magnetic data show an apparent sharp truncation and even parallelism of anomalies along the tectonically active edges of the North and South American Plates, whereas across passive continental margins prominent anomalies tend to continue into the ocean, perhaps reflecting modified oceanic crust. When plotted on an early Cambrian reconstruction of Gondwanaland, many of the radially polarized anomalies of the continents demonstrate remarkably detailed correlation across the continental boundaries to verify the pre-rift origin of their sources. Accordingly, these anomalies provide fundamental constraints on the geologic evolution of the continents and their reconstructions.

CITATION # 17

THE SOUTH-CENTRAL U.S. MAGNETIC ANOMALY

P.J. Starich, W.J. Hinze and L.W. Braile

SEG 55th Annual International Meeting and Exposition
Technical Program (Abstracts & Biographies), 204-206, 1985

The south-central United States magnetic anomaly is the most prominent positive feature in the Magsat scalar magnetic field over North America. The anomaly correlates with increased crustal thickness, above average crustal velocity, negative Free-air gravity anomalies and an extensive zone of Middle Proterozoic anorogenic felsic basement rocks.

The anomaly and the magnetic crust are bounded on the west by the north-striking Rio Grande rift, a zone of lithospheric thinning and high heat flow in central New Mexico. The anomaly extends eastward over the Grenville age basement rocks of central Texas and is terminated to the south and east at the buried extension of the Ouachita Orogenic system which is the southern edge of the North American craton. The anomaly also extends eastward across Oklahoma and Arkansas to the Mississippi Embayment. A subdued northeasterly extension of the anomaly continues into the Great Lakes region. The feature terminates along the east-west boundary of the felsic terrain in southern Kansas.

Spherical dipole source inversion of the Magsat scalar data and subsequent calculation of a reduced-to-pole (Figure 1) map provide additional constraints for a crustal magnetic model which corresponds geographically to the extensive Middle Proterozoic felsic rocks trending northeasterly across the U.S. These felsic rocks contain insufficient magnetization or volume to produce the anomaly, but are rather indicative of a crustal zone which was disturbed during a Middle Proterozoic thermal event which enriched magnetic material deep in the crust.

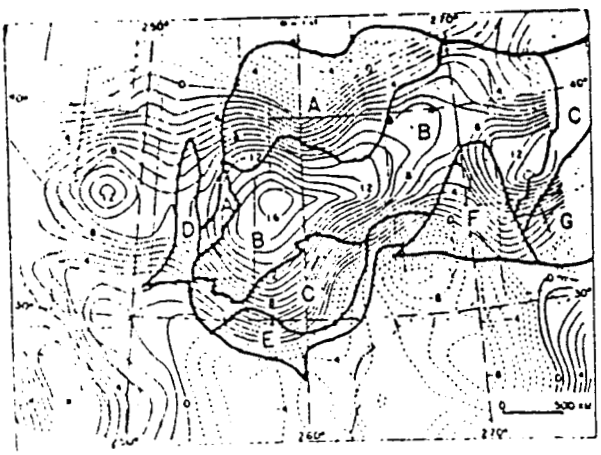

FIG. 1. Reduced-to-pole Magsat map with basement structural provinces: A. Early Proterozoic plutonic rocks. B. Middle Proterozoic granite and rhyolite. C. Grenville age plutonic rocks. D. Rio Grande rift zone. E. Ouachita system. F. Mississippi embayment. G. Appalachian system.

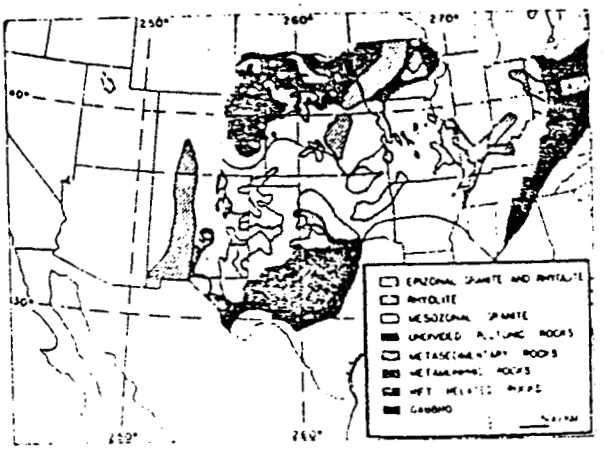

FIG. 2. Basement lithology of the central U.S. (after Van Schmus and Bickford, 1981; Denison et al., 1984; Hinze et al., 1984).

CONTINENTAL AND OCEANIC MAGNETIC ANOMALIES: ENHANCEMENT THROUGH GRM

by

Ralph R. B. von Frese
Dept. of Geology & Mineralogy
The Ohio State University
Columbus, Ohio 43210

William J. Hinze
Dept. of Geosciences
Purdue University
W. Lafayette, Indiana 47907

Earth-orbiting satellites over the past two decades have provided consistent global magnetic anomaly data sets which have given us unique insight on regional petrologic variations of the crust and upper mantle, and crustal thickness and thermal perturbations. Verification of the satellite magnetic data has been demonstrated by quantitative comparisons with aeromagnetic anomalies of the conterminous U.S. and western Canada. In contrast to the POGO and MAGSAT satellites, the GRM satellite system will orbit at a minimum elevation to provide significantly better resolved lithospheric magnetic anomalies for more detailed and improved geologic analysis. In addition, GRM will measure corresponding gravity anomalies to enhance our understanding of the gravity field for vast regions of the earth which are largely inaccessible to more conventional surface mapping. Crustal studies will greatly benefit from the dual data sets as modeling has shown that lithospheric sources of long-wavelength magnetic anomalies frequently involve density variations which may produce detectable gravity anomalies at satellite elevations. Furthermore, GRM will provide an important replication of lithospheric magnetic anomalies as an aid to identifying and extracting these anomalies from satellite magnetic measurements.

After the question of the formation of the earth itself, the most fundamental problem of the geosciences concerns the origin and characterization of the continents and oceans. An essential difference in the earth is between the continents and the oceans which is reflected in gravity via the Bouguer anomaly. However, as in the case of free-air and isostatic gravity anomalies, satellite magnetic measurements indicate no overwhelming difference between these regions. This is illustrated in Figure 1 which shows scalar 2°-averaged MAGSAT anomalies differentially reduced to the radial pole of intensity 60,000 nT at 400 km elevation for the eastern Pacific Ocean, North and South America, the Atlantic Ocean, and Euro-Africa. These radially polarized anomalies have been adjusted for differential inclination, declination and intensity effects of the geomagnetic field, so that in principle these anomalies directly reflect the geometric and magnetic polarization attributes of crustal magnetic sources. Characteristics of the data given in Figure 1 include the amplitude range (AR), amplitude mean (AM), contour interval (CI), and the normalization amplitude (AMP) for the radially polarizing field.

A subtle indication of the difference between oceans and continents is obtained by computing mean magnetic anomalies for the region shown in Figure 1. The analysis indicates that the mean magnetic anomaly of the continents (0.3 nT) is greater than the average for the oceans (-1.8 nT). This observation is compatible with the shallow crust of the ocean basins and evidence that suggests that the Moho is a magnetic boundary between

crustal magnetic and upper mantle non-magnetic rocks. However, this result may be muted by remanence effects which for regional crustal magnetic sources are generally not well known and at MAGSAT elevations are not well resolved.

Low-level observations of the oceans indicate that most of the magnetic anomalies reflect the age of the crust and are caused by the acquisition of remanent magnetization in the reversing magnetic field as the rocks pass through their Curie Point. However, as shown in Figure 1, only the broader scale Mesozoic and Cretaceous quiet zones seem to be clearly affiliated, respectively, with pronounced negative and positive radially polarized anomalies at MAGSAT elevations. In contrast, the satellite elevation magnetic anomalies of the continents seem to have a predominance of induction effects. There are remanent effects, but these are characteristically high wavenumber anomalies and are attenuated at higher elevations in the continental areas. The increased anomaly resolution derived from GRM's 160 km elevation orbits will significantly contribute to an understanding of the role which remanence has in causing regional anomalies of the oceans and continents.

Continental satellite magnetic data show an apparent sharp truncation and even parallelism of the anomalies along the leading edges of the North and South American plates, whereas across trailing plate continental margins prominent anomalies tend to continue into the ocean. Detailed analysis of the MAGSAT orbital data for South America indicates that the trailing edge anomalies have no apparent relationship to external fields, so these anomalies appear to be internally derived. Many of these anomalies show a striking parallelism with the tracks of hotspots particularly in the south Atlantic, although there is little consistency in the sign of the radially polarized anomalies and the hotspot tracks. Gravity and bathymetric correlations also suggest possible affiliation of some of these anomalies with subsided continental fragments. Clearly, information on these features is very limited and their origin is an important area of inquiry. High resolution magnetic data and correlative gravity anomalies provided by GRM will significantly facilitate understanding their origin and possible role in the evolution and dynamics of the continents and oceans.

The radially polarized anomalies of Figure 1 permit testing the reconstruction of the continents prior to the origin of the present day Atlantic Ocean in the Mesozoic Era. Indeed, as demonstrated in Figure 2, the radially polarized MAGSAT anomalies of North and South America, Euro-Africa, India, Australia and Antarctica exhibit remarkably detailed correlation of regional magnetic crustal sources across rifted margins when plotted on a reconstruction of Pangea. Obviously, these results suggest great ages for the geologic conditions which these anomalies desribe and provide new and fundamental constraints on the geologic evolution of the continents. The high resolution regional magnetic and correlative gravity anomaly data potentially available from the GRM offer the clear promise to improve quantitative geologic modeling of these features and to detail their development through geologic time.

FIGURE 1

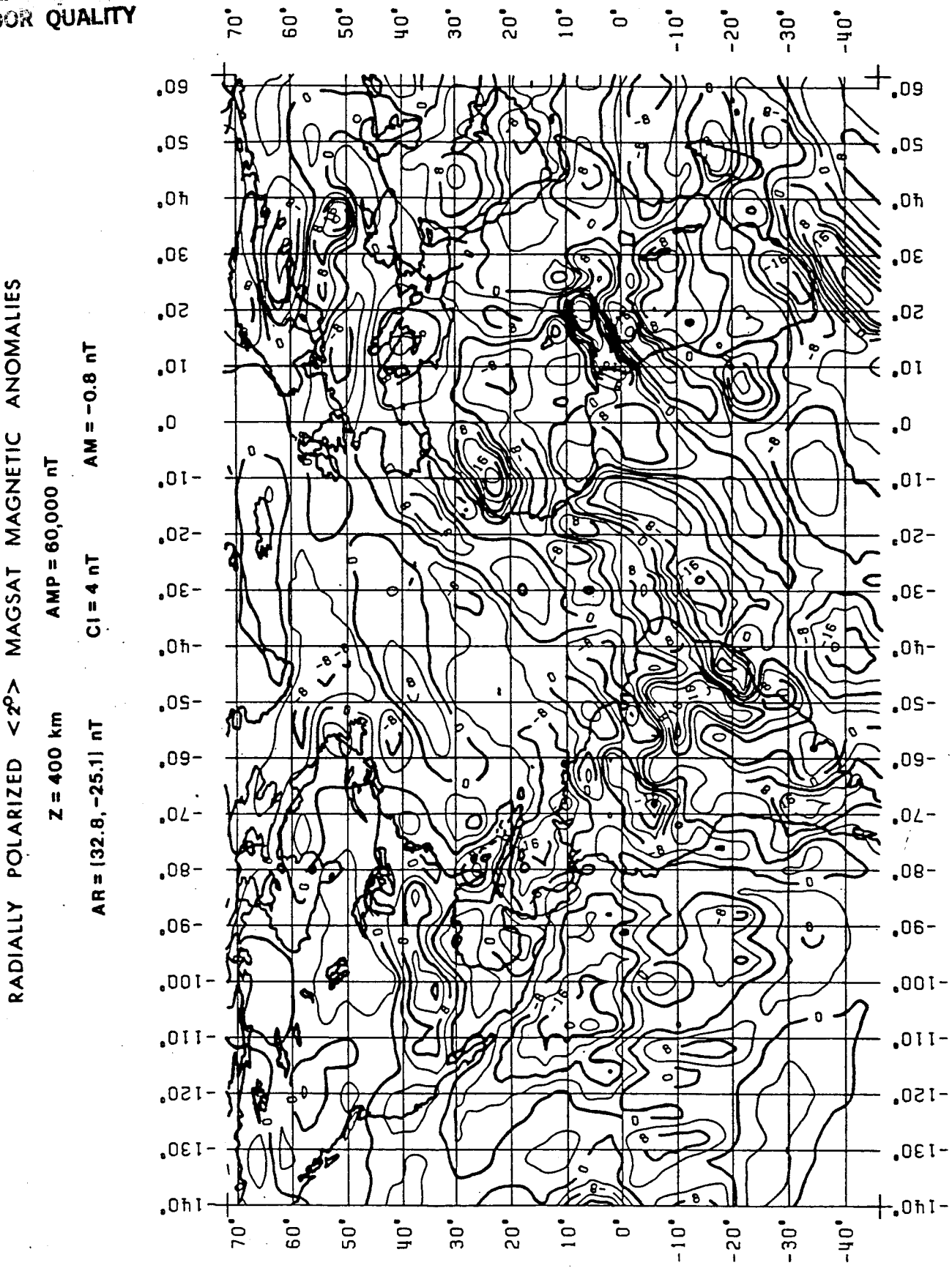

FIGURE 2

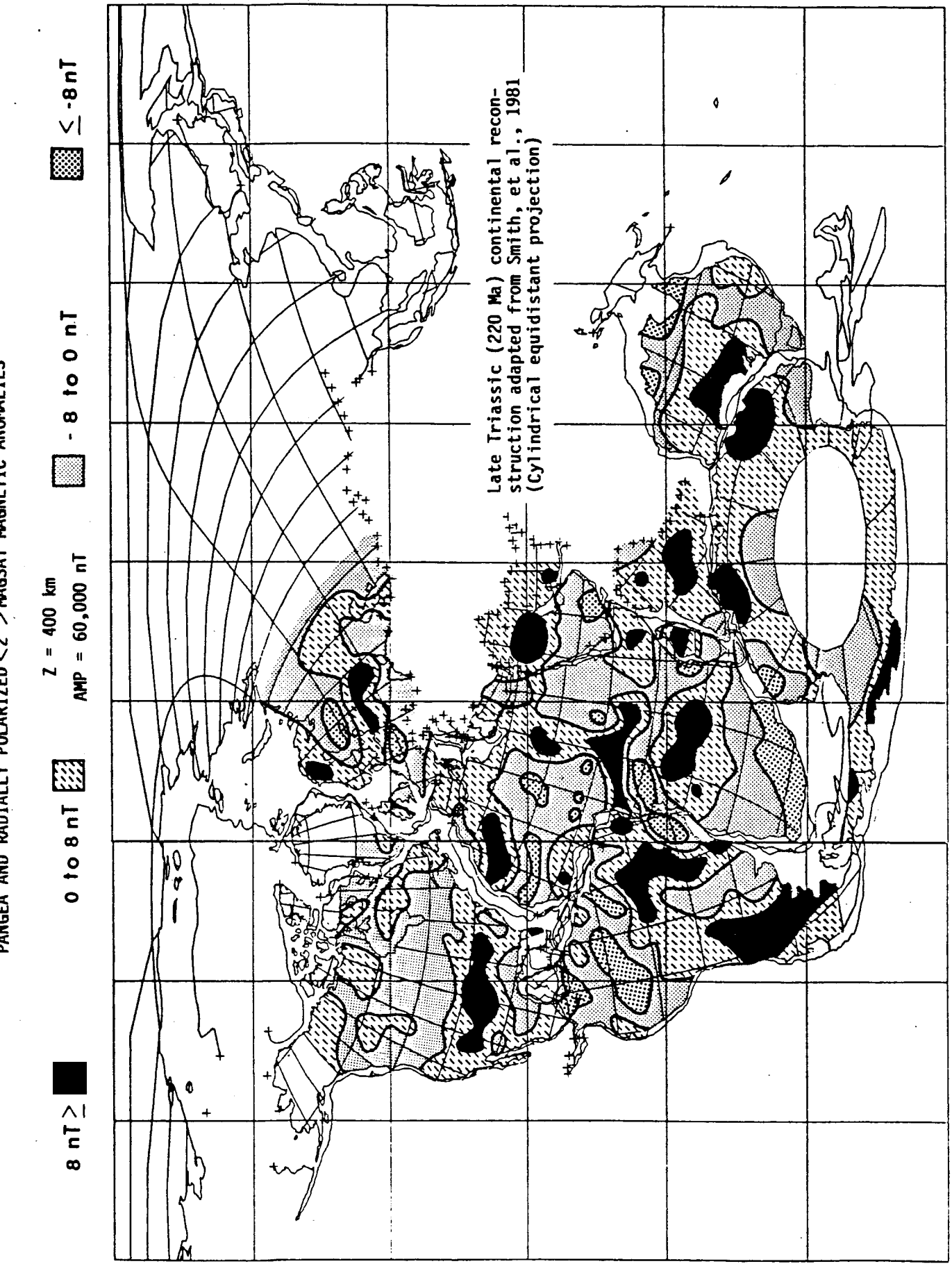

CRUSTAL APPLICATIONS OF GASP

R. R. B. von Frese

The utility of GASP for studying the earth's crust can be characterized in terms of lithospheric contributions by past satellite programs such as the POGO and MAGSAT missions. In general, these programs have provided consistent global magnetic anomaly data sets in harmonic degrees greater than about 13 which have yielded unique insight on regional petrologic variations of the crust and upper mantle, and crustal thickness and thermal perturbations. In contrast to the POGO and MAGSAT satellites, GASP will orbit at a lower elevation (≈ 270 km) to provide better resolved lithospheric magnetic anomalies for more detailed and improved geologic analysis. Furthermore, GASP will provide an important replication of lithospheric magnetic anomalies as an aid to identifying and extracting these anomalies from satellite magnetic measurements.

In the geological representation of satellite magnetic anomaly data, two approaches are current that can serve the analysis of GASP observations. When global scale coverge is available spherical harmonic expansions of the observations may be utilized. For lithospheric investigations, high degree representations are required comparable to the 720-by-720 degree spherical harmonic expansions of the earth's gravity field which geodesists are currently producing using routine mainframe computers.

More typically, lithospheric investigations utilizing satellite elevation data are performed on spatial scales which are smaller than global scale. For these studies, a useful and efficient approach is to determine the physical properties of an array of point equivalent sources by least-squares matrix inversion of the observations which will closely duplicate the observed field (Figure 1). Linear transformations of the equivalent source field then can be used to isolate or enhance geologically meaningful attributes of the observational data.

An important preliminary step in the representation of satellite magnetic observations either by high degree spherical harmonic expansion or by equivalent point source inversion is to register the data at constant elevation over uniform intervals of latitude and longitude. Most recently, we have learned to grid satellite magnetic data accurately by least-squares collocation which is a statistical procedure widely applied to problems in physical geodesy. As shown in Figure 2, this approach essentially involves using the variance/covariance statistics of the observational data in terms of the distances that they are from the point of prediction.

In conventional geodetic predictions of gravity, the observations are continued to the surface of a constant elevation sphere where they are then estimated at uniform intervals of latitude and longitude. This standard approach will be appropriate for GASP missions which will be designed to maintain nearly constant elevation orbits. However, we have also extended collocation to three dimensions to grid at constant elevation magnetic data with altitude variations, such as produced by MAGSAT where orbital elevation differences of over 120 km are commonly encountered.

Gridding satellite magnetic observations also greatly facilitates direct modeling of lithospheric sources to help validate and further detail

interpretations. Lithospheric modeling of satellite magnetic (and gravity) data can be readily performed in spherical or any other generalized coordinates by Gauss-Legendre quadrature integration. As shown in Figure 3, the procedure involves distributing point sources within the lithospheric body as determined by body's surface envelope, and computing the integrated effects of the point sources for comparison with observed anomalies.

Typical source representations for lithospheric modeling by Gaussian quadrature integration are shown in Figure 4. A geologic body whose surface envelop is sampled by an arbitrary number of points, for example, may be subdivided into generalized tetrahedra for modeling purposes (Figure 4-A). Because the magnetic thickness of the lithosphere is small compared to the elevation of satellite observations, magnetic sources also may frequently be modeled by a series of generalized triangular wedges which define a polygonal prismatic body (Figure 4-B). Finally, geologic sources with gridded surface envelopes (e.g., digital terrain models) can be subdivided into gridded prismatic elements (Figure 4-C) for accurately modeling their magnetic and gravity effects in any generalized coordinate system.

Quantitative geologic analyses of satellite measured anomalies derived from inductively magnetized sources in the lithosphere can be enhanced considerably by reducing the observations for the variable attitude and intensity attributes of the core field. As an example, consider the region in Figure 5 where the inclination, declination, and intensity variations of the IGS'75 geomagnetic reference field updated to 1980 at the earth's surface are plotted. The attitudinal characteristics of the core field as approximated by this model operate over the geometries of the lithospheric sources and at the observation points to vary the attributes of magnetic anomalies continuously from the poles to the equator where inversion of the anomaly signs ocurs. Assuming induced magnetization, the anomaly amplitudes are a function of the susceptibility of the sources, and the ambient field strength which varies as shown in Figure 5 from roughly 23,000 nT to 62,000 nT. Thus, an inductively magnetized source located in central southeastern South America produces an anomaly which is only about a third to one-half as strong as the anomaly produced by the same source at high magnetic latitudes.

Figure 6-A gives <2°> MAGSAT scalar magnetic anomalies over this region which are contoured at 2 nT intervals. In general, the sign, shape and strength of these anomalies are not simple functions of the magnetic and geometric properties of the lithospheric sources because of the effects of the core field. To minimize core field distortions, the data of Figure 6-A were inverted by least-squares matrix methods, using the IGS'75 reference field updated to 1980, for the magnetic susceptibilities of a 4°-array of point dipoles as shown in Figure 1. This procedure yielded stable point sources which modeled the observed anomalies in Figure 6-A with negligible error. Core-field-adjusted magnetic anomalies were then obtained as shown in Figure 6-B by computing the anomalies at a fixed elevation (400 km) from the equivalent point dipoles assuming a radial field of constant strength (60,000 nT). The radially polarized anomalies in Figure 6-B are contoured at 4 nT intervals.

The effects of differential reduction to the radial pole are readily appreciated by comparing Figures 6-A and 6-B. Note the marked shift of the radially polarized anomalies relative to their total field counterparts along isogonic lines towards the poles. At low geomagnetic latitudes this shift is as great as several degrees, whereas along the geomagnetic equator the radially polarized anomalies are reversed in sign relative to corresponding total field anomalies. These effects have a major impact on relating satellite elevation magnetic anomalies to regional lithospheric features. Also, the radially polarized anomalies indicate the presence of relatively strong lithospheric magnetic sources, particularly in east-central and southern South America, which are not readily apparent in the total field anomaly data due to the weak polarization characteristics of the core field in this region.

One of the fundamental questions in geology is the difference between continents and oceans. It is reflected in the definition of the Bouguer gravity anomaly, but other types of anomalies like free-air gravity or isostatic anomalies do not show this difference very well. The MAGSAT data as given in Figure 6 also indicate no overwhelming difference between these regions.

However, subtle evidence for the magnetic difference between oceans and continents can be obtained by computing the mean anomalies of these regions from the radially polarized data of Figure 6-B. Histograms of the radially polarized anomalies for the various continents and ocean basins are given in Figure 7, along with the mean (μ), standard deviation (S), and number (N) of anomaly values of each distribution. The continental regions all have greater mean magnetic anomaly values than the oceans which are characterized by negative mean anomalies. This is an impressive statistical result as there is only 1 chance in 64 that it is a random outcome.

In Figure 8, all the radially polarized anomalies for the oceans are collected into a histogram which is compared to the histogram for all the continental anomalies. The analysis shows that the mean magnetic anomaly of the continents (0.3 nT) is greater than the average for the oceans (-1.8 nT) at the 99.9% confidence level. These observations are compatible with the shallow crust of the ocean basins and evidence that suggests that the Moho is a magnetic boundary between crustal magnetic and upper mantle non-magnetic rocks. However, this result may be muted by remanence effects which for regional crustal magnetic sources are generally not well known and at MAGSAT elevations are not well resolved.

Low-level observations of the oceans indicate that most of the magnetic anomalies reflect the age of the crust and are caused by the acquisition of remanent magnetization in the reversing magnetic field as the rocks pass through their Curie Point. However, as shown in Figure 6-B, only the broader scale Mesozoic and Cretaceous quiet zones seem to be clearly affiliated, respectively, with pronounced negative and positive radially polarized anomalies at MAGSAT elevations. In contrast, the satellite elevation magnetic anomalies of the continents seem to have a predominance of induction effects. There are remanent effects, but these are characteristically high wavenumber anomalies and are attenuated at higher elevations in the continental areas. The increased anomaly resolution derived from the 270 km elevation orbits of GASP will contribute to an

understanding of the role which remanence has in causing regional anomalies of the oceans and continents.

Continental satellite magnetic data in Figure 6-B show an apparent sharp truncation and even parallelism of the anomalies along the leading edges of the North and South American plates, whereas across trailing plate continental margins prominent anomalies tend to continue into the ocean. Detailed analysis of the MAGSAT orbital data for South America indicates that the trailing edge anomalies have no apparent relationship to external fields, so these anomalies appear to be internally derived. Many of these anomalies show a striking parallelism with the tracks of hotspots particularly in the south Atlantic, although there is little consistency in the sign of the radially polarized anomalies and the hotspot tracks. Gravity and bathymetric correlations also suggest possible affiliation of some of these anomalies with subsided continental fragments. Clearly, information on these features is very limited and their origin is an important area of inquiry. Higher resolution magnetic data provided by GASP will facilitate understanding their origin and possible role in the evolution and dynamics of the continents and oceans.

The radially polarized anomalies of Figure 6-B permit testing the reconstruction of the continents prior to the origin of the present day Atlantic Ocean in the Mesozoic Era. Indeed, as demonstrated in Figure 9, the radially polarized MAGSAT anomalies of North and South America, Euro-Africa, India, Australia and Antarctica exhibit remarkably detailed correlation of regional magnetic crustal sources across rifted margins when plotted on a reconstruction of Pangea. Obviously, these results suggest great ages for the geologic conditions which these anomalies describe and provide new and fundamental constraints on the geologic evolution of the continents. The higher resolution regional magnetic anomaly data potentially available from GASP missions offer the promise to improve quantitative geologic modeling of these features and to detail their development through geologic time.

Finally, GASP offers the opportunity to sample lithospheric anomalies with non-polar orbits in contrast to the POGO and MAGSAT missions which were flown over nearly polar orbits. Reducing the data of the previous missions for lithospheric anomalies normally involves procedures which are applied on an orbit-by-orbit basis. In general, it is felt that along-track-processing of polar orbits tends to attenuate N/S anomaly components, producing E/W striping patterns such as those shown in Figure 6. GASP missions operated at oblique to nearly equatorial orbits will contribute to resolving this issue and thereby to improving the utility of satellite magnetic anomalies for lithospheric studies.

Acknowledgements

This paper includes results from investigations which were partially supported by NASA contract NAGW-736 from the Goddard Space Flight Center, and by grant DPP-8313071 from the National Science Foundation.

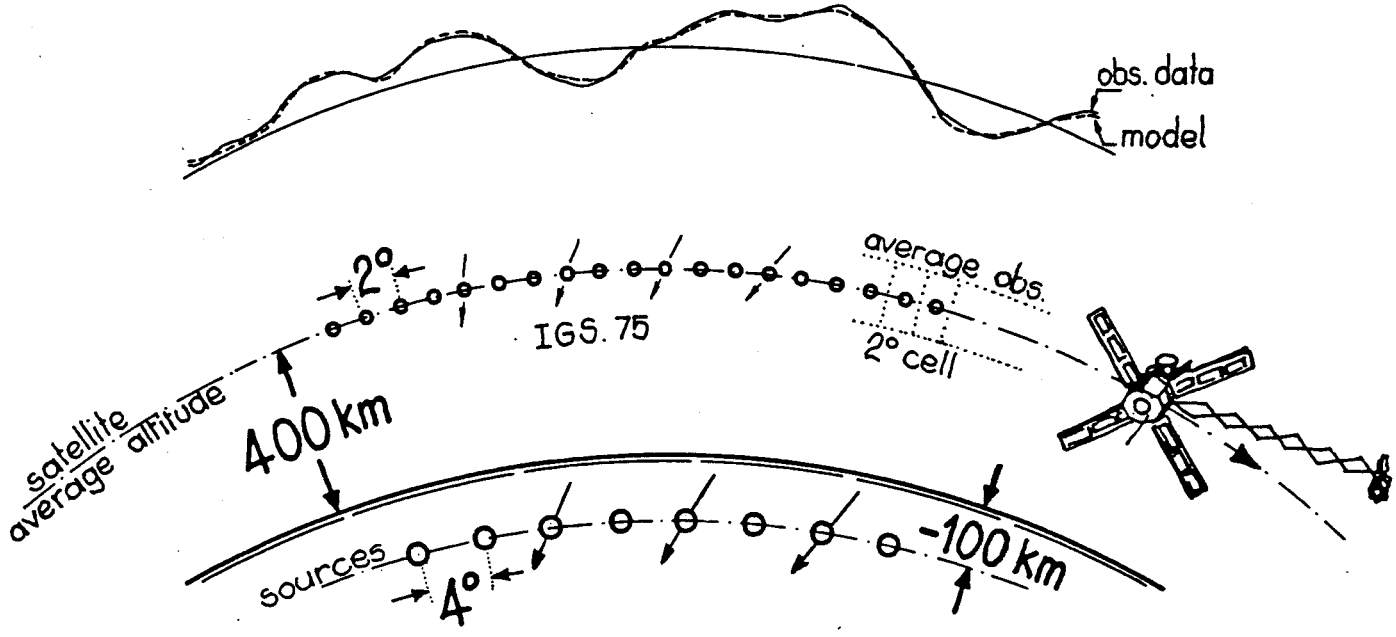
obs. data
model
2°
IGS.75
average obs.
2° cell
satellite
average altitude
400km
sources
4°
100km

FIGURE 1

LEAST-SQUARES COLLOCATION

(Moritz, 1972)

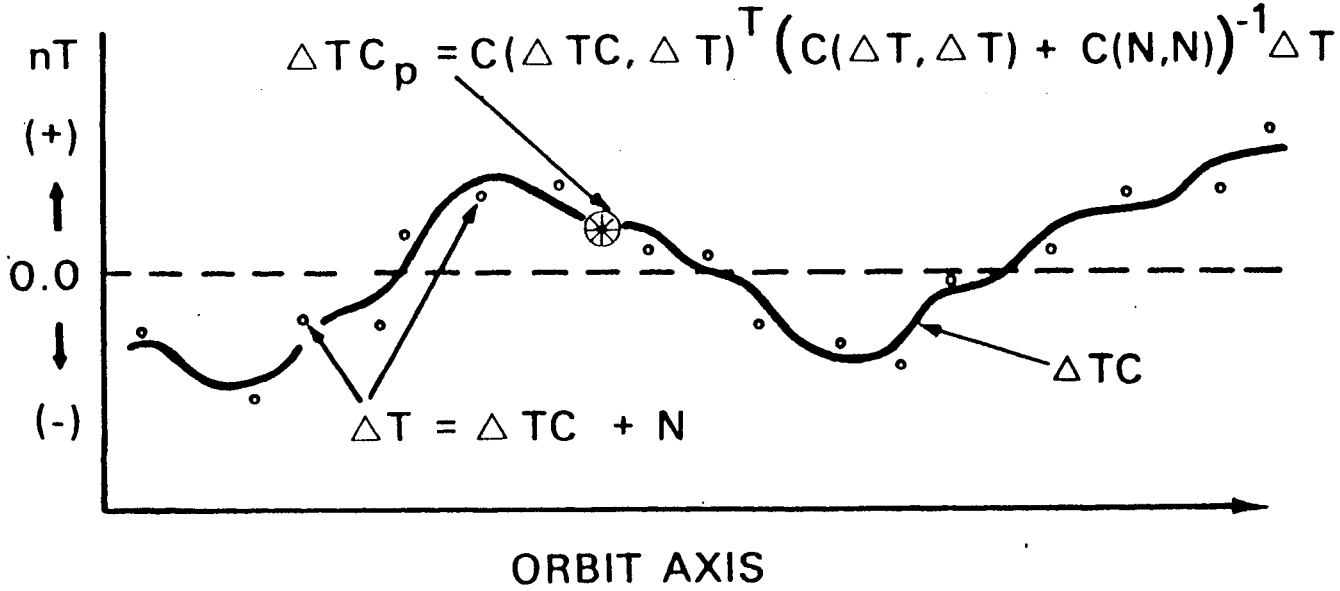

FIGURE 2

$C(\Delta TC, \Delta T)$ is the Cross-Covariance matrix between signal and observations.

$C(\Delta T, \Delta T)$ is the Covariance matrix of obserations.

C(N,N) is the Covariance matrix of observational noise which simplifies to (EV*I) if the noise is purely random with variance = EV.

GRAVITY AND MAGNETIC MODELING BY GAUSS-LEGENDRE QUADRATURE

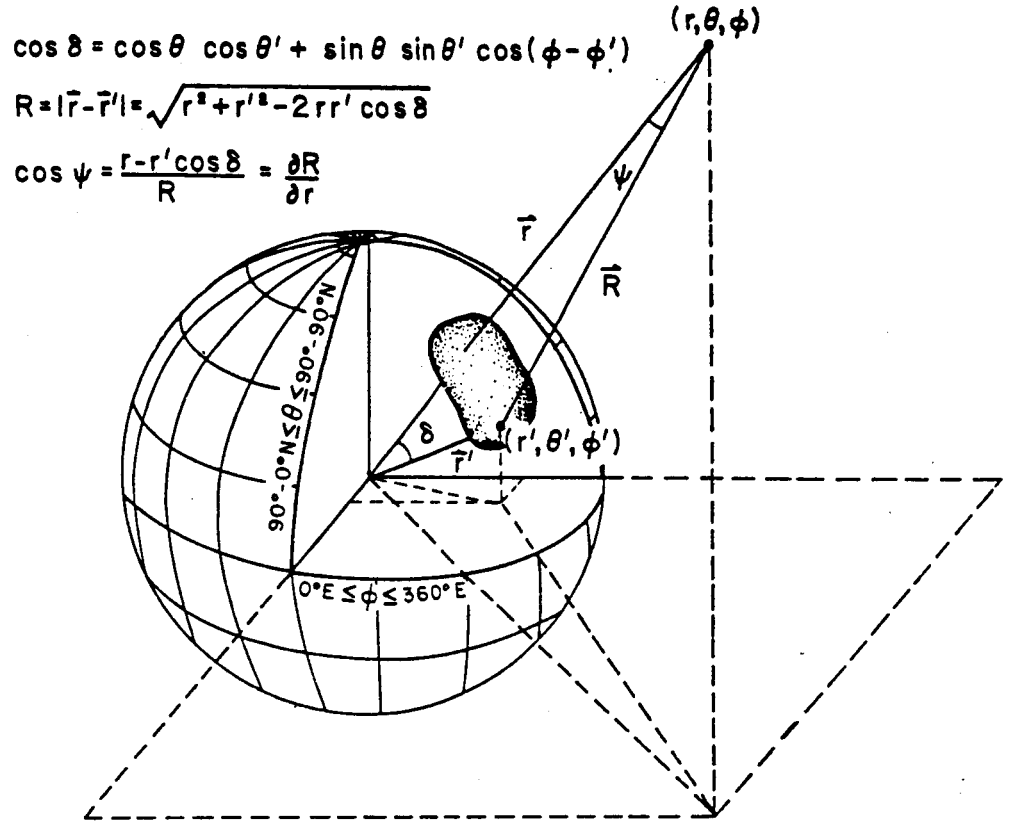

$$\cos\delta = \cos\theta\,\cos\theta' + \sin\theta\,\sin\theta'\cos(\phi-\phi')$$

$$R = |\vec{r}-\vec{r}'| = \sqrt{r^2+r'^2-2rr'\cos\delta}$$

$$\cos\psi = \frac{r-r'\cos\delta}{R} = \frac{\partial R}{\partial r}$$

GRAVITY ANOMALY

$$\Delta g = \left[-G\,\frac{\partial}{\partial R}\left(\frac{1}{R}\right)\frac{\partial R}{\partial r}\right] * \Delta m$$

MAGNETIC ANOMALY

$$\Delta T = \left[-\vec{u}\cdot\vec{\nabla}\left\{\vec{u}'\cdot\vec{\nabla}'\left(\frac{1}{R}\right)\right\}\right] * \Delta j$$

$$q(r,\theta,\phi;\, r',\theta',\phi') * \Delta x$$

GENERALIZED ANOMALY

$$\int_{\phi'_a}^{\phi'_b}\int_{\theta'_a}^{\theta'_b}\int_{r'_a}^{r'_b}\left(q(r',\theta',\phi') * \Delta x\right) dr'\,d\theta'\,d\phi'$$

$$\left(\frac{\phi'_{kb}-\phi'_{ka}}{2}\right)\sum_{k=1}^{nk}\left\{\left(\frac{\theta'_{jb}-\theta'_{ja}}{2}\right)\sum_{j=1}^{nj}\left[\left(\frac{r'_{ib}-r'_{ia}}{2}\right)\sum_{i=1}^{ni}\left(q(r'_i,\theta'_j,\phi'_k) * \Delta x\right)A_i\right]A_j\right\}A_k$$

FIGURE 3 Gravity and magnetic anomaly modeling in spherical coordinates of a geologic body with arbitrary shape and physical properties by Gauss-Legendre quadrature integration (see text for details).

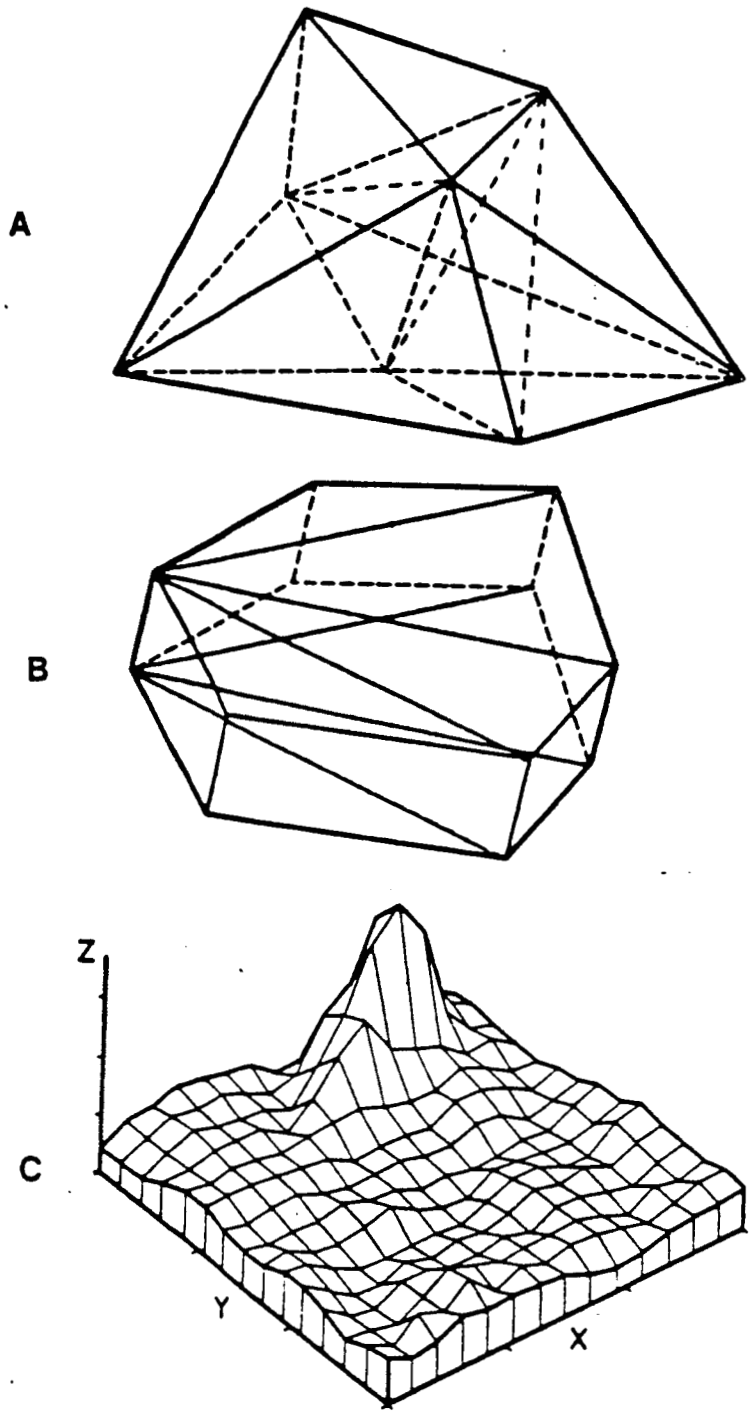

FIGURE 4 Typical geologic source representations: A) arbitrary source subdivided into tetrahedra, B) polygonal prism subdivided into triangular wedges, and C) source subdivided into gridded prismatic elements.

FIGURE 5

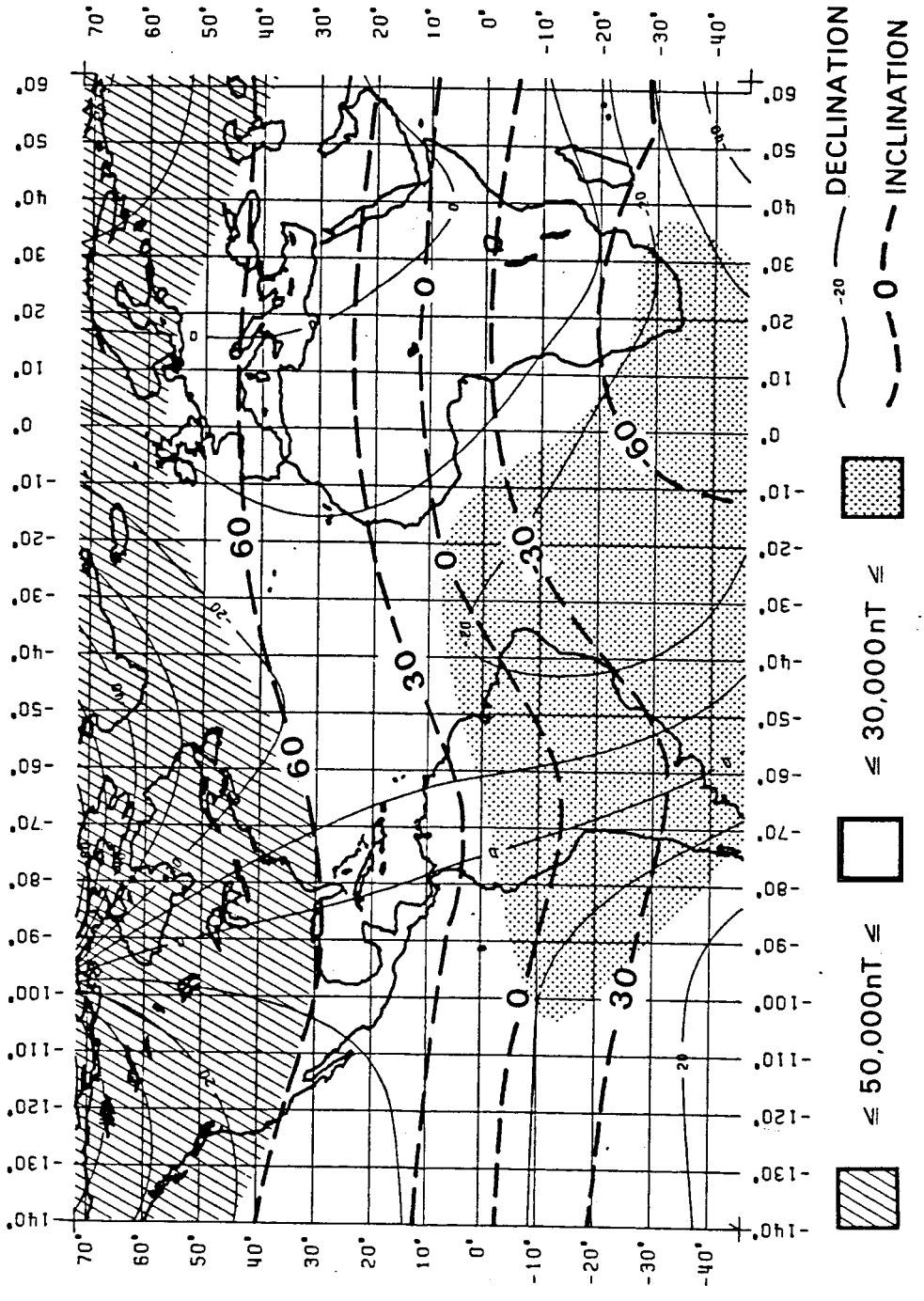

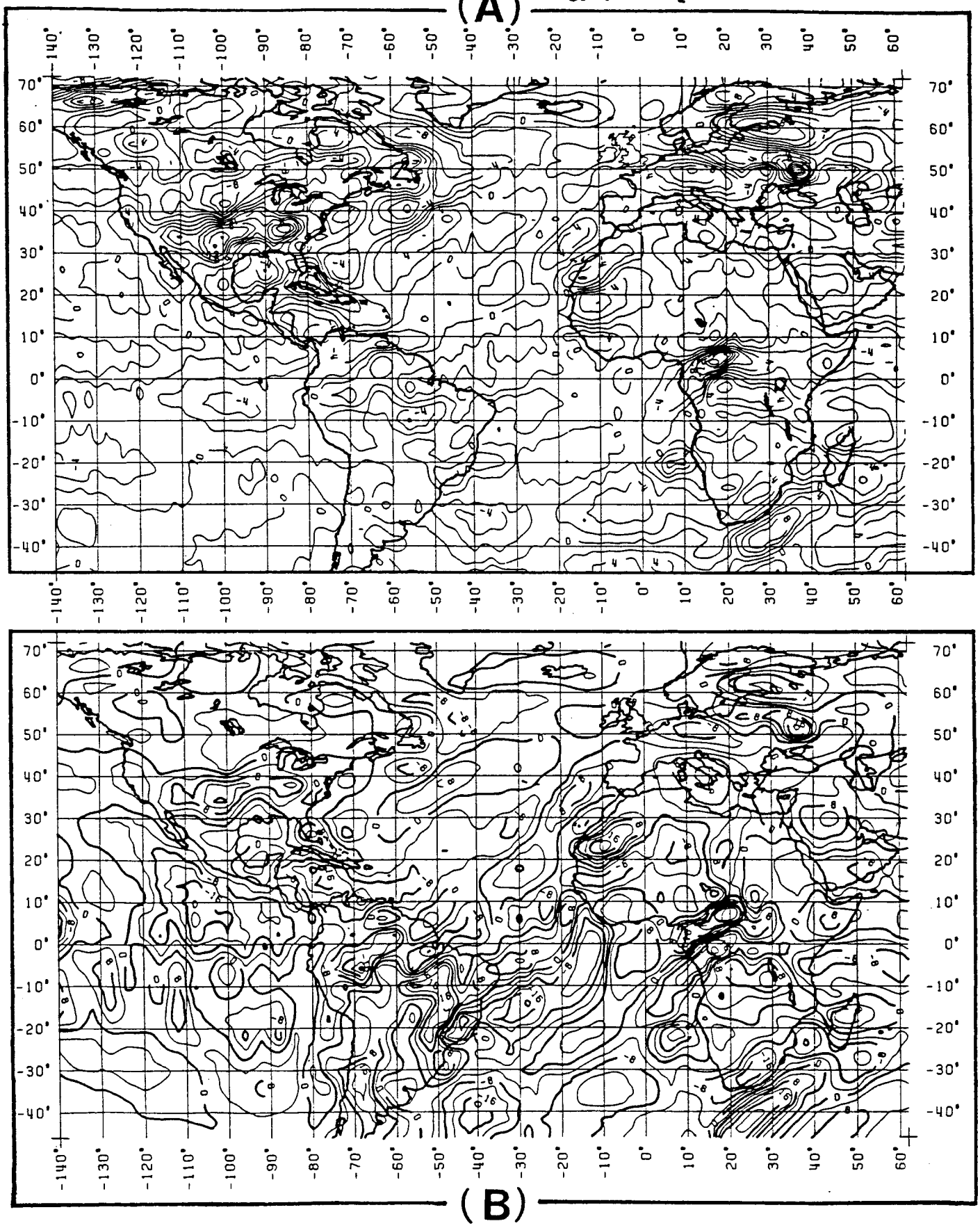

FIGURE 6

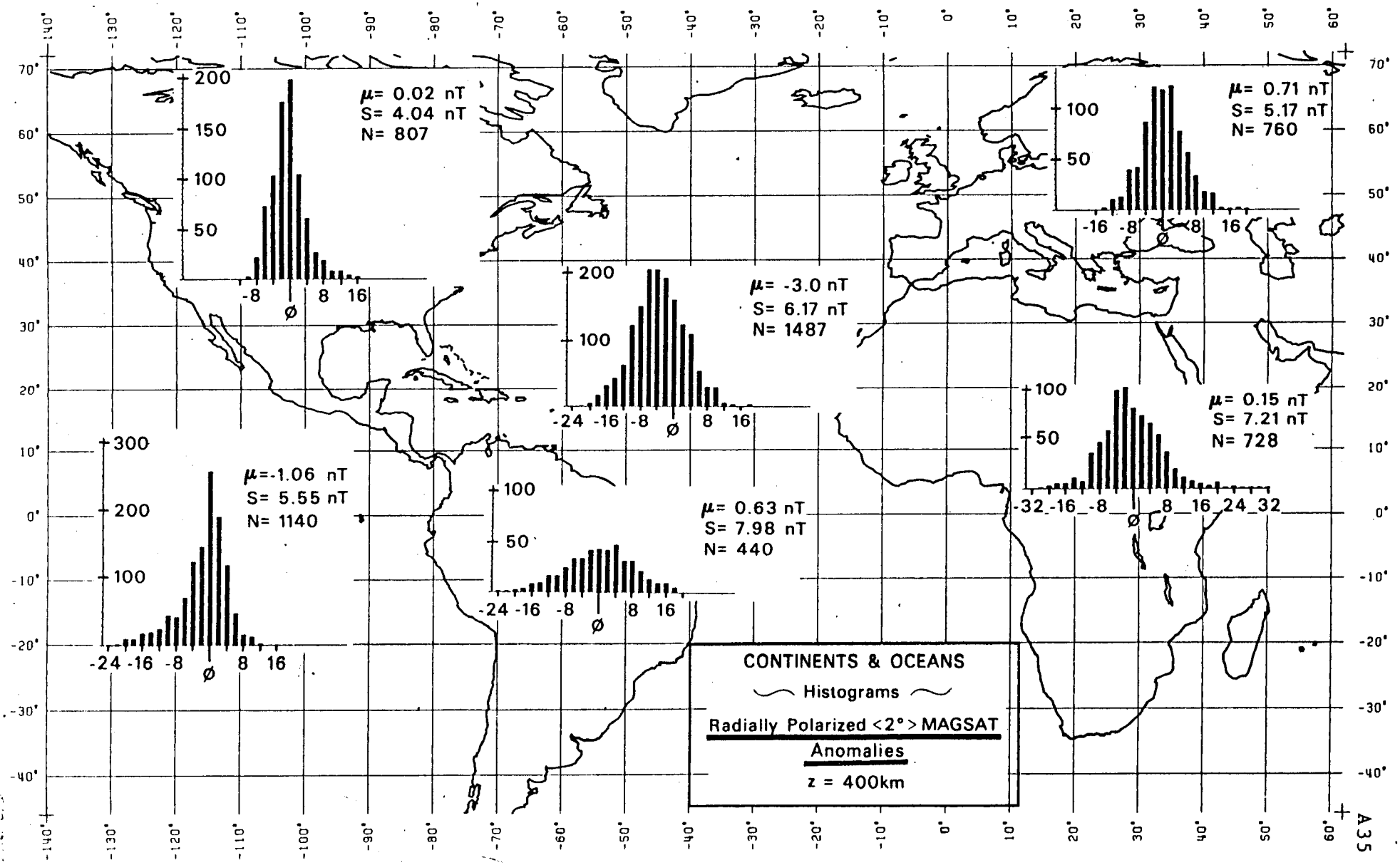

FIGURE 7

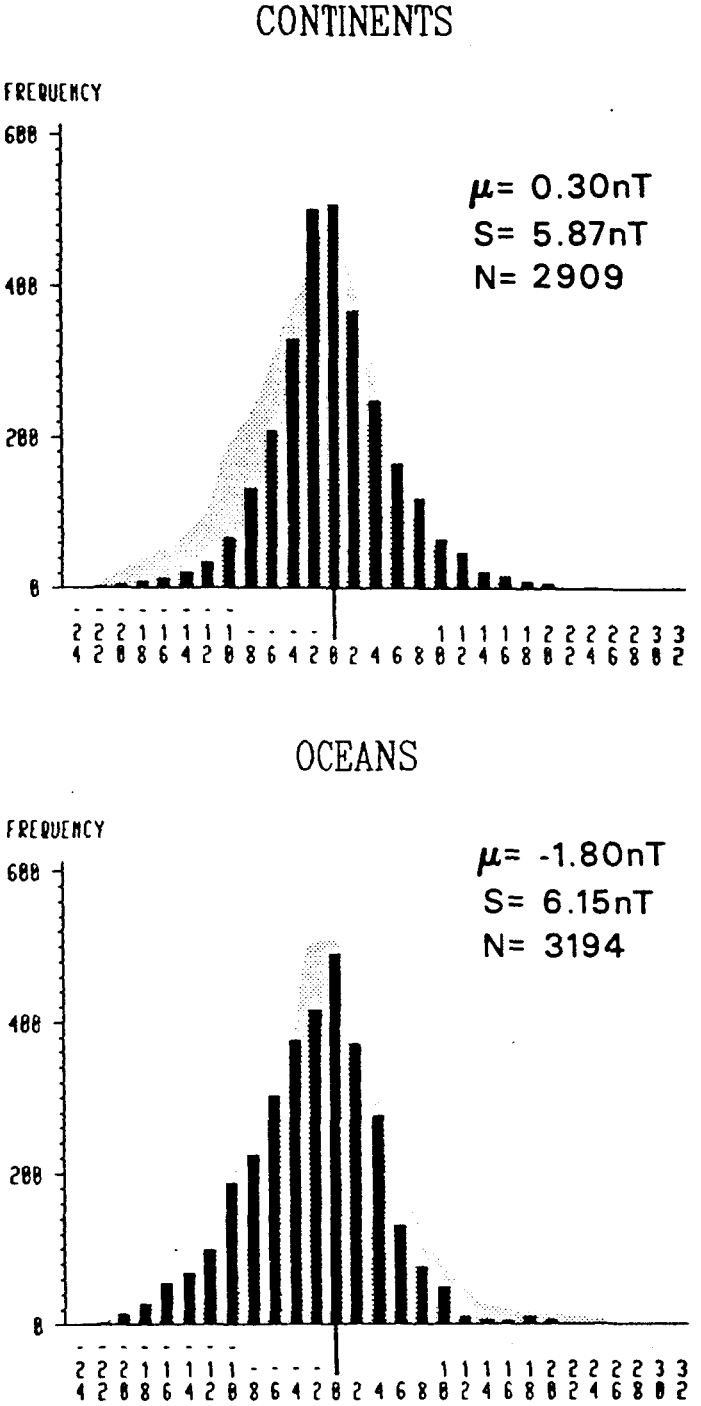

Frequency distributions for oceanic and continental radially polarized <2°> MAGSAT magnetic anomalies at 400 km elevation for the eastern Pacific Ocean, North and South America, Atlantic Ocean, and Euro-Africa. For each of the distributions a shaded representation of the other histogram is given to facilitate comparisons.

FIGURE 8

PANGEA AND RADIALLY POLARIZED MAGSAT MAGNETIC ANOMALIES

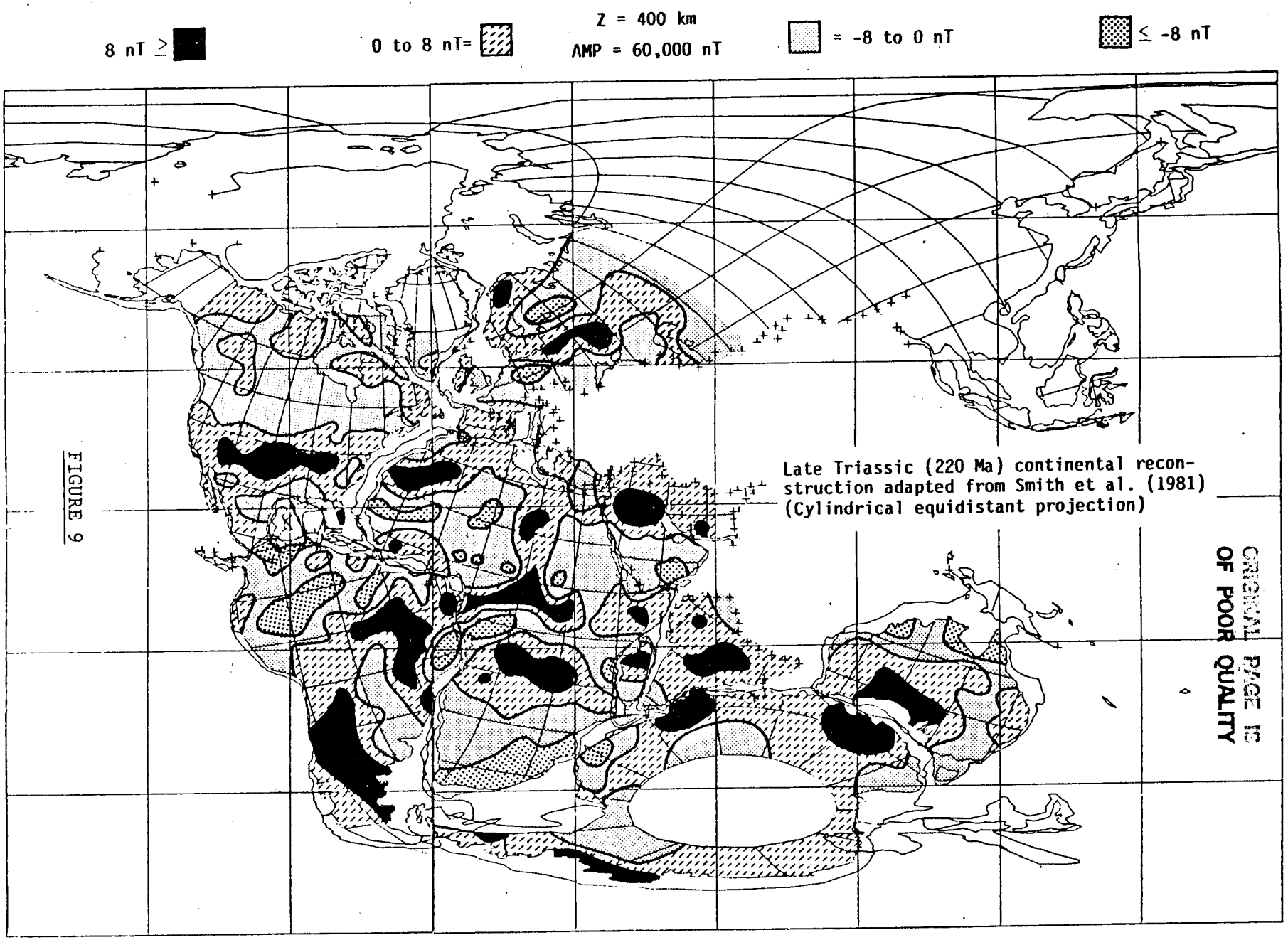

FIGURE 9

APPENDIX B

Preprints

1) Goyal, H.K., R.R.B. von Frese and W.J. Hinze, 1986, Statistical prediction of satellite magnetic anomalies, submitted to Geophysics for publication.

2) von Frese, R.R.B., D.N. Ravat, W.J. Hinze and C.A., McGue, 1986, Improved inversion of geopotential field anomalies for lithospheric investigations, submitted to Geophysics for publication.

3) von Frese, R.R.B., W.J. Hinze, R. Oliver and C.R. Bentley, 1986, Satellite magnetic anomalies of Gondwana, AGU Monograph (in press).

STATISTICAL PREDICTION OF SATELLITE MAGNETIC ANOMALIES

by

H. K. Goyal[1], R. R. B. von Frese[1], and W. J. Hinze[2]

[1] Dept. of Geology & Mineralogy
The Ohio State University
Columbus, OH 43210

[2] Dept. of Geosciences
Purdue University
W. Lafayette, IN 47907

Abstract

The errors of numerically averaging satellite magnetic anomaly data for geologic analysis are investigated using orbital anomaly simulations of lithospheric magnetic sources over a spherical earth. These simulations suggest that numerical averaging errors constitute small and relatively minor contributions to the total error-budget of higher orbital estimates ($\gtrsim$ 400 km), whereas for lower orbital estimates the error of averaging may increase substantially. Least-squares collocation in three dimensions is also investigated as an alternative to numerical averaging and found to produce substantially more accurate anomaly estimates as the elevation of prediction is decreased towards the lithospheric sources. Three-dimensional collocation is applied to MAGSAT magnetic observations of South America to demonstrate the utility of this statistical procedure for producing accurately gridded magnetic anomalies at constant elevation for geologic analysis.

Introduction

Geopotential anomaly field data are collected at micro through regional or global scales for a variety of important geological applications. As coverage is being increasingly extended, the problem of generating accurate anomaly values at larger scales from smaller-scale survey data is becoming evermore

commonplace and significant. Typically, the approach is to subdivide the higher density data sets into windows or bins which are analyzed for more regional-scale anomaly values. In general, binning of potential field data is a subject of considerable current interest and it will continue to be of interest in the future as we attempt to decimate oversampled data for regional geologic applications.

An important class of binning problems involves artificial, earth-orbiting satellites which are making increasingly available consistent,. regional-scale magnetic anomaly data for lithospheric studies. Satellite magnetometer observations for geologic applications are frequently presented as numerically averaged values of orbital profile anomalies within equal-angle or equal-area parallelepipeds or bins (e.g., Regan et al., 1975; Langel et al., 1982; Ritzwoller & Bentley, 1983). The averaged anomaly is normally assigned to the center of the area at the arithmetically averaged elevation of the data within the bin. In general, it is felt without quantitative basis that the averaging process limits the utility of anomaly maps prepared from these data in geologic analysis, but the advantages to geologic interpretation of more sophisticated and costlier data processing are also not clear. The objective of this study is to investigate the errors of numerical averaging for satellite magnetic anomaly estimation under spherical-earth conditions and to evaluate, as an alternative to arithmetic averaging, magnetic anomaly estimation by least-squares collocation. Of particular interest is the use of these relatively rapid statistical procedures for accurate production of magnetic anomaly values at arbitrary spatial coordinates. An important practical application of this capability is to grid satellite magnetic anomalies at constant elevation to facilitate geologic analysis and modeling at regional and global scales.

To obtain basic results for the statistical estimation of lithospheric magnetic anomalies, a series of numerical experiments are performed at satellite elevations involving the magnetic signals of crustal prisms. These results are then extended to MAGSAT observations over South America to produce a 1°-gridded anomaly map at constant elevation for gelogic analysis.

Statistical Magnetic Anomalies of Crustal Prisms at Satellite Elevations

The basic data of the numerical simulations are orbital scalar magnetic anomaly values of two dimensional, 40 km thick crustal spherical prisms with widths of 50, 100, 200, 300, and 500 km (Figure 1). The magnetic anomalies of these radially (normally) polarized prisms were calculated assuming 3 A/m magnetization by the Gauss-Legendre quadrature integration procedure (von Frese et al., 1981b). The anomaly values were computed at 0.25° intervals on 40°-length orbits that are at 25 km levels over elevations ranging from 100 to 700 km. The radial polarization and two dimensional assumptions were made to generalize the results while simplifying the computations.

Numerical averaging simulations were conducted using the statistical weighting procedure outlined by Langel et al. (1982) to obtain <2°> scalar magnetic anomalies from MAGSAT*. This procedure involves computing the mean and standard deviation of the anomaly values within a 2°-parallelepiped, eliminating anomaly values which are not within two standard deviations of the mean, and then recomputing the mean of the remaining values as the <2°> anomaly estimate. To evaluate numerical averaging errors, the averaged anomaly values were computed from the simulated 2°-bins with elevations ranging from 100 to 300 km, 300 to 500 km, and 500 to 700 km, and compared to

*Langel et al. (1982) also used only one anomaly value from each orbit in a 2°-bin, but this study does not test their sampling procedure.

the modeled anomaly values at the center of each bin at elevations, respectively, of 200 km, 400 km, and 600 km.

Least-squares collocation, a statistical estimation technique which is widely applied to problems in physical geodesy (e.g., Moritz, 1972), was also used in this study. For satellite magnetic anomaly prediction, residualized anomaly observations, ΔT, within a bin, may be modeled as shown in Figure 2 by

$$\Delta T = \Delta TC + N. \tag{1}$$

When the crustal anomaly, ΔTC, and random noise, N, are not correlated, a least-squares estimate of the crustal anomaly can be obtained from

$$\Delta TC_p = C(\Delta TC,\Delta T)^T(C(\Delta T,\Delta T) + C(N,N))^{-1}\Delta T, \tag{2}$$

where $C(\Delta TC,\Delta T)$ is the cross-covariance matrix between ΔTC and ΔT, $C(\Delta T,\Delta T)$ is the covariance matrix of observations, and C(N,N) is the covariance matrix of noise or measuring errors. If the observational noise is purely random with variance (EV), then

$$C(N,N) = (EV*I), \tag{3}$$

where (I) is the identity matrix.

For optimal prediction, the statistical behavior of the anomalies can be assessed through an appropriate covariance function. Conventional geodetic applications for anomaly interpolation involve the covariances for angular separations between observations scattered over a spherical surface at constant elevation. The present study, by contrast, extends collocation to three dimensions by considering the covariances of separation distances which are also variable in the radial coordinates of the anomalies. For a spherical earth the separation distance, R_{12}, between points $P(r_1,\theta_1,\phi_1)$ and $Q(r_2,\theta_2,\phi_2)$ is given by

$$R_{12} = (r_1^2 + r_2^2 - 2r_1r_2(\cos\theta_1\cos\theta_2 + \sin\theta_1\sin\theta_2\cos(\phi_1 - \phi_2))^{1/2}, \tag{4}$$

where (r_1,θ_1,ϕ_1) and (r_2,θ_2,ϕ_2) represent the radial, co-latitude and longitude coordinates for P and Q, respectively. In these simulations, the covariances for all separation distances between observations within a 2°-bin were computed by forming the corresponding anomaly products which were, in turn, sorted into successive uniform intervals of the separation distance. For each interval of the separation distance, the average of the anomaly products, normalized to the covariance value at zero separation distance, was plotted against the mean separation distance to obtain the normalized covariance function shown in Figure 3.

The normalized covariance functions for all bins considered in these simulations were found to follow in a least-squares sense the functional form given by

$$C_n(R) = 1.00 - (0.78*10^{-2})R - (0.2*10^{-4})R^2, \qquad (5)$$

where $C_n(R)$ is the normalized covariance value at separation distance, R. Covariance values for the various separation distances are given by

$$C(R) = C_n(R)*C(0), \qquad (6)$$

where C(0) is the value of the covariance function in nT^2 at zero separation, and R is the separation distance in km. This relationship was observed to hold for $R \lesssim 100$ km in these experiments. For the covariance values in each bin, the correlation length was close to 56 km, where the correlation length, ξ, is the value of R for which $C(\xi) = C(0)/2$. Accordingly, observations within a radius of about 100 km of the prediction point were used to form the elements of the covariance matrix $C(\Delta T,\Delta T)$.

Typical examples of the radially polarized anomaly signals considered in these simulations are shown in Figure 4. The upper panel (Figure 4.A) illustrates how the anomalies broaden and increase in amplitude at 200 km elevation with increasing source widths, whereas the lower panel (Figure 4.B) shows how

the magnetic anomaly of a crustal prism of width 200 km increases in amplitude and wavenumber with decreasing orbital elevation. Similar observations hold at the other elevations for all the source widths considered in these experiments.

Figure 5 provides characteristic results of how the averaging procedure described by Langel et al. (1982) performed in these simulations. The dotted line in each panel shows the small relative deviations of the estimates which are defined as the modeled (true) anomaly (solid line) minus the <2°> anomaly value obtained from analysis of all the computed anomalies within each bin, which in this case has no values perpendicular to the profile. However, in the normal preparation of satellite magnetic anomaly maps, orbits with large external magnetic field activity indices are routinely rejected to enhance lithospheric anomaly components. This frequently results in severely decimated coverage with respect to the anomaly values available for averaging within a bin. To simulate this condition, the computed values within each bin were randomly decimated to 20% of the original coverage. Characteristic <2°> anomaly deviations for the sparse data coverage are plotted as the dashed curves on the panels of Figure 5.

In general, Figure 5 shows that maximum deviations for both dense and sparse data coverage principally occupy the flank and peak regions of the anomalies, where the <2°> anomalies derived from sparse data coverage show the largest and most erratic deviations. Accordingly, to further evaluate errors of averaging, subsequent study focused on <2°> anomaly predictions from the decimated data for the various crustal prisms at the locations of the peak amplitude, 50% peak amplitude, and 10% peak amplitude of the true (modeled) anomaly profiles over the principal elevations of 200 km, 400 km, and 600 km. An overview of these results is presented in TABLE I, where at each of the

principal elevations the root mean squared (RMS) errors for predicting magnetic anomalies by averaging and three-dimensional collocation are given.

These results suggest that the simple averaging procedure provides remarkably good anomaly estimates at elevations of 400 km and greater for the simulations considered here. In practice, the location of a satellite magnetometer measurement is typically known only to within plus or minus several tens of meters of the true position. This mislocation can produce errors in the calculation of the geomagnetic reference field as large as a few nanoTeslas at 400 km and which increase with increasing orbital elevations. These errors are introduced when the reference field is subtracted from the observations to obtain the lithospheric anomaly residuals. External magnetic field effects, which are currently not well understood and difficult to account for, constitute an even greater error source in these residuals. Hence, inaccuracies due to numerical averaging represent only a minor contribution to the overall error-budget of satellite magnetic anomalies at these elevations. For lower elevations on the other hand, such as at 200 km where future satellite missions may be orbited, mislocation of the magnetometer sensor introduces errors of only 1 or 2 nT or less, yet numerical averaging can produce significantly large errors according to these simulations.

For comparison with the numerical averages, predictions based on least-squares collocation (with EV = 0) were also obtained for these sparsely populated bins. Differences between the anomaly estimates produced by the two methods smaller than or equal to 1.0 nT were attributed to numerical roundoff errors. For any differences above this cutoff, collocation yielded a significantly more accurate estimate than numerical averaging. Out of the 45 sparsely populated bins tested at the various elevations and source widths, collocation yielded significantly improved anomaly estimates for roughly 33%

of them. The improvement of collocation predictions over averaging as defined by (1 - |collocation deviation/averaging deviation|)*100% was found to range from 51% to 99% over all the source widths (Figure 6.A). However, improvement was more concentrated and significant at the lowest principal elevation (200 km) considered in this study (Figure 6.B and TABLE I).

Statistical MAGSAT Anomaly Predictions for South America

The crustal prism anomaly experiments described above suggest that least-squares collocation can be adapted for accurately gridding magnetic anomaly values which are arbitrarily distributed in three-dimensional, source-free space. This result has considerable practical significance for regional magnetic anomaly studies in particular, where these gridding efforts commonly involve anomaly inversions on equivalent source models (Mayhew, 1979; von Frese et al., 1981a) that are by several orders of magnitude more numerically intensive and laborious to apply than collocation.

To demonstrate the utility of three-dimensional collocation, a data set of nearly 11,000 anomaly values derived by Ridgway & Hinze (1986) from MAGSAT observations over South America is considered. This data set is the result of extensive screening and processing which attempted to isolate magnetic signals of the lithosphere on the basis of their temporal and spatial coherency. The geologic utility of these data are restricted, however, by orbital altitude variations which range between plus and minus 60 km about a mean elevation of 405 km, and by large lateral gaps in coverage that are associated with the selected orbits as shown in Figure 10.A.

Accordingly, Ridway & Hinze (1986) normalized the three-dimensional variability of the satellite magnetic data to a grid of anomaly values at constant elevation for geologic applications using the equivalent point source

inversion procedures of von Frese et al. (1981a). To normalize accurately these MAGSAT orbital tracks onto a 1°-grid of anomaly values at 350 km elevation by equivalent point source inversion requires a minimum of over 12 CPU-minutes and 1 megabyte of disk storage on a supercomputer (e.g., Cyber 205). Three-dimensional collocation, by contrast, can be implemented on a common mainframe computer (e.g., IBM 3081) to interpolate very accurate grids through these orbital tracks using less than 2 CPU-minutes and roughly 0.4 megabytes of disk space.

To obtain criteria for evaluating the performance of collocation in this application, a simulation study was conducted using a lithospheric equivalent point source model of the South American MAGSAT data. The NASA averaging procedure was applied to the orbital profiles of Ridgway & Hinze (1986) to obtain <2°> magnetic anomalies at an average elevation of 405 km. This grid of <2°> anomalies was then inverted on a point source grid with 4° spacing at 100 km below the earth's surface by least-squares methods. In this way a set of dipole susceptibilities was obtained such that the anomalies computed from the grid of point dipoles matched the <2°> magnetic anomalies with negligible error. The gridded dipole model was next evaluated at the spatial coordinates of each of the nearly 11,000 anomaly values derived by Ridgway & Hinze (1986) to produce a set of simulated anomalies. Predictions from the application of collocation to the simulated data were then compared to predictions computed directly from the equivalent point dipole model to evaluate the performance of the statistical procedure.

Efforts to determine the covariance function, C(R), for the selected MAGSAT anomaly values showed that the data were too sparsely distributed to produce a meaningful picture of the covariance properties. The covariance function given in equation (6) can be used to obtain reasonably accurate

anomaly predictions. However, it was found that predictions with improved accuracies could be obtained using a covariance function due to Moritz (1980) given by

$$C(R) = (C(0))*EXP(-A^2R^2), \qquad (7)$$

where C(0) is the variance of the data used in any particular prediction from which their mean value has been subtracted. For the South American data, the correlation length was chosen to be 300 km to facilitate scaling of the covariance matrix $C(\Delta T,\Delta T)$ in the comuter using anomaly values within about 2° of a prediction point. The coefficient, A, in equation (7) was found accordingly to be 0.00276/km. Figure 7.A shows the covariance function of equation (7) normalized against C(0) which was used for predicting gridded anomaly values from the selected MAGSAT orbits over South America.

Applications of three-dimensional collocation to the simulated MAGSAT orbital tracks assumed that these anomalies were representative of lithospheric signals which are free of measuring errors (i.e., EV = 0). Figure 8.A gives the map obtained when collocation was performed on the simulated data to produce 71*71 anomaly predictions over a 1°-grid at 405 km elevation. Figure 8.B is the anomaly map computed at the elevation of 405 km from the gridded point dipole model that collocation attempted to predict in Figure 8.A. Both maps are almost identical with a correlation coefficient equal to 0.999. Comparable results were obtained when collocation was applied to produce a gridded anomaly map at 350 km elevation (Figure 9.A) from the simulated orbits and checked against the map computed from the equivalent point dipole model at the same elevation (Figure 9.B). These two maps also correlate very well, attaining a correlation coefficient of 0.998.

These results suggest that three-dimensional collocation applied to the MAGSAT orbital data tracks should yield accurate estimates of the anomaly

field at altitudes of 405 km and 350 km. However, when applied to the actual MAGSAT data to obtain a 1°-grid of values at 405 km elevation, the collocation predictions yielded high frequency features which tend to align along gaps in the orbital coverage as shown in Figure 10.A. These features are related to instabilities in the inversion of the covariance matrix which may be minimized by adding the diagonal matrix (EV*I) to $C(\Delta T, \Delta T)$ as in equation (2), where (EV) is the error variance (Schwarz, 1978; Gerstl & Rummel, 1981).

For the MAGSAT data of South America then, an appropriate choice of (EV) must be made to control the numerical stability of the three-dimensional predictions by least-squares collocation. In practice, this choice is conveniently facilitated by plotting the error variance (EV) against the sum of squared residuals (SSR) between predictions for (EV = 0) and positive values of the error variance. Such an EV-spectrum is given in Figure 7.B for MAGSAT anomaly predictions at 405 km elevation over South America. As the error variance increases, the curve initially rises very rapidly and then it tends to flatten, suggesting little change in the residuals beyond an error variance of about 0.25 nT^2. In general, as the error variance is increased, the predictions become less sensitive to the higher frequency characteristics of the data and the resultant maps exhibit smoother, longer wavelength features. At sufficiently large values of the error variance, the anomaly predictions begin to approach zero so that the residuals continue to increase.

These results suggest that the predictions tend to stabilize for the South American MAGSAT data at error variances of about 0.25 nT^2 or greater. The collocation map of the MAGSAT data calculated with an error variance of 0.25 nT^2 at 405 km elevation is shown in Figure 10.B. This map is significantly more consistent with the behavior of lithospheric signals at satellite

elevations that the map given in Figure 10.A which was produced with zero error variance. Increasing the error variance to 1.0 nT^2 does not significantly affect the predictions as shown in Figure 11.A. At a considerably larger error variance of 9.0 nT^2, long wavelength features dominate the map and local high frequency predictions are significantly attenuated as shown in Figure 11.B. This effect is clearly evident by comparing Figures 11.A and 11.B where the characteristics of high frequency anomalies less than -4 nT or greater than 4 nT are severely attenuated, but the longer wavelength features are relatively unaffected. The MAGSAT anomalies computed over a grid at 350 km elevation by three-dimensional collocation using an error variance of 1.0 nT^2 are shown in Figure 12. This map, which took less than 2 minutes to compute, compares very favorably to the MAGSAT scalar anomalies which Ridgway & Hinze (1986) produced at 350 km elevation by compositing the results of nine separate inversions of smaller, overlapping regions within the study area.

The positive values of error variance in these applications are required to stabilize the predictions. However, they may also be interpreted as purely random error components in the data which propagate into the predictions so that the true values are within plus or minus $(EV)^{1/2}$ of the predicted values. This characterization of error variance may or may not have any relationship with the actual observation errors of the data. On the other hand, if the observational error can be determined for each data point, then these errors can be included for each prediction to produce a map of the prediction deviations or errors as is typically done for statistical gravity anomaly determinations (Moritz, 1972).

Conclusions

Crustal magnetic anomaly signals over satellite orbits were simulated to investigate numerical averaging as an anomaly estimator. Averaging is a convenient procedure for reducing satellite magnetometer data to manageable proportions for geologic analysis, although the precision of averaging as an anomaly estimator involves significant problems concerning spatial and amplitude smoothing of the satellite magnetic observations. The results of the simulations considered in this study suggest that the error of numerical averaging constitutes a small and relatively minor component of the total error-budget of higher orbital anomaly estimates ($\gtrsim$ 400 km), whereas for lower orbital estimates numerical averaging error increases substantially.

As an alternative to numerical averaging, least-squares collocation was investigated and observed to produce substantially more accurate anomaly estimates, particularly as the orbital elevation of prediction was decreased towards the lithospheric sources. In contrast to averaging, three-dimensional collocation is a significantly more resource-intensive procedure to apply because of the practical, but surmountable problems related to establishing and inverting the covariance matrix for accurate anomaly prediction. However, as demonstrated by these simulations, collocation may be used much more effectively than numerical averaging to exploit the anomaly details contained in the lower orbital satellite magnetic data for geologic analysis.

Statistical predictions of MAGSAT observations over South America were investigated for improving the geological analysis of regional magnetic anomalies. In general, three-dimensional collocation is a most efficient and cost-effective approach for obtaining accurate, altitude-normalized anomaly grids from orbital or arbitrarily distributed data. Once in gridded

format, the anomaly data are especially ameanable to modeling and representation by equivalent source transformations or harmonic expansions for enhanced geologic interpretation.

Acknowledgements

The authors thank Prof. R. H. Rapp and Dr. J. Y. Cruz of the Dept. of Geodetic Science at Ohio State for stimulating discussions and initial software for implementing least-squares collocation. This investigation was partially supported by NASA contract NAGW-736 from the Goddard Space Flight Center and grant DPP-8313071 from the National Science Foundation.

References Cited

Gerstl, M., and R. Rummel, 1981, Stability investigations of various representatives of the gravity field, Rev. of Geophys. and Space Phys., v. 3, p. 415-420.

Langel, R. A., J. D. Phillips and R. J. Horner, 1982, Initial scalar magnetic anomaly map from MAGSAT, Geophys. Res. Lett., v. 9, p. 269-272.

Mayhew, M. A., 1979, Inversion of satellite magnetic anomaly data, J. Geophys., v. 45, p. 119-128.

Moritz, H., 1972, Advanced Least-Squares Methods, Rept. #175, Dept. of Geodetic Sci., The Ohio State University, Columbus, OH.

Moritz, H., 1980, Advanced Physical Geodesy, Herbert Wichmann Verlag, West Germany.

Regan, R. D., J. C. Cain and W. M. Davis, 1975, A global magnetic anomaly map, J. Geophys. Res., v. 80, p. 794-802.

Ridgway, J. R., and W. J. Hinze, 1986, MAGSAT scalar anomaly map of South America, Geophysics, v. 51, p. 1472-1479.

Ritzwoller, M. H. and C. R. Bentley, 1983, Magnetic anomalies over Antarctica measured from MAGSAT, in (Olivier, R. L., P. R. James and J. B. Jago, eds.) Antarctic Earth Science-Fourth International Symposium, Cambridge Univ. Press, NY, p. 504-507.

Schwarz, K. P., 1978, On the Application of Least-Squares Collocation Models to Physical Geodesy, Herbert Wichmann Verlag, West Germany.

von Frese, R. R. B., W. J. Hinze, and L. W. Braile, 1981a, Spherical earth gravity and magnetic anomaly analysis by equivalent point source inversion, Earth Planet. Sci. Lett., v. 53, p. 69-83.

von Frese, R. R. B., W. J. Hinze, L. W. Braile and A. J. Luca, 1981b, Spherical earth gravity and magnetic anomaly modeling by Gauss-Legendre quadrature integration, J. Geophys., v. 49, p. 234-242.

TABLE I

Root Mean Squared (RMS) Errors - Averaging vs. Collocation
(Sparse Data Coverage Simulations)

Orbital Elevation [km]	RMS Error of Averaging [nT]	RMS Error of Collocation [nT]
200	12.70	1.48
400	1.31	0.44
600	0.23	0.43

Figure Captions

Figure 1
Geometric and physical properties used for the satellite orbital magnetic anomaly simulations. This study focused on anomaly estimates for A = 2°.

Figure 2
Elements of signal prediction by least-squares collocation.

Figure 3
The least-squares polynomial curve in separation distance, R, fitting the normalized covariance functions of the crustal prism profiles is given by $C_n(R) = 1.00 - (0.78*10^{-2})R - (0.20*10^{-4})R^2$.

Figure 4
Characteristics of radially polarized magnetic anomalies for different crustal prism widths at 200 km elevation (A), and at different satellite elevations for a crustal prism 200 km wide (B).

Figure 5
Comparison of true anomalies due to a 200 km wide crustal prism with corresponding deviations of <2°> magnetic anomalies derived from dense (dotted) and sparse (dashed) data coverage at (A) 200 km elevation, (B) 400 km elevation, and (C) 600 km elevation.

Figure 6
Percent improvement of collocation estimates over those obtained by averaging plotted as a function of (A) the source widths and (B) the principal satellite elevations considered in the crustal prism experiments. Numbers beside superimposed data points give the number of data points in the cluster.

Figure 7
Plots of (A) the normalized covariance function $C_n(R) = EXP(-A^2R^2)$ and (B) the error variance (EV) spectrum used for predicting MAGSAT magnetic anomalies over South America by three-dimensional collocation.

Figure 8
Magnetic anomaly maps at 405 km altitude produced by (A) collocation (EV = 0.0) of the simulated data orbits, and by (B) the equivalent point dipole model. Contour interval is 2 nT.

Figure 9
Magnetic anomaly maps at 350 km altitude produced by (A) collocation (EV = 0.0) of the simulated data orbits, and by (B) the equivalent point dipole model. Contour interval is 2 nT.

Figure 10
Collocation anomaly predictions at 405 km altitude produced from selected dawn orbits of MAGSAT with (A) EV = 0.0 and satellite tracks superimposed on the study area, and with (B) EV = 0.25 nT^2. Contour interval is 2 nT.

Figure 11
Collocation anomaly predictions at 405 km altitude produced from selected dawn orbits of MAGSAT with (A) EV = 1.0 nT^2 and (B) EV = 9.0 nT^2. Contour interval is 2 nT.

Figure 12
Collocation anomaly predictions at 350 km altitude produced from selected dawn orbits of MAGSAT with EV = 1.0 nT^2. Contour interval is 2 nT.

PARAMETERS FOR MAGNETIC SATELLITE ANOMALY AVERAGING SIMULATIONS

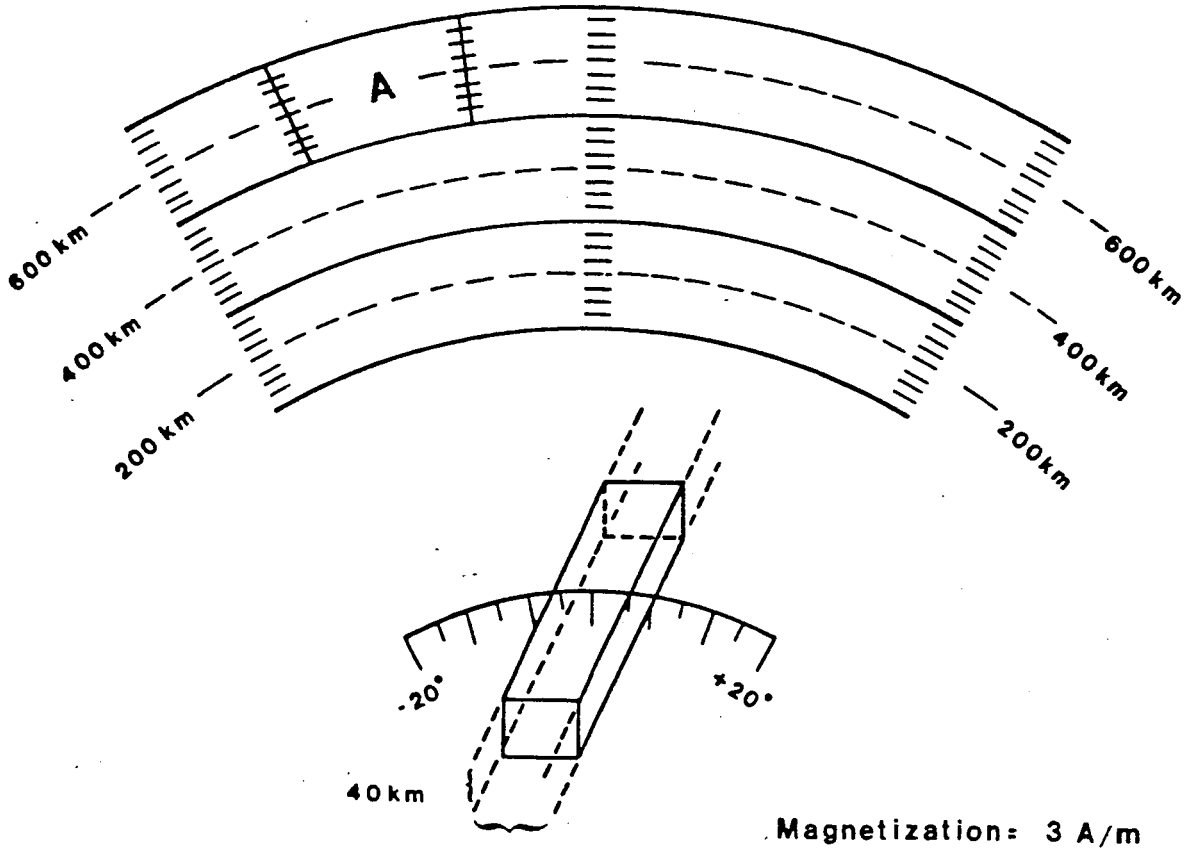

FIGURE 1

LEAST-SQUARES COLLOCATION

(Moritz, 1972)

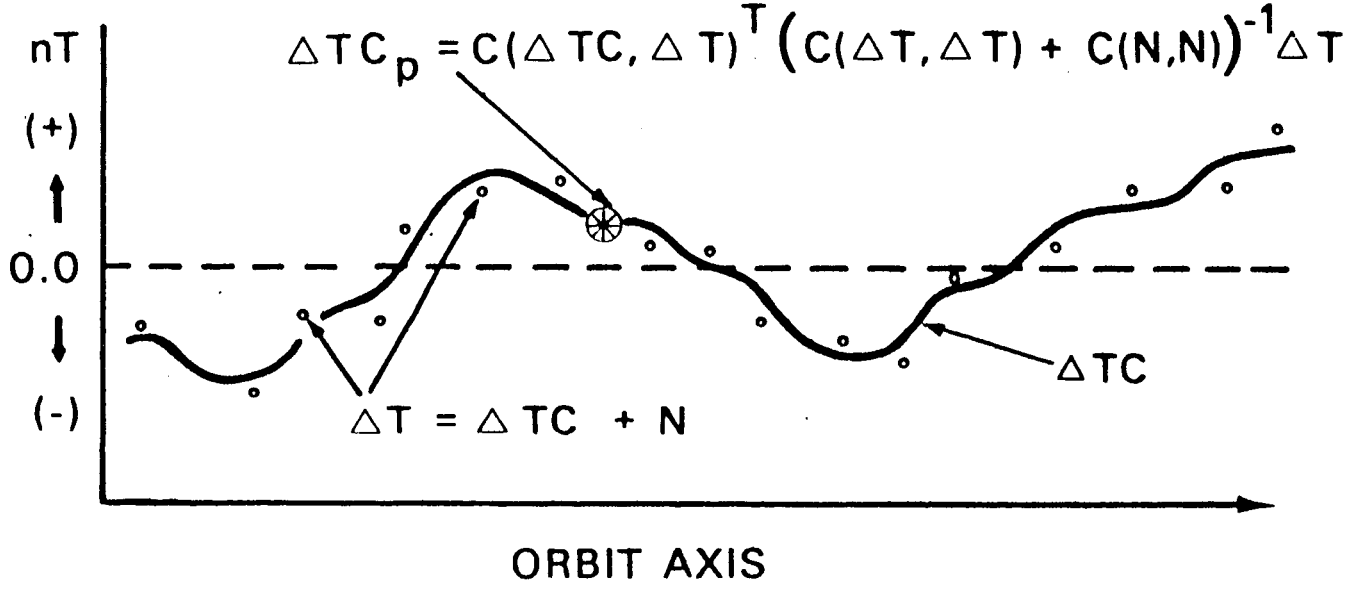

FIGURE 2

$C(\Delta TC, \Delta T)$ is the Cross-Covariance matrix between signal and observations.

$C(\Delta T, \Delta T)$ is the Covariance matrix of obserations.

C(N,N) is the Covariance matrix of observational noise which simplifies to (EV*I) if the noise is purely random with variance = EV.

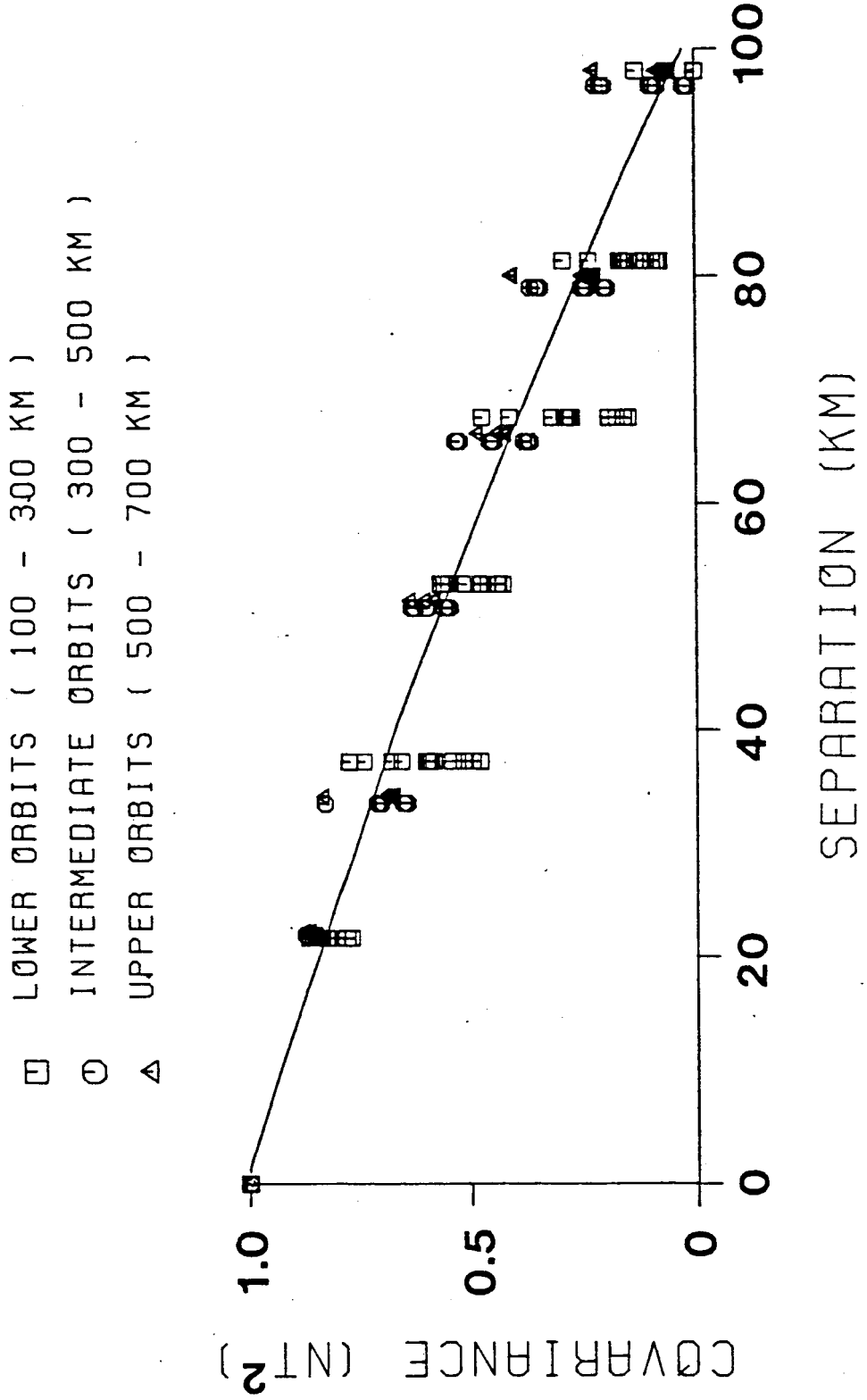
LOWER ORBITS (100 - 300 KM)
INTERMEDIATE ORBITS (300 - 500 KM)
UPPER ORBITS (500 - 700 KM)
COVARIANCE (NT²)
1.0
0.5
0
SEPARATION (KM)
0
20
40
60
80
100

FIGURE 3

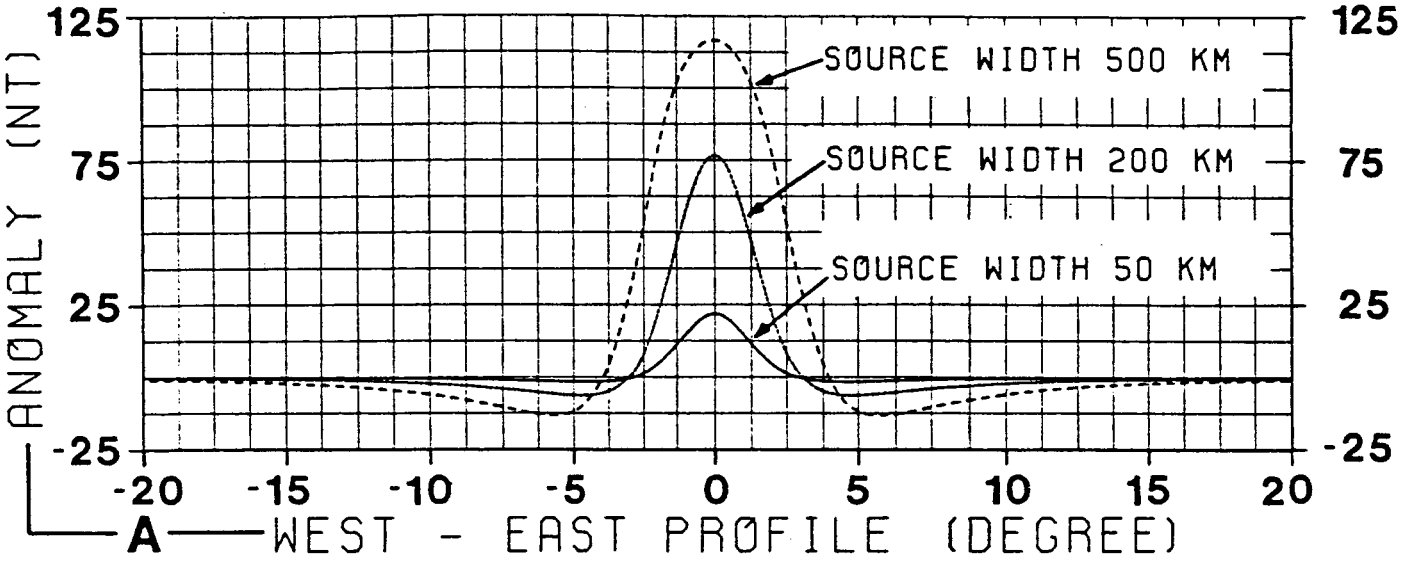
125
75
25
-25
ANOMALY (NT)
SOURCE WIDTH 500 KM
SOURCE WIDTH 200 KM
SOURCE WIDTH 50 KM
-20 -15 -10 -5 0 5 10 15 20
A—WEST - EAST PROFILE (DEGREE)

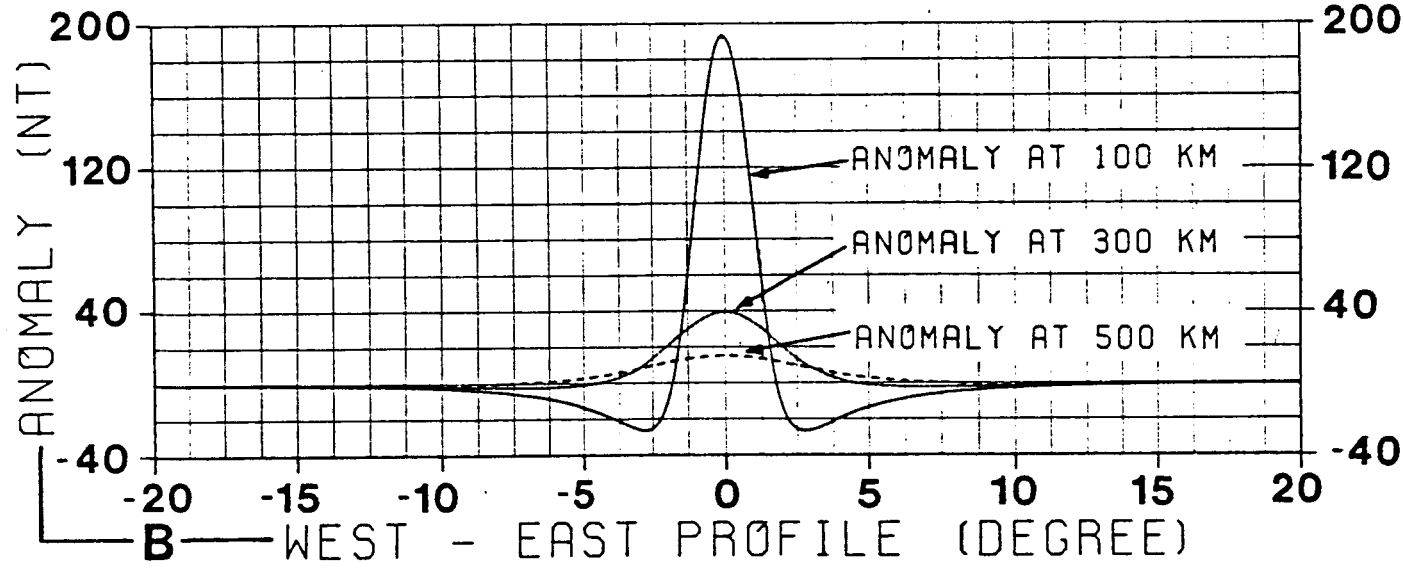
200
120
40
-40
ANOMALY (NT)
ANOMALY AT 100 KM
ANOMALY AT 300 KM
ANOMALY AT 500 KM
-20 -15 -10 -5 0 5 10 15 20
B—WEST - EAST PROFILE (DEGREE)

FIGURE 4

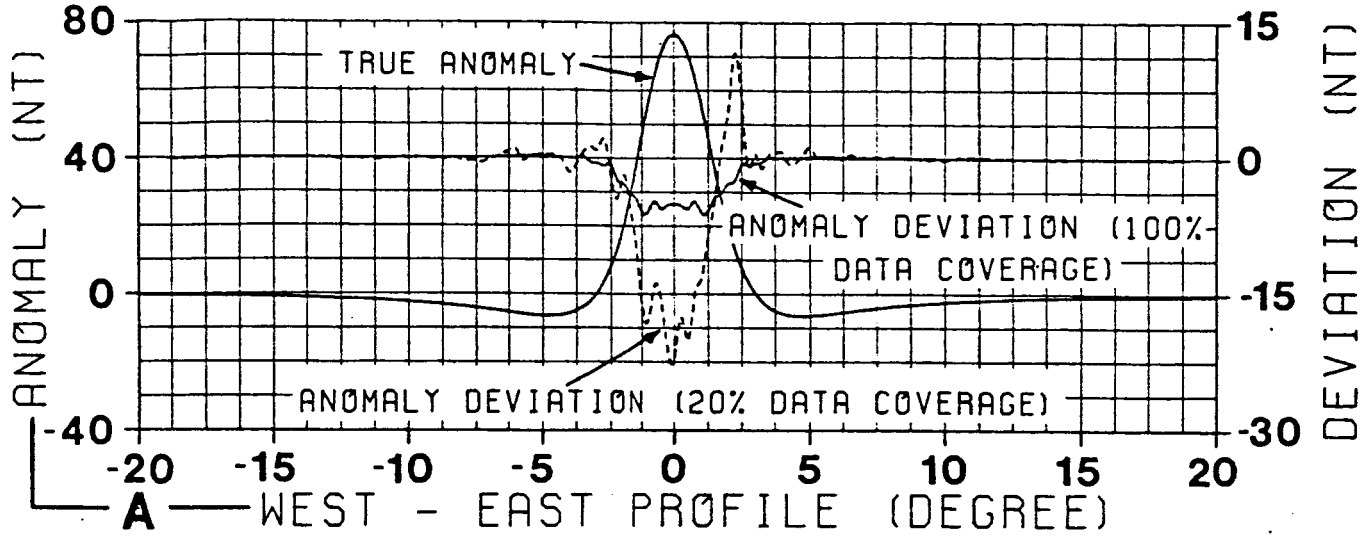
80
40
0
-40
ANOMALY (NT)
15
0
-15
-30
DEVIATION (NT)
TRUE ANOMALY
ANOMALY DEVIATION (100% DATA COVERAGE)
ANOMALY DEVIATION (20% DATA COVERAGE)
-20 -15 -10 -5 0 5 10 15 20
A — WEST - EAST PROFILE (DEGREE)

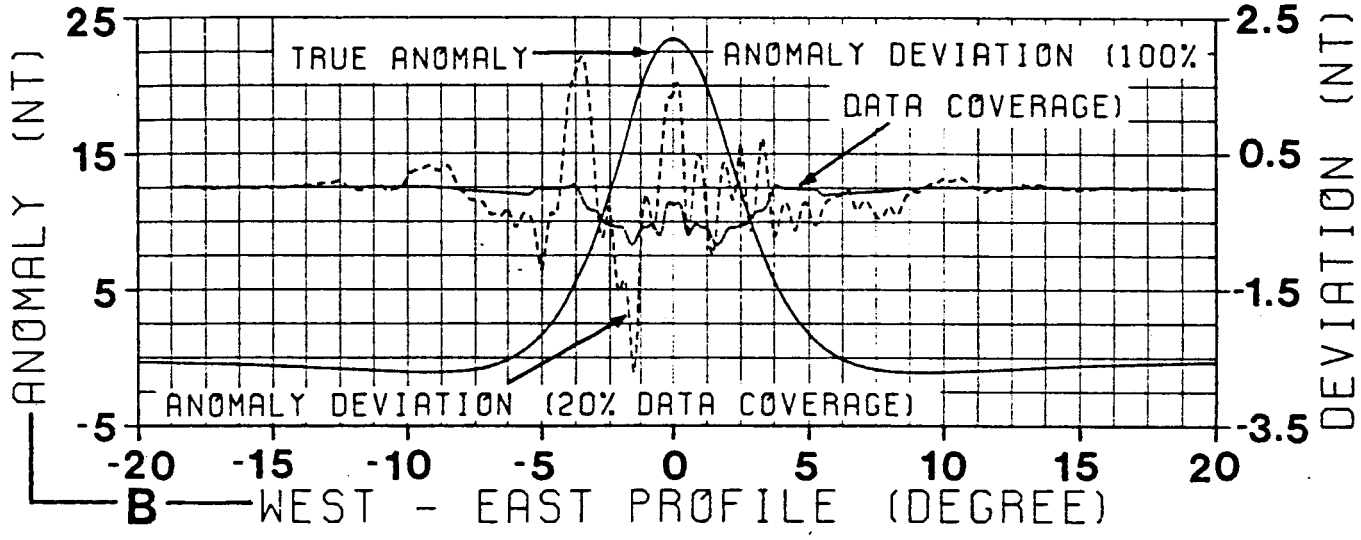
25
15
5
-5
ANOMALY (NT)
2.5
0.5
-1.5
-3.5
DEVIATION (NT)
TRUE ANOMALY
ANOMALY DEVIATION (100% DATA COVERAGE)
ANOMALY DEVIATION (20% DATA COVERAGE)
-20 -15 -10 -5 0 5 10 15 20
B — WEST - EAST PROFILE (DEGREE)

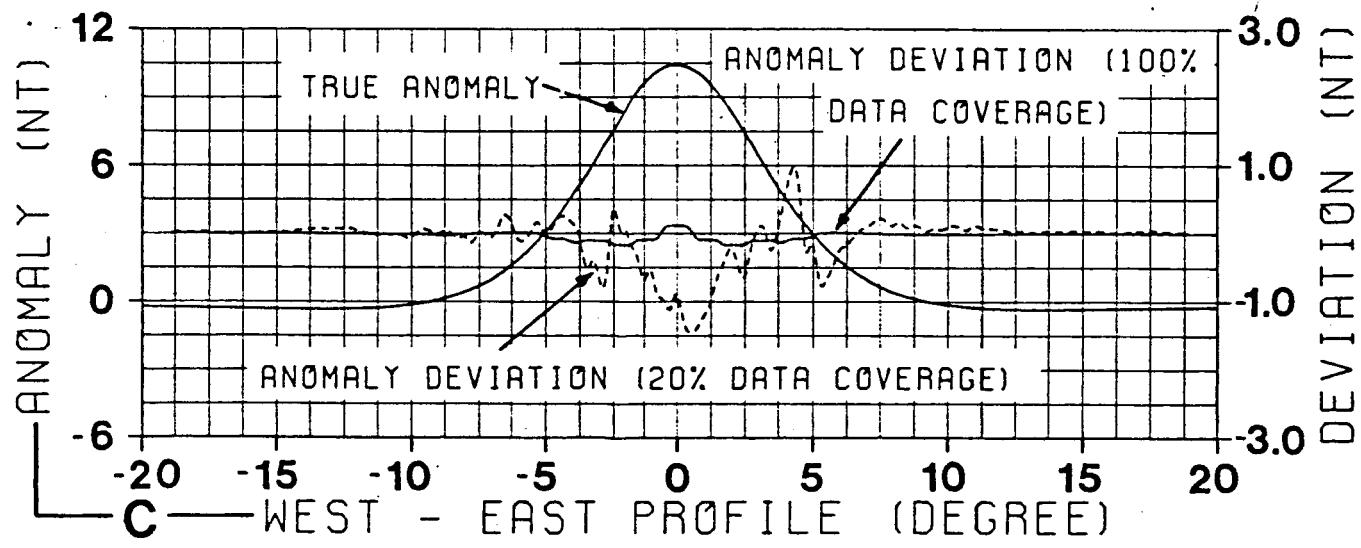
12
6
0
-6
ANOMALY (NT)
3.0
1.0
-1.0
-3.0
DEVIATION (NT)
TRUE ANOMALY
ANOMALY DEVIATION (100% DATA COVERAGE)
ANOMALY DEVIATION (20% DATA COVERAGE)
-20 -15 -10 -5 0 5 10 15 20
C — WEST - EAST PROFILE (DEGREE)

FIGURE 5

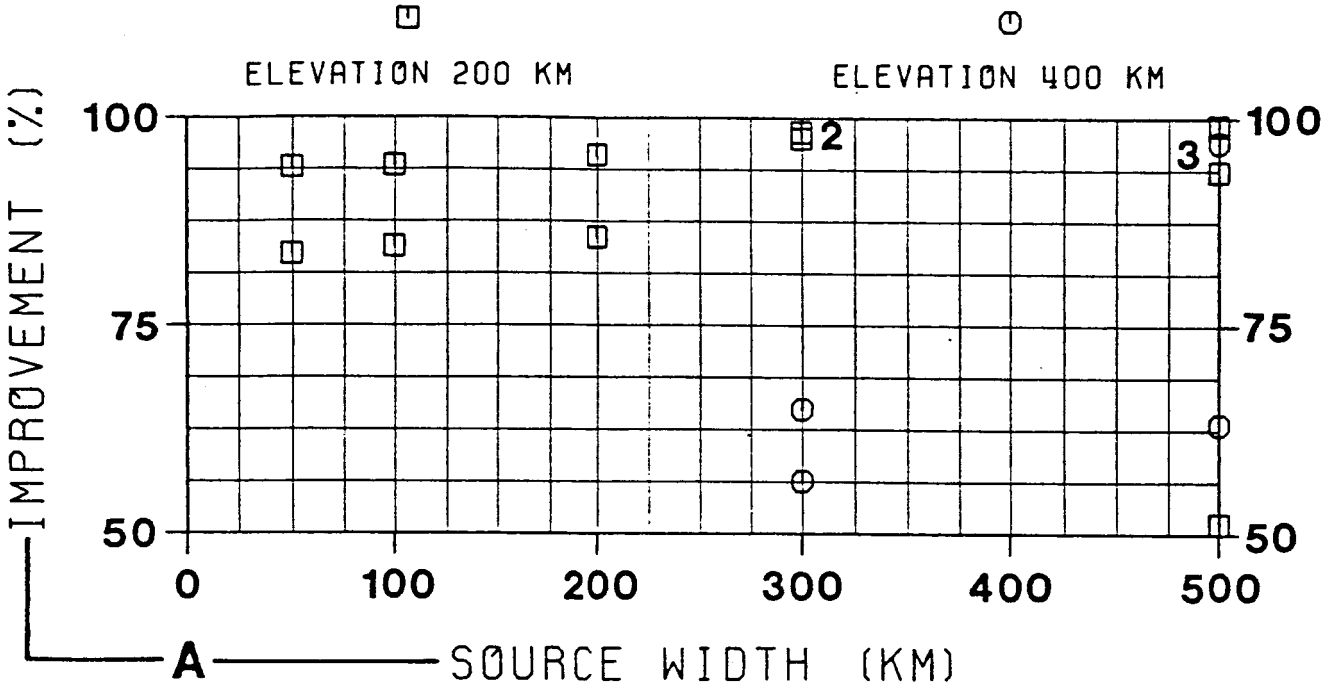
ELEVATION 200 KM
ELEVATION 400 KM
IMPROVEMENT (%)
100
75
50
0
100
200
300
400
500
2
3
A
SOURCE WIDTH (KM)

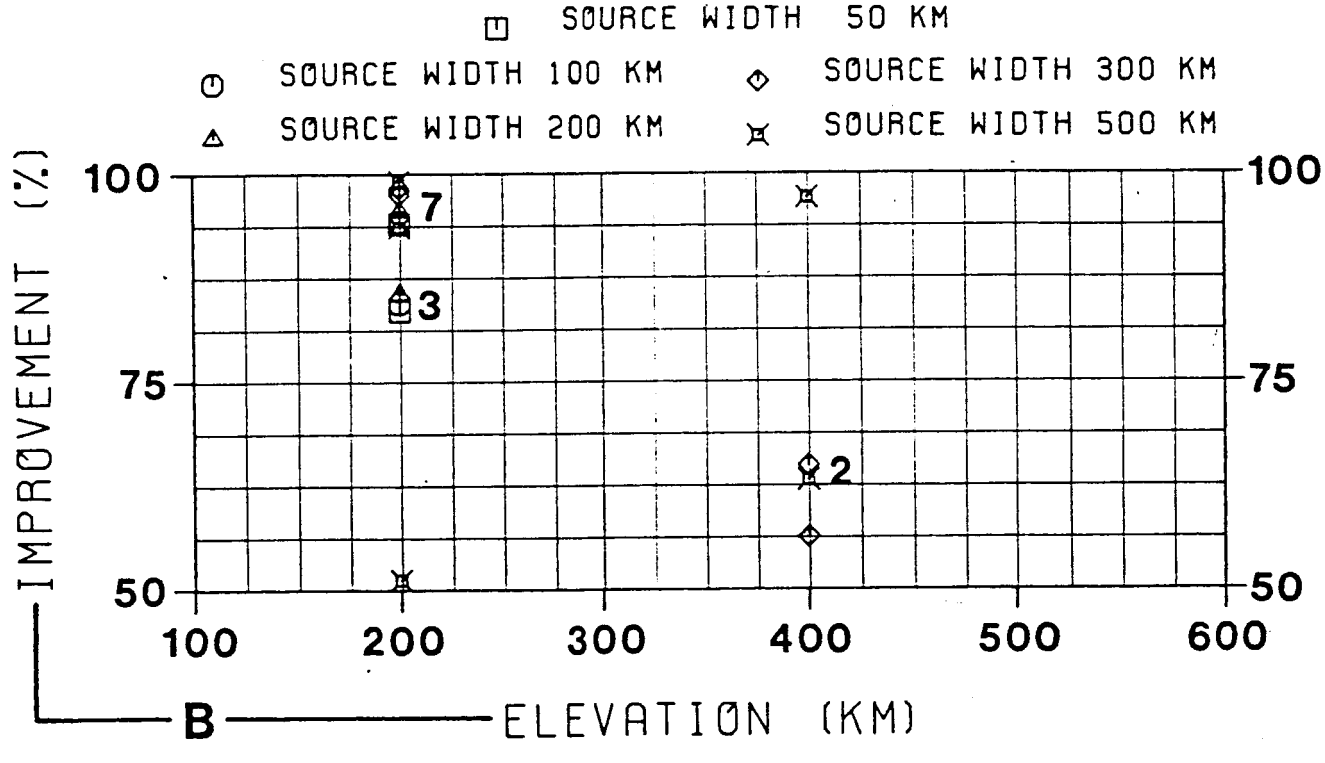
SOURCE WIDTH 50 KM
SOURCE WIDTH 100 KM
SOURCE WIDTH 200 KM
SOURCE WIDTH 300 KM
SOURCE WIDTH 500 KM
IMPROVEMENT (%)
100
75
50
100
200
300
400
500
600
7
3
2
B
ELEVATION (KM)

FIGURE 6

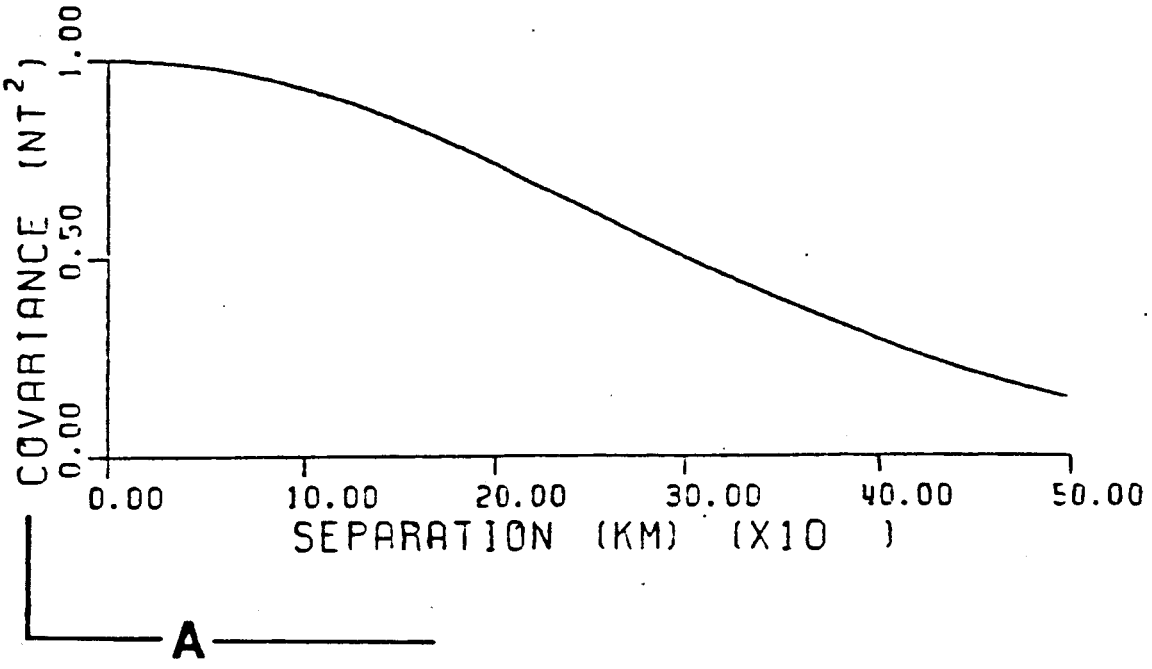
COVARIANCE (NT²)
1.00
0.50
0.00
0.00
10.00
20.00
30.00
40.00
50.00
SEPARATION (KM) (X10)
A

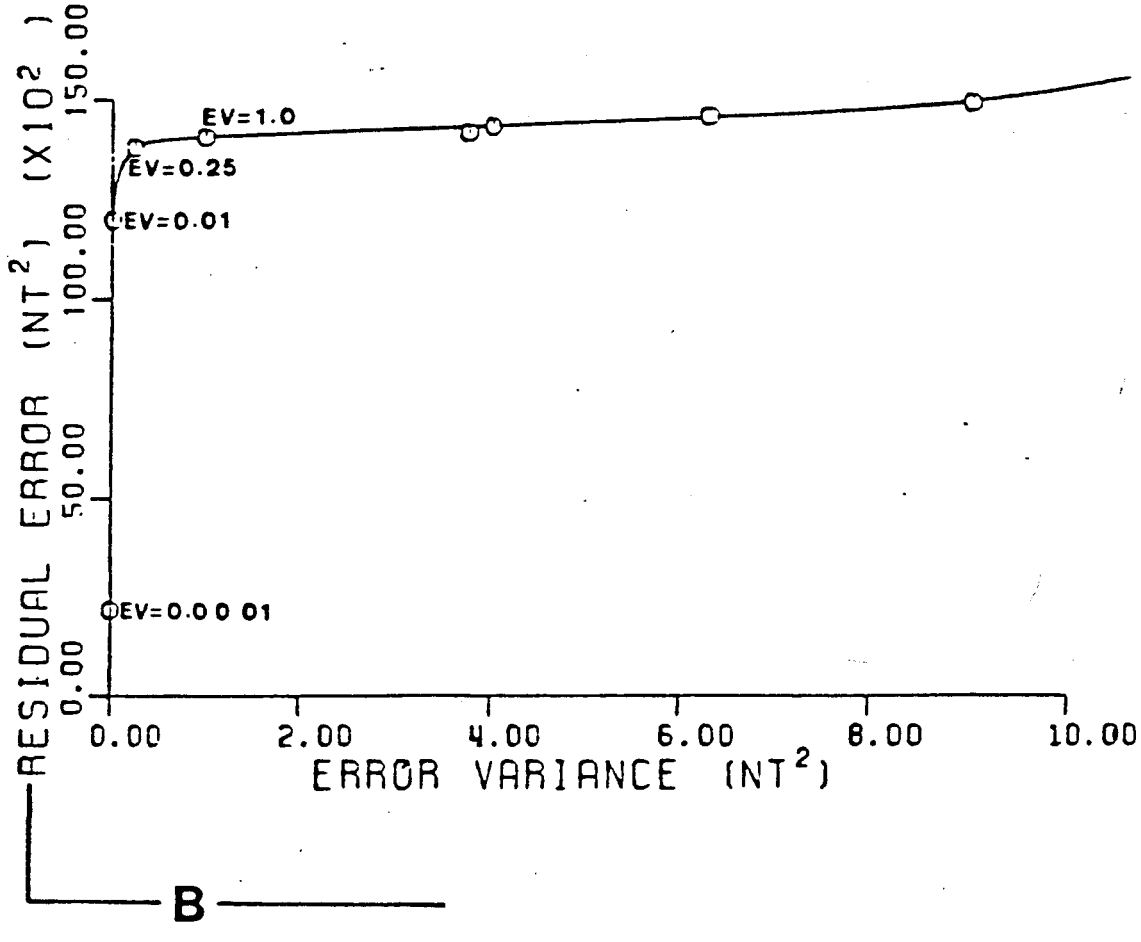
RESIDUAL ERROR (NT²) (X10²)
150.00
100.00
50.00
0.00
EV=1.0
EV=0.25
EV=0.01
EV=0.0 0 01
0.00
2.00
4.00
6.00
8.00
10.00
ERROR VARIANCE (NT²)
B

FIGURE 7

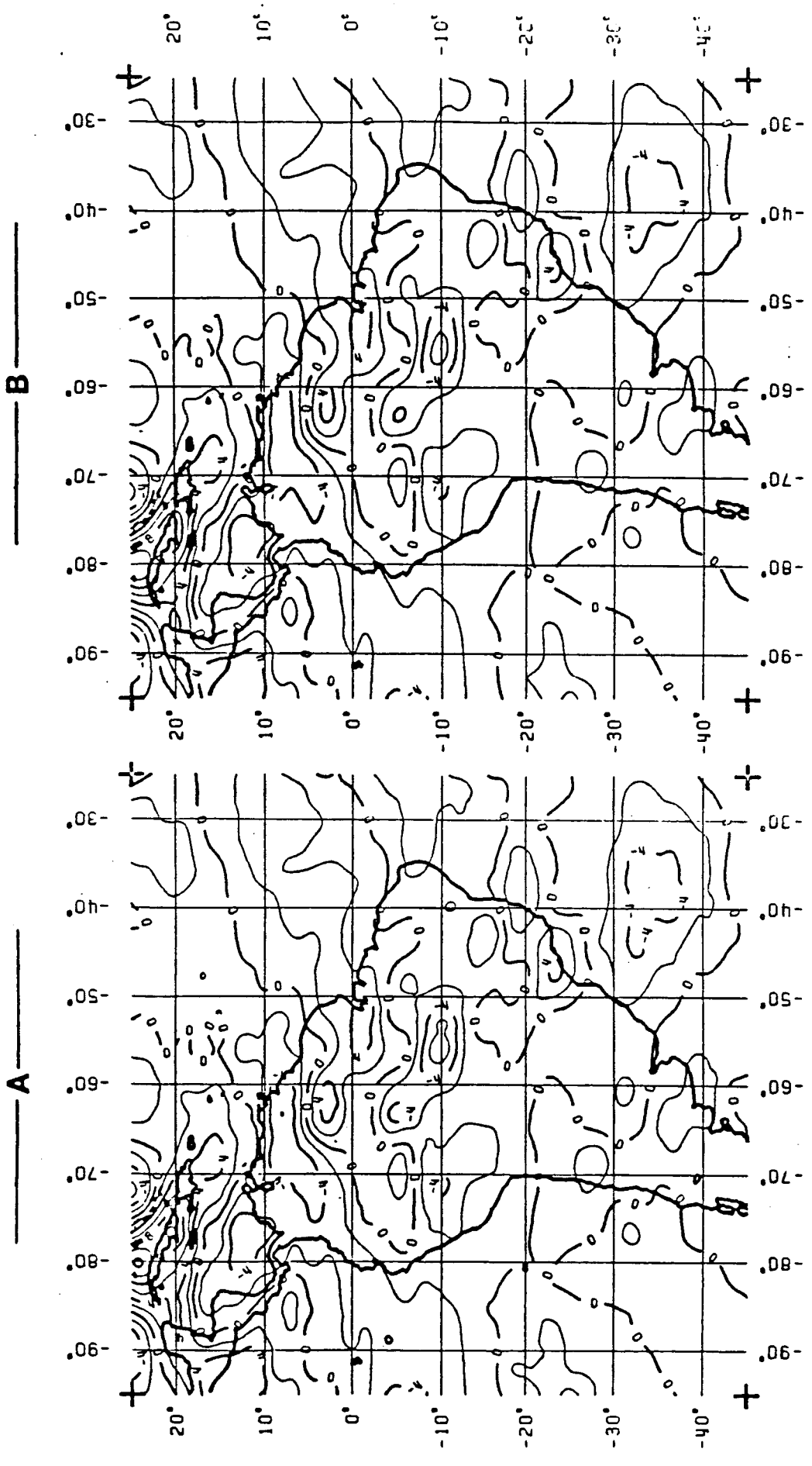

FIGURE 8

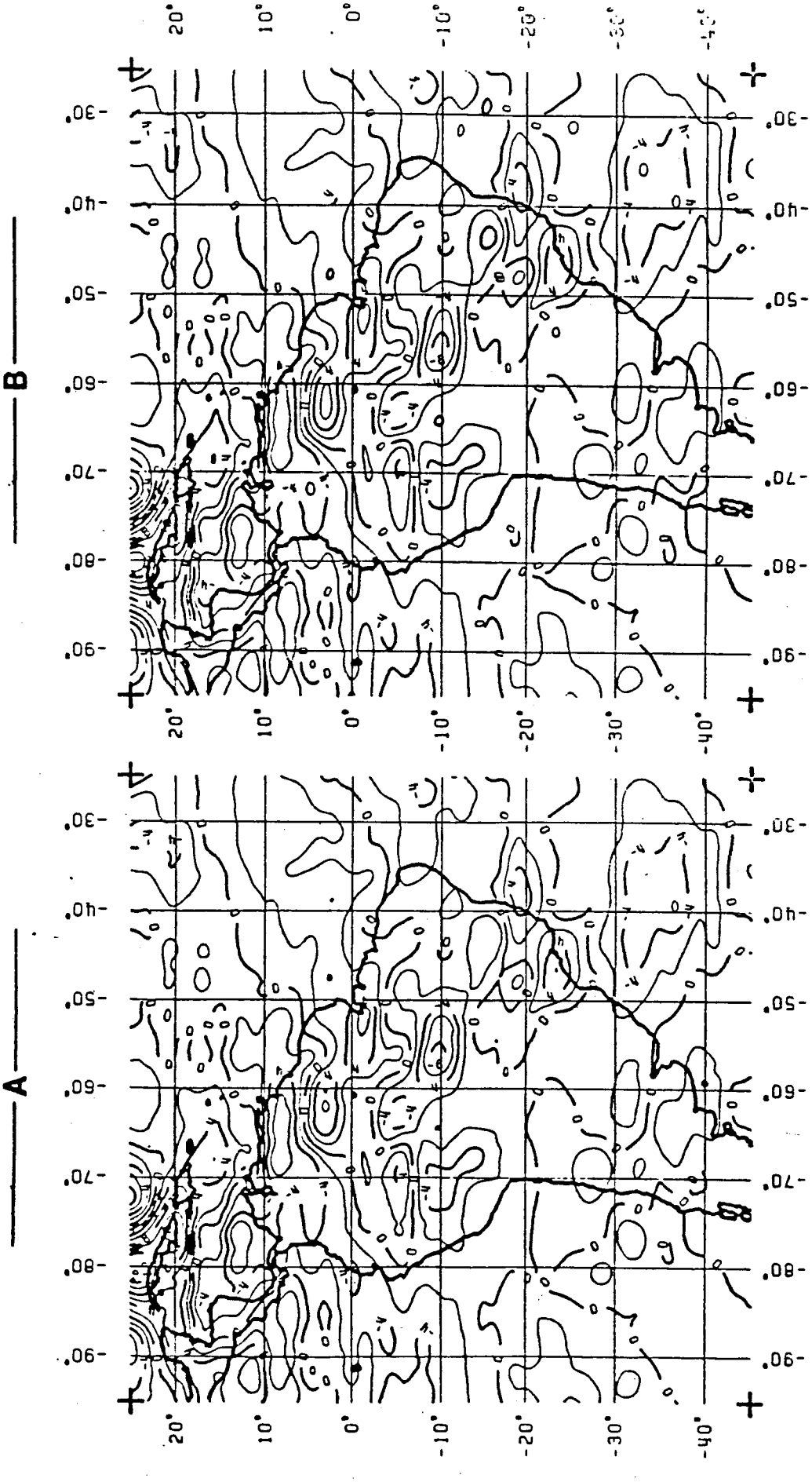

FIGURE 9

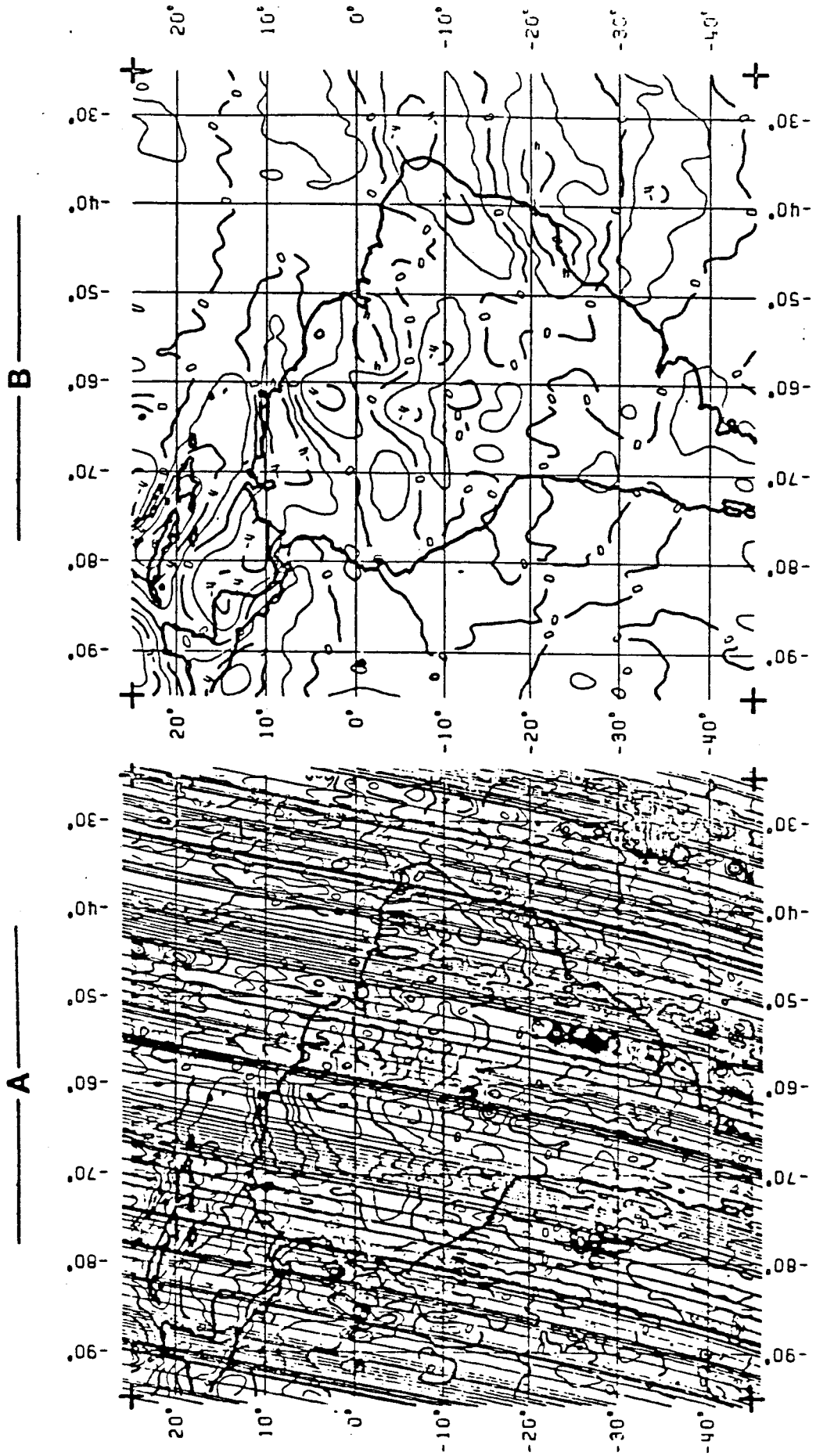

FIGURE 10

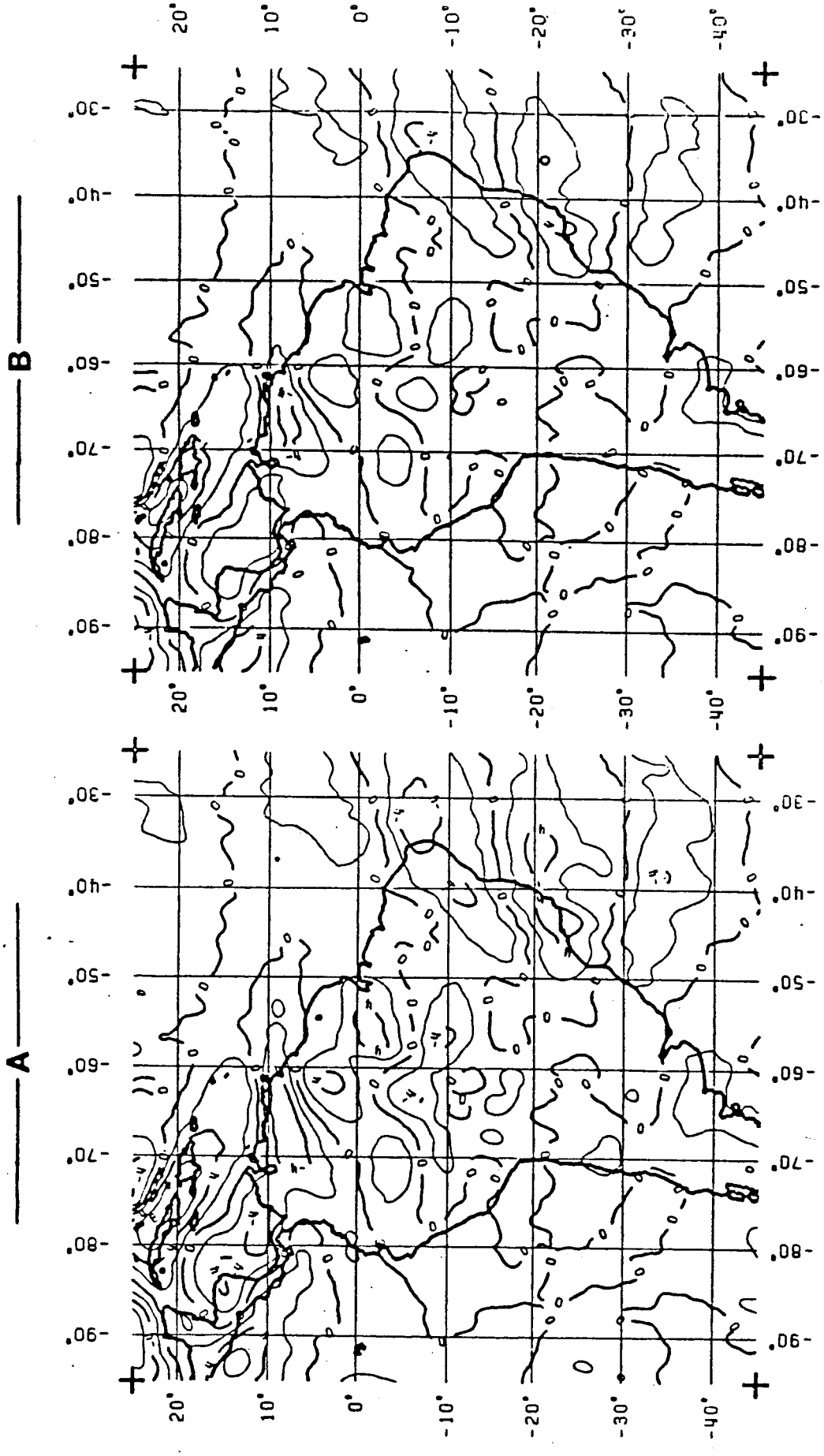

FIGURE 11

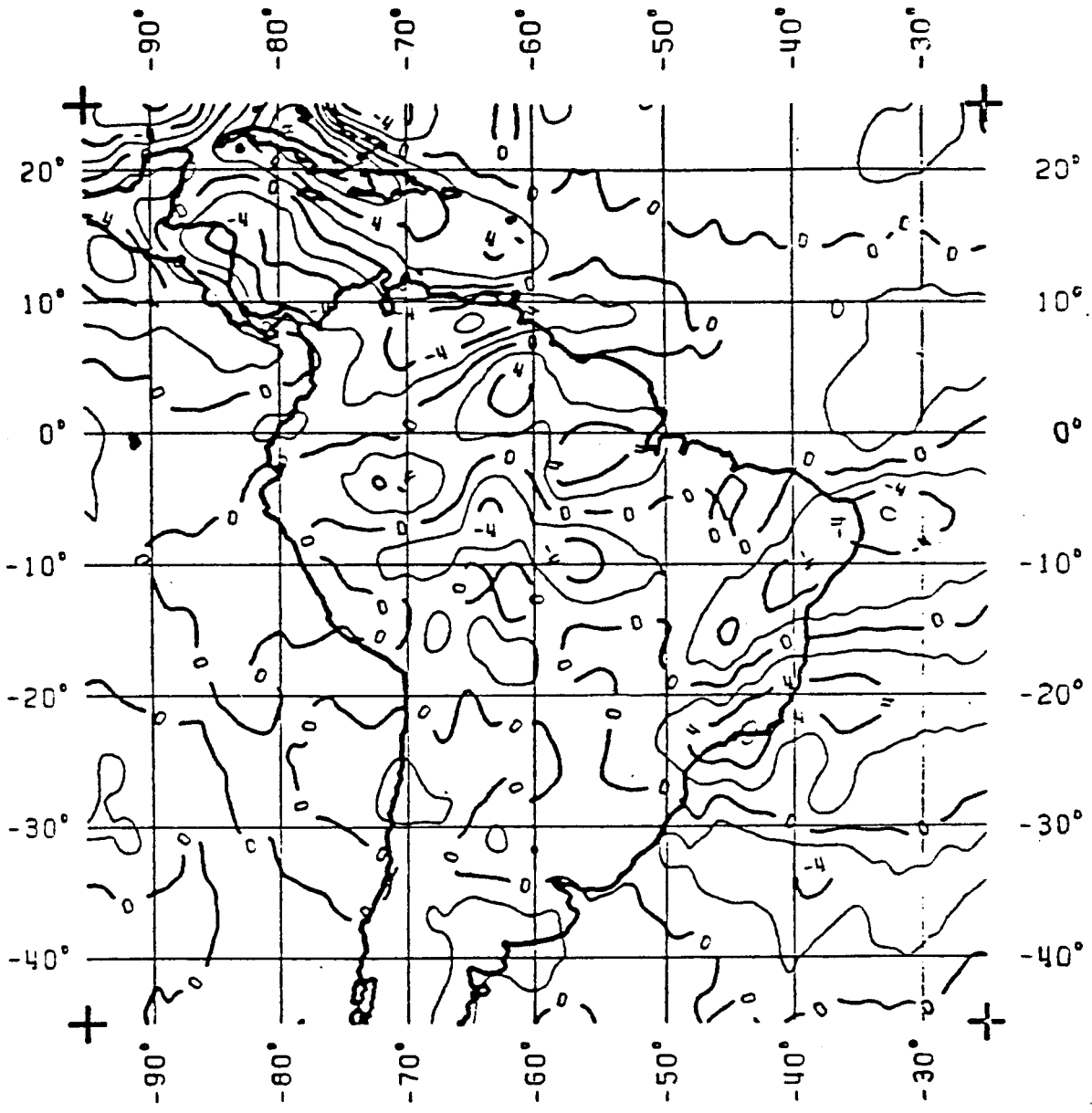

FIGURE 12

IMPROVED INVERSION OF GEOPOTENTIAL FIELD ANOMALIES FOR LITHOSPHERIC INVESTIGATIONS

by

R.R.B. von Frese[1], D.N. Ravat[2], W.J. Hinze[2], and C.A. McGue[1]

[1]Dept. of Geology & Mineralogy
The Ohio State University
Columbus, OH 43210

[2]Dept. of Geosciences
Purdue University
W. Lafayette, IN 47907

Abstract

Instabilities and the large scales of inversions which are common to geologic analyses of regional magnetic and gravity anomalies often complicate the use of efficient least-squares matrix procedures. Inversion stability profoundly affects anomaly analysis and hence it must be considered in any application. Wildly varying or unstable solutions are the products of errors in the anomaly observations and the integrated effects of observation spacing, source spacing, elevation differences between sources and observations, geographic coordinate attributes, geomagnetic field attitudes, and other factors which influence the singularity conditions of inversion. Solution instabilities caused by these singularity parameters can be efficiently minimized by the application of ridge regression. An effective damping factor large enough to stabilize the inversion, but small enough to produce an analytically useful solution can be chosen by comparing the curves where damping factors are plotted, respectively, against the residuals between observed and modeled anomalies and against the solution variance or the residuals between predicted anomaly maps which represent the processing objective (e.g., downward continuation, differential reduction to the radial pole, etc.).

To obtain accurate and efficient mega-scale inversions of anomaly data, a procedure based on the superposition principle of potential fields may be used. This method involves successive inversions of residuals between the observations and various stable model fields which can be readily accommodated by available computer memory. Integration of the model fields yields a well-resolved representation of the observed anomalies corresponding to an integrated model which normally could not be obtained by direct inversion due to excessive memory requirements.

MAGSAT magnetic anomaly inversions over India demonstrate the utility of these procedures for improving the geologic analysis of potential field anomalies.

Introduction

Current geopotential studies aimed either at characterization of the lithosphere or investigation of current geodynamical processes are noted for their broad, regional scope. Increasingly these studies are taking advantage of the data sets obtained from regional surveys, the compositing of areally-restricted data sets, and the global data sets derived from satellite-elevation surveys. A continuation of this trend is anticipated because of the international appreciation for the importance of studying geologic processes and their effects through the geologic history of the earth over the entire globe and because of the increasing availability of improved-quality data over large regions of the earth. Of particular importance in this regard are data, both magnetic and gravity, which are obtained from satellites. These data are especially advantageous because they provide broad coverage with consistent survey specifications and have minimum disturbance from

near-surface geologic noise. These are characteristics which are seldom achieved in surface regional or composited data sets. The satellite measurements do suffer from a deterioration in the geologic resolution of the data because of the height of the observations above the sources, but this problem is minimized by focusing in the interpretation upon broad-scale geologic processes and their regional effects.

An efficient technique for processing satellite elevation data is equivalent source inversion which was initially used for geologic applications in Cartesian coordinates by Dampney (1969) and Emilia (1973). The procedure was adapted to spherical coordinates by Mayhew (1979) for reducing orbital tracks of satellite magnetic observations with arbitrary spatial coordinates to a grid of anomaly values at constant elevation and for obtaining crustal magnetization models from the satellite data. von Frese et al. (1981a) generalized the method for lithospheric analysis of both magnetic and gravity anomalies and extended the capabilities of the procedure to include the spherical earth computation of geoidal anomalies, pseudo-anomalies, vector anomaly components, spatial derivatives, continuations, and differential magnetic pole reductions.

For the least-squares inversion of geopotential field anomalies, von Frese et al. (1981a) recommended the use of efficient linear equation solvers based on classical matrix manipulations over the eigenvalue-eigenvector decomposition procedure which requires substantially greater CPU time and memory commitments to implement. However, their study did not consider problems concerning the numerical stability of inversions which can greatly complicate applications of the efficient matrix procedures for anomaly analysis. More recently, Langel et al. (1984) investigated these problems as they relate to

equivalent source inversion of satellite data for producing and analyzing global magnetic anomaly maps. To overcome inversion stabilities, they proposed a method based on eigenvalue-eigenvector decomposition of the problem which increases substantially the computational logistics of these applications.

A further factor profoundly influencing the efficiency and effectiveness of inversion analyses includes computer limitations which determine the number of unknowns or the scale of inversion. The scale of anomaly inversion for many geologic applications is so large that it can only be accomplished by piecing together a series of adjoining or overlapping smaller scale inversions (e.g., Langel et al., 1984; Ridgway and Hinze, 1986). A particularly bothersome and time-consuming aspect of these efforts is the requirement of adjusting the smaller-scale solutions for edge effects in compositing an accurate large-scale solution.

In general, instabilities and the large-scales of inversion which are common to geological applications of regional gravity and magnetic anomalies complicate the use of efficient least-squares matrix procedures. Accordingly, this study investigates the role which these factors play in anomaly inversion and procedures are suggested for using least-squares matrix methods to obtain stable, large-scale inversions of geopotential anomaly field data.

Inversion Practice and Stability

A useful and efficient approach to lithospheric analysis of regional geopotential field anomalies is to determine the physical properties of an array of point equivalent sources by least-squares matrix inversion of the observations which will closely duplicate the observed field. Linear

transformations of the equivalent source field then can be used to isolate or enhance geologically meaningful attributes of the observational data.

von Frese et al. (1981a) have shown that the inversion problem for both magnetic and gravity anomalies can be generalized in matrix notation by

$$(Q)*(\Delta X) = (OBS), \tag{1}$$

where (Q) is a (n-row by p-column) matrix with coefficients that are completely determined from the known geometric coordinates of the observation and source points, (ΔX) is a (p by 1) column matrix containing the solution of physical property values, and (OBS) is a (n by 1) column matrix of the anomaly observations. For geological applications, the number of unknowns is generally less than the number of observations (i.e., $p < n$) and the system of linear equations given in (1) is related to an incomplete set of anomaly data which contain inaccuracies in measuring the anomaly values and their spatial coordinates and other errors. Accordingly, a least-squares solution of equation (1) is normally considered as given by

$$(\Delta X) = \left((Q^T Q)^{-1}\right)*(Q^T)*(OBS) \tag{2}$$

which minimizes the Eucleadian vector norm of the residual, $|OBS - Q*\Delta X|^2$.

Efficient procedures for obtaining the least-squares solution in (2) avoid the necessity of computing the inverse of $(Q^T Q)$ directly, using instead rapid Gaussian elimination techniques to process the system of normal equations given by

$$(Q^T Q)*(\Delta X) = (Q^T)*(OBS). \tag{3}$$

In theory, (Q^TQ) is a symmetric, positive definite, real matrix, and hence there is an upper triangular matrix (R) so that $(Q^TQ) = (R^TR)$ (Lawson and Hanson, 1974). Replacing the matrix (Q^TQ) by its Choleski factorization (R^TR) permits especially rapid and efficient processing of the system in (3) for the least-squares solution (ΔX).

In general, the Choleski decomposition procedure is the fastest method for obtaining the solution of equation (2) (Bhattacharyya, 1980). It is also a method which has minimal storage requirements in computing. By taking advantage of the symmetry of the product matrix (Q^TQ), maximum storage requirements for producing the solution of equation (2) consist of a singly-dimensioned array of length $\left(p(p+1)/2\right)$ into which is sequentially packed the columns of either the upper or lower triangle of the product matrix. Software is readily streamlined to compute directly these $\left(p(p+1)/2\right)$-coefficients of (Q^TQ) and the (p)-coefficients of the column vector $\left((Q^T)*(OBS)\right)$. Subsequent efforts to determine the Choleski factorization of (Q^TQ) and to evaluate (3) for the least-squares solution (ΔX) require only about 10% of the time it takes to compute these coefficients.

An important provision for obtaining a least-squares solution with these procedures is that (Q^TQ) be non-singular. Singularity of the linear system occurs if a row (or column) contains only zeroes or if two or more rows (or columns) can be related by a linear transformation. A more common condition in geologic practice is for the system to be near-singular so that in the computer's working precision, the elements of a row (or column) are nearly zero or two or more of the rows (or columns) are nearly linear multiples of each other. Near-singularity of the linear system is characterized by a solution with large and erratic values, and hence large variance. In this

instance, the solution is said to be unstable and its linear transformations may be geologically meaningless, even though the solution may model the anomaly observations with great accuracy.

The variance of the least-squares solution to equation (2) is related to the variance in the anomaly observations by the well-known result (e.g., Draper and Smith, 1966)

$$\text{var}(\Delta X) = \left((Q^T Q)^{-1}\right)\text{var}(OBS). \qquad (4)$$

When the problem is ill-conditioned or near-singular, several of the eigenvalues of $(Q^T Q)$ can be very much smaller than one (Hoerl and Kennard, 1970a; 1970b). The effect of these eigenvalues on equation (4) may be seen by considering the singular value decomposition of the design matrix given by $(Q) = (UDV^T)$ (Lanczos, 1961). Here, (V) is a (p by p) matrix whose columns are the eigenvectors of $(Q^T Q)$ and (D) is a square, diagonal matrix containing the (p)-eigenvalues of (Q) which are the square roots of the eigenvalues of $(Q^T Q)$. Also, (U) is a (n by p) matrix whose columns are the eigenvectors of (QQ^T) that correspond to the (p)-eigenvalues of (Q). However, $(U) = (QVD^{-1})$ so that it is not necessary to evaluate (QQ^T) directly for its eigenvalues and eigenvectors. It is easy to show that $\left((Q^T Q)^{-1}\right) = (VD^{-2}V^T)$ because (U) and (V) are orthogonal matrices and hence their inverses are equal to their respective transpositions. By inserting this result into equation (4), the presence of very small eigenvalues corresponding to near-singularities of the system can be seen to cause the elements of (D^{-2}) to blow up and dominate the stability of the solution. Uncertainties in the anomaly amplitudes (OBS) do not influence the singularity conditions of the system, but rather they

combine with these conditions via equation (4) to produce uncertainties in the least-squares solution (ΔX).

In theory, the linear system can be made singular only if source and observation points are specified at the same locations. In practice, however, singularity or near-singularity may be introduced by many factors including errors in specifying the variables used to compute the coefficients in (Q), or improper scaling of these computations where the significant figures of the variables are only partially accounted for within the computer's working precision. With respect to satellite magnetic data inversion, previous studies have characterized solution stability in terms of source function parameters such as the dipole spacing (Mayhew, 1982) and low inclination of the geomagnetic field (Langel et al., 1984). In general, however, a myriad of singularity parameters related to the inverse distance function between sources and anomaly observations may combine to influence the stability of the inversion solution in lithospheric applications.

These effects can be conveniently studied using the concept of the condition number of the product matrix (Q^TQ) which is given by the ratio of the largest eigenvalue to the smallest nonzero eigenvalue of (Q^TQ). If the condition number is one, then the linear system is said to be orthogonal in the sense that each coefficient of the solution displays a minimum of linear dependency or correlation, and uncertainties in its solution are in constant proportion to uncertainties in the observations. As the condition number increases, however, the linear system becomes more singular or linearly dependent and its solution less stable. An estimate of the condition number can be efficiently evaluated from the Choleski factorization of (Q^TQ) which avoids the necessity of directly computing the eigenvalues of the system (Lawson and Hanson, 1974).

In particular, the reciprocal condition number may be determined from this Choleski factorization (Cline et al., 1979; Dongarra et al., 1979) as a measure of the sensitivity of the solution (ΔX) to errors in the product matrix (Q^TQ) and the weighted observation vector $((Q^T)*(OBS))$. The elements of (ΔX) can usually be expected to have (K) fewer significant figures of accuracy than the elements of (Q^TQ) if the reciprocal condition number is approximately equal to (10^{-K}). Consequently, (ΔX) may have no significant figures if the reciprocal condition number is so small that in floating point arithmetic it is negligible when compared to one.

The use of the reciprocal condition number for treating mathematical solutions for the system in equation (1) may be demonstrated by considering inversions of the magnetic anomaly data presented in Figure 1-A. The remaining panels of Figure 1 show the effects on inversion stability of varying several of the inversion parameters individually in terms of (K) which estimates the relative loss of significant figures in the solution (ΔX) while holding the remaining parameters fixed. For comparison, our inversion experiences with satellite elevation magnetic and gravity anomalies have shown that when our software produces reciprocal condition numbers such that ($K \gtrsim 8$), the corresponding solutions are typically so unstable as to prove useless for lithospheric applications.

The basic data set contoured in Figure 1-A consists of an arbitrary 10*10 array of magnetic anomaly values. The inversion experiments performed on these data obtained magnetic susceptibility solutions for a 10*10 array of equivalent point dipole sources according to procedures described by von Frese et al. (1981a). Figure 1-B shows how the inversion tends to destabilize, thus causing K to expand, as the elevation difference between source

and observation grids is increased. These results were obtained for a nodal spacing of 1° for both source and observation grids. A normally inclined geomagnetic field was also assumed over the observation and source grids with a polarizing field intensity of 60,000 nT.

Figure 1-C demonstrates how the attributes of the coordinate space involved in the inversion of these anomaly data affect solution stability. These results were obtained by moving the observation and source grids along constant longitude in the northern hemisphere and performing the inversions at different latitudes. The other inversion parameters were the same as used in Figure 1-B, except that the elevation difference between the source and observation grids was kept at 125 km. The results suggest a strong dependence of the inversion on the coordinate parameterization, particularly at high latitudes where observation and source spacing which is constant in degrees of a spherical earth becomes increasingly smaller in the linear dimension of kilometers.

Figure 1-D demonstrates the capacity for variations in inclination and declination of the core magnetic field to influence inversion stability. These experiments were performed by moving the observation and source grids along 10° swaths north (curve A) and south (curve B) from 0° latitude. Inversions were obtained assuming that the 10°*10° set of observations at the earth's surface and the 10°*10° source grid at 125 km in the subsurface were operated upon by the IGS'75 geomagnetic field model (Barraclough et al., 1975) updated to (1976.8). By contrast, results are also included (curve C) where the updated IGS'75 field model was replaced by a radial field with polarizing intensity of 60,000 nT to show the significant advantage to

inversion that is obtained when dealing with normal component data such as radially polarized magnetic anomalies or gravity anomalies.

Figure 1-E shows the stability effects on inversions of these data where the grid spacing of the observations has been varied at a fixed source spacing of 1° (curve A) and where the source grid spacing was varied for a constant observation grid spacing of 1° (curve B). These inversions were obtained for an elevation difference of 400 km between source and observation grids which were subjected to a radial field with a polarization strength of 60,000 nT. For any particular data set, results such as presented in Figures 1-B and 1-E can be obtained to initiate a sensible inversion strategy, although it is clear that the inversion may be influenced more strongly by other parameters over which the investigator has little control, such as the examples in Figures 1-C and 1-D. In general, inversion stability is likely to be a complicated function of the integrated effects of many parameters for any application. In the effort to engineer a useful solution, the investigator may be able to modify readily some of the parameters, but for others it may prove very difficult if not impossible to reparameterize the inversion problem effectively.

The need for detailed reparameterization of an inversion can be mitigated somewhat in practice by the use of the general linear inverse (Jackson, 1972; Wiggins, 1972) to obtain a least-squares solution which principally reflects the less singular portion of the linear system established by a chosen parameterization. The procedure involves computing eigenvalues and associated eigenvectors of the linear system from (Q^TQ) and forming the Lanczos or natural inverse (Lanczos, 1961) given by $(VD^{-1}U^T) = (((Q^TQ)^{-1})*(Q^T))$ to evaluate equation (2). The variance or stability of the

solution (4) is inversely related to the eigenvalues, so that solution variance can be made unacceptably large by the presence of very small, non-zero eigenvalues which characterize near-singularities in the system. To manage the variance of the least-squares solution, the procedure is simply to generalize the Lanczos inverse by considering an eigenvalue to be zero if it is less than some appropriate threshold value. Fuller details of the procedure and its use for designing inverses for ill-posed linear systems are given in Jackson (1972) and Wiggins (1972).

Langel et al. (1984) describe an elegant adaptation of the generalized inverse for the stability analysis of MAGSAT anomalies. However, the inversion of regional geopotential field anomalies for lithospheric applications commonly involves more than a thousand unknowns, so that the numerical determination of the eigensystem components of the problem often is not feasible due to the large matrices which must be processed. Also, criteria are required to discriminate between the larger, relevant eigenvalues of the problem and the smaller, unimportant ones which must be discarded. For many types of problems, the appropriate division of eigenvalues is suggested by a break or sharp change in gradient of the eigenvalue spectrum. However, as shown by the example considered in Langel et al. (1984), lithospheric inversions of geopotential field anomalies can yield eigenvalue spectra which provide relatively little explicit insight for choosing appropriate threshold limits.

An alternative least-squares procedure for obtaining a stable solution is to retain the smaller, problematic eigenvalues, but weighted now by the addition of a small, positive constant (EV) to dampen their effects on the

linear system. This approach is equivalent to solving the linear system in equation (1) for the damped least-squares solution given by

$$(\Delta X') = \left((Q^T Q + (EV)*I)^{-1}\right)*(Q^T)*(OBS), \qquad (5)$$

where (I) is the identity matrix and the constant (EV) is called by various names including damping factor, Marquardt parameter, and error variance. For ill-conditioned systems, an appropriate choice of the damping constant (EV) will reduce solution variance and hence substantially improve the mean square error of least-squares estimation and prediction.

The use of a weighting factor (EV) for solving non-linear least-squares problems was discussed by Levenberg (1944) and a well-known algorithm for implementing the method was developed by Marquardt (1963). Consideration of the damped solution in equation (5) shows that it is the same as the solution of equation (2), except that the diagonal elements of the product matrix $(Q^T Q)$ have been modified by the addition of the constant (EV). The study of these types of problems as a function of (EV) also has been called ridge regression (Hoerl and Kennard, 1970a; 1970b). In a statistical context, the symmetric positive definite matrix $\left((Q^T Q)^{-1}\right)$ is also known as the unscaled covariance matrix (e.g., Lawson and Hanson, 1974) and the solution in equation (5) is related to the matrix (Q) whose elements have been perturbed by purely random noise drawn from a distribution with variance (EV) and zero mean. Further details concerning ridge regression and its mean square error properties are given by Hoerl and Kennard (1970a; 1970b) and Marquardt (1970).

The great practical advantage of the solution in equation (5) to equivalent source inversion of geopotential anomaly field data is that the fast and elegant Choleski factorization procedure can now be implemented to minimize the destabilizing effects of ill-posed parameters of the inversion. For any particular parameterization of a problem, the $(p(p+1)/2)$-coefficients of (Q^TQ) and the (p)-coefficients of $((Q^T)*(OBS))$ need to be computed only once and stored. The problem then reduces to finding a value for the damping factor (EV) which is just large enough to stabilize the solution, yet small enough that the predictive properties of the solution are maximized.

For geopotential anomaly inversion, a fairly straightforward procedure for estimating the optimal value of the damping factor is to investigate the EV-spectrum as a function of the variance of the solution or a parameter which reflects some desirable property of a prediction of the solution (e.g., the sum of squared residuals between model and observations, the variance of downward continued or radially polarized models, etc.). Experience indicates that EV-spectra for ill-conditioned inversions are typically characterized by second or higher order curves which are sufficiently diagnostic of the over- and under-damped attributes of the solution that a reasonable value of (EV) may be chosen for optimizing the trade-off between the predictive properties of the solution and stability. An example can help to clarify the use of (EV) and its spectra for obtaining geologically useful solutions of regional magnetic and gravity anomaly inversions.

In their study of the potential for using regional magnetic anomalies to constrain continental breakup, von Frese et al. (1986) used equivalent point source inversion to adjust averaged MAGSAT anomalies of the continents to a common elevation and to differentially reduce the magnetic anomaly data to

the radial pole. During the course of the study it was determined that the continents definitely do not all invert equally with respect to the MAGSAT data. The nature of the problem can be demonstrated by considering the <2°> MAGSAT anomalies produced by Langel et al. (1982) for the region of the Indian subcontinent shown in Figure 2. The MAGSAT observations in Figure 2-A consist of a 16*16 array of values distributed over a spherical grid with 2° nodal spacing at an average elevation of 400 km above the earth's surface. To reduce the observations differentially to the pole, the data were inverted for the susceptibilities of a 16*16 array of equivalent point dipoles also spaced at 2° intervals, but located 100 km below the earth's surface. The IGS'75 geomagnetic field model updated to (1980) was assumed to be operating over the source and observation grids for this inversion.

The inversion using the solution of equation (2) produced a reciprocal condition number which indicated a poorly constrained solution with few significant figures (i.e., K ≈ 10). However, as shown by Figure 2-B, the solution still permitted the equivalent point dipole array to model the observed total field anomalies of Figure 2-A with considerable accuracy, despite its great variance. When the equivalent dipole model is used to estimate the radially polarized anomalies assuming a 60,000 nT polarization intensity, however, the instabilities of the solution become clearly manifest as the wildly varying, large amplitude anomaly features shown in Figure 2-C. The magnetic equator of the IGS'75 field updated to (1980) lies along the southern boundary of the study area, and hence the results suggest an ill-conditioning of the inversion here which may well be related to the low inclination effects of the core field model.

The use of the damped solution in (5) for effectively reducing the MAGSAT observations differentially to the pole is demonstrated with the aid of the lithospheric model shown in Figure 2-D. The model consists of a series of spherical prisms, all 30 km thick and with their tops located 10 km below the earth's surface. The lateral boundaries of the spherical prism sources are given in Figure 2-D which are keyed to the magnetic susceptibility properties listed in Table I. The total magnetic field anomalies at 400 km elevation due to these lithospheric prisms are shown in Figure 2-E as calculated by the spherical-earth modeling procedure of von Frese et al. (1981b). A substantial portion of the observed MAGSAT anomalies is accounted for by these lithospheric prism anomalies as indicated by Figure 2-F which is the difference map obtained by subtracting the anomaly field of Figure 2-E from the anomalies in Figure 2-A.

For the purposes of this simulation, the MAGSAT observations in Figure 2-A can be thought of as being due to the lithospheric model anomalies of Figure 2-E which are contaminated by "data errors" as given in Figure 2-F. Hence, an appropriate test for recognizing a solution which effectively reduces the MAGSAT observations differentially to the pole is to find that solution which produces radially polarized anomalies that deviate least from the radially polarized anomalies of the lithospheric model. These anomalies are shown in Figure 2-G where they were modeled from the lithospheric prisms assuming a radial polarization intensity of 60,000 nT.

Efforts to construct EV-spectra in terms of the various solution characteristics are facilitated by the fact that the $(p(p+1)/2)$-coefficients of the upper triangle of (Q^TQ) have already been computed by the inversion which produced Figure 2-B. Several EV-spectra for solutions obtained

according to equation (5) are shown in Figure 3. Curve A gives the sum of squared residuals (SSR) between Figure 2-G and the radially polarized anomalies predicted by solutions for various values of (EV) to reflect the control provided by the simulation of radially polarized signals from the lithosphere. The initial sharp gradient of curve A shows the inversion to be ill-conditioned, where the horizontal run of the gradient is roughly indicative of the amount of error variance which must be added to the system to stabilize it. There then follows a trough encompassing a range of EV-values which can produce effective solutions for reducing the MAGSAT observations differentially to the pole. As the error variance is increased further, the radially polarized anomalies from the solutions become smoother to reflect increasing degradation of the predictive properties of the solution. Curve A rises as the solution becomes over-damped and it eventually reaches a plateau where predicted anomaly fields show little variation.

The results presented in curve A suggest approximately the amount of error variance which is required for damping this system to produce radially polarized magnetic anomalies of the lithosphere from the anomaly observations. This under-damping of the system can also be derived directly in terms of some of the properties of the solution. For example, curve B gives the behavior of the sum of squared residuals (SSR) between the radially polarized anomalies at (EV = 1) and the differentially reduced to pole anomaly maps from solutions which were obtained using smaller positive values of the error variance. This curve exhibits relatively good definition of the range of error variance values indicated in curve A for which the solutions are under-damped.

However, the characteristics of curve B are difficult to interpret for values of the error variance which over-damp the solution. A test for over-damping can be obtained by comparing the observed anomalies against modeled anomalies produced by the solution for various values of the error variance. For example, curve C presents variations of the sum of squared residuals (SSR) between the observations in Figure 2-A and various models of these data predicted by the nonzero values of (EV). As the error variance is increased, the predictions become smoother so that the sharp rise on this curve for all ($EV \gtrsim 10^{-6}$) provides a fairly straightforward indicator of the range of error variance over which the solutions are over-damped.

Figure 3 also includes spectra of error variance plotted against (K) (curve D) and the variance of the solutions (curve E). These curves require less numerical effort to determine than curves B and C which are based on forward calculations of the solutions. However, curve D does not appear to be readily interpretable for the under- and over-damping conditions of this problem. Curve E also indicates little apparent sensitivity to over-damping conditions, although a major break in the inital slope at ($EV = 10^{-6}$) suggests a possible constraint on the range of error variance yielding under-damped solutions.

The results of curves B, C, and E suggest an optimal range of error variance (10^{-8}-10^{-6}) for obtaining radially polarized anomalies from the MAGSAT anomalies in Figure 2-A by equivalent source inversion. These values are consistent with results of curve A based on the lithospheric model, which in fact shows a minimum of the residuals for ($EV = 10^{-6}$). This value of the error variance does not necessarily produce the best solution, however, because the prism model is only a rough approximation of the lithospheric

component in MAGSAT anomalies. In fact, the principal use of the prism model is to provide assurance that the analysis of the EV-spectra yields results which are consistent with the numerical properties of magnetic anomalies from the lithosphere. Presumably, the MAGSAT anomalies of Figure 2-A are completely due to lithospheric sources, and hence a smaller value of the error variance is likely to be more appropriate for estimating the radially polarized anomalies of these data.

The variability of radially polarized anomaly predictions encompassed by the range of approximately optimal values of error variance is indicated by the difference map in Figure 2-H. This map was obtained by subtracting the anomalies predicted by the solution at ($EV = 10^{-6}$) from the anomaly field predicted at ($EV = 10^{-8}$). To minimize this difference, an "optimal" value ($EV = 10^{-7}$) was chosen to produce the radially polarized anomalies in Figure 2-I. In lieu of any other constraints then, Figure 2-I is taken as a nearly optimal estimate of the MAGSAT data of Figure 2-A reduced differentially to the radial pole at 400 km elevation.

Bootstrap Inversion

Equivalent source inversions of geopotential fields are commonly of such great scale with respect to computing limitations that solutions must be obtained by combining a series of smaller-scale solutions. For these applications, the superposition principle of potential fields can be used to produce smaller-scale solutions which integrate very efficiently into a large-scale solution because they essentially have no edge-effects within the integrated solution.

The procedure involves using a source function where the number of unknowns is of a size that can be handled conveniently by available computer time and storage resources. The entire set of anomaly observations is inverted on this source function for the physical properties by least-squares methods. A model of the observed anomalies is then obtained by forward calculations of the source function using the derived solution. Subtracting the modeled anomalies from the observed anomalies produces a residual field which is inverted on another source function with different parameters. This procedure is continued until the integrated effects of the solutions drive the residual to an acceptable level for the objectives of the investigation.

Olivier et al. (1982) used this procedure, which they called bootstrap inversion, to reduce MAGSAT anomalies of Euro-Africa differentially to the pole by inversions on two independent sets of equivalent point sources. The process was initiated by inversion of the observed anomalies using a set of equivalent point dipoles distributed over the southern half of their study area. The residual anomalies obtained by subtracting the model anomalies from the observed anomalies were then inverted over a distribution of point dipoles in the remaining half of the area. The integrated effects of the two solutions directly modeled the observed anomalies with negligible error, producing no edge effects which required adjustment. This bootstrap inversion strategy was also used to compute first order radial derivatives of surface <1°> free-air gravity anomalies at 400 km elevation to help constrain lithospheric analysis of the radially polarized MAGSAT anomalies of Euro-Africa (von Frese et al., 1983).

Equivalent point source grids are particularly convenient for manipulation by bootstrap inversion because of their efficient programming

characteristics for automated computation. Coordinates of the grid can be computed internally as inverse or forward calculations proceed, and key grid parameters such as the density, depth, and spacing of the unknowns can be easily manipulated to reflect available computer resources or some desired level of spectral fidelity in modeling the anomaly observations. Also as shown by Figures 1-B and 1-E, the stability of inversion can be profoundly influenced by straightforward adjustments of source grid elevation and spacing. Hence, bootstrap inversion, particularly when implemented using gridded source functions, is a powerful procedure for obtaining large-scale solutions, with considerable sensitivity to practical constraints of geopotential anomaly analysis.

To demonstrate the flexibility which is inherent to the method, consider again the inversion problem presented by the MAGSAT anomalies in Figure 2-A. Previous inversion efforts involved a 16*16 array of point dipoles spaced at 2° with an elevation difference of 500 km between source and observation grids to produce the radially polarized anomalies in Figure 2-I. However, comparable results can also be obtained by bootstrap inversion using a smaller scale source function derived by modifying the previous grid so that every second and third dipole is deleted from consideration. Implementation of this new 6*6 source function with 6° spacing results in roughly an 86% reduction in the working memory required by the previous inversion. Also, because the source spacing is larger, these inversions are inherently more stable in conformance with the results in Figure 1-E.

A bootstrap solution for an 11*11 source grid with 3° dipole spacing was produced by merging the results of four inversions of 6*6 source grids which were intermeshed according to the shift strategy indicated in Figure 4. For

applications such as this one, experience has shown that a maximum amount of residual error of the fit is modeled when the source grid is shifted so that the new occupation sites are located farthest from the previous sites. Accordingly, the second iteration involved a diagonal shift as shown in Figure 4. Initial solutions for the four inversions all yielded reciprocal condition numbers corresponding to ($K \approx 3$). However, inspection of the corresponding EV-spectra indicated a requirement for damping for each of the inversions, despite the relative stability suggested by the small values of (K).

In comparison to Figures 2-A and 2-I, Figures 5-A and 5-B show, respectively, the poor resolution of the models for the observations and the radially polarized anomalies which are produced by the damped solution of the initial inversion. By contrast, Figures 5-C and 5-D illustrate, respectively, the significant improvement in the total field and differentially reduced to pole anomaly models obtained from integrating the results of all four inversions. Figure 5-E indicates the decrease in the sum of squared residuals (SSR) between the observations of Figure 2-A and the integrated total field anomaly model resulting from each inversion. Comparable results are shown in Figure 5-F for the radially polarized anomalies of Figure 2-I and the bootstrap model integrated for each inversion iteration.

The bootstrap procedure in this example produced a solution for an 11*11 array of point dipoles spaced at 3° intervals from four damped inversions of the anomaly observations and their residuals using a 6*6 source function with 6° spacing which was manipulated according to the strategy in Figure 4. The radially polarized anomalies derived from the bootstrap inversion as shown in Figure 5-D compare well with the results in Figure 2-I. Further improvement in the bootstrap solution may be possible by continued inversion on shifted

source functions. However, each iteration must be checked to insure that a decrease in the residual between observed and modeled anomalies occurs. When a particular campaign of inversions begins to produce no decrease or an increase of the residual, a practical limit has been reached in its capacity to model further details of the anomaly observations. Additional improvements in the solution are still possible, however, but they will require the use of fundamentally new source functions such as denser point dipole grids located closer to the observations. In general, as suggested by these results, bootstrap inversion using damped solutions can provide a powerful and flexible approach to lithospheric analysis of geopotential field anomalies.

Conclusions

Experience with equivalent source analyses of regional gravity and magnetic anomalies indicates that these inversions are nearly always ill-conditioned for lithospheric applications. Accordingly, variations in the least-squares solution may not reflect variations of the anomaly observations as much as they may reflect the integrated effects of observation spacing, source spacing, elevation differences between sources and observations, characteristics of the coordinate parameterization, geomagnetic field attitudes, and other factors related to the computation of the coefficients of (Q^TQ). However, by adding an appropriate constant (EV) to the elements of the diagonal of the product matrix, the system may be biased to reduce this variance and thus improve substantially the mean square error of estimation and prediction.

The optimal value of (EV) which is large enough to stabilize the solution, yet small enough to maximize its predictive power can be estimated

from trade-off diagrams consisting of EV-spectra plotted against various properties of the solution or its predictions. In particular, constraints on under-damped conditions of the system may be obtained from spectra of the damping factors against solution variance or the residuals between predicted anomaly maps which represent the processing objective (e.g., downward continuation, differential reduction to the radial pole, anomaly gradients, etc.). Constraints on over-damping, on the other hand, are available by considering the EV-spectrum against the residuals between observed and modeled anomalies.

In addition to improving substantially the accuracy of prediction, the damped least-squares solution of equation (5) also optimizes computer time and storage resources because it can be obtained by efficient Choleski decomposition procedures. Available resources of computer storage can be further extended by bootstrap inversion which is based on the superposition principle of potential fields. The procedure involves successive inversions of the residuals between the observed and modeled anomalies on different source function parameters. When an acceptable fit has been achieved, the series of damped solutions may be merged, with no requirements for edge-effect adjustments, to produce a large-scale solution which normally could not be obtained by direct inversion due to excessive memory requirements.

The ability of these procedures for improving lithospheric analyses of geopotential field anomalies was demonstrated by considering an ill-conditioned inversion problem involving the differential reduction of MAGSAT magnetic anomalies of India to the radial pole. In general, the use of damped least-squares in combination with bootstrap inversion represents a

flexible and efficient approach for obtaining geologically useful inversions of potential field anomalies.

Acknowledgements

This study was partially supported by the Goddard Space Flight Center under NASA contract NAGW-736, and the NSF under grant DDP-8313071.

References Cited

Barraclough, D.R., Harwood, J.M., Leaton, B.R., and Malin, S.R.C., 1975, A model of the geomagnetic field at epoch 1975, Geophys. J. R. Astro. Soc., v. 43, p. 111-121.

Bhattacharyya, B.K., 1980, A generalized multibody model for inversion of magnetic anomalies, Geophysics, v. 45, p. 255-270.

Cline, A.K., Moler, C.B., Stewart, G.W., and Wilkinson, J.H., 1979, An estimate for the condition number of a matrix, SIAM Numerical Analysis, v. 16, p. 368-375.

Dampney, C.N.G., 1969, The equivalent source technique, Geophysics, v. 34, p. 39-53.

Dongarra, J.J., Bunch, F.R., Moler, C.B., and Stewart, G.W., 1979, LINPACK User's Guide, SIAM, Philadelphia, PA.

Draper, N.R., and Smith, H., 1966, Applied Regression Analysis, John Wiley & Sons, New York, NY.

Emilia, D.A., 1973, Equivalent sources used as an analytical base for processing total magnetic field profiles, Geophysics, v. 38, p. 339-348.

Hoerl, A.E., and Kennard, R.W., 1970a, Ridge regression: Biased estimation for nonorthogonal problems, Technometrics, v. 12, p. 55-67.

Hoerl, A.E., and Kennard, R.W., 1970b, Ridge regression: Applications to nonorthogonal problems, Technometrics, v. 12, p. 69-82.

Jackson, D.D., 1972, Interpretation of inaccurate, insufficient, and inconsistent data, Geophys. J. R. Astro. Soc., v. 28, p. 97-109.

Lanczos, C., 1961, Linear Differential Operators, D. Van Nostrans, London.

Langel, R.A., Phillips, J.D., and Horner, R.J., 1982, Initial scalar magnetic anomaly map from MAGSAT, Geophys. Res. Lett., v. 9, p. 269-272.

Langel, R.A., Slud, E.V., and Smith, P.J., 1984, Reduction of satellite magnetic anomaly data, J. Geophys., v. 54, p. 207-212.

Lawson, C.L., and Hanson, R.J., 1974, Solving Least Squares Problems, Prentice-Hall, Princeton, NJ.

Levenberg, K., 1944, A method for the solution of certain nonlinear problems in least squares, Quart. Appl. Math., v. 2, p. 164-168.

Marquardt, D.W., 1963, An algorithm for least-squares estimation of nonlinear parameters, J. Soc. Indust. Appl. Math., v. 11, p. 431-441.

Marquardt, D.W., 1970, Generalized inverses, ridge regression, biased linear estimation, and nonlinear estimation, Technometrics, v. 12, p. 591-612.

Mayhew, M.A., 1979, Inversion of satellite magnetic anomaly data, J. Geophys., v. 45, p. 119-128.

Mayhew, M.A., 1982, An equivalent layer magnetization model for the United States derived from satellite altitude magnetic anomalies, J. Geophys. Res., v. 87, p. 4837-4845.

Olivier, R., Hinze, W.J., and von Frese, R.R.B., 1982, Satellite magnetic anomalies of Africa and Europe, SEG 52nd Annual International Meeting and Exposition, Technical Program (Abstracts & Bibliographies), p. 413-415.

Ridgway, J.R., and Hinze, W.J., 1986, MAGSAT scalar anomaly map of South America, Geophysics, v. 51, p. 1472-1479.

von Frese, R.R.B., Hinze, W.J., and Braile, L.W., 1981a, Spherical earth gravity and magnetic anomaly analysis by equivalent point source inversion, Earth Planet Sci. Lett., v. 53, p. 69-83.

von Frese, R.R.B., Hinze, W.J., Braile, L.W., and Luca, A.J., 1981b, Spherical earth gravity and magnetic anomaly modeling by Gauss-Legendre quadrature integration, J. Geophys., v. 49, p. 234-242.

von Frese, R.R.B., Olivier, R., and Hinze, W.J., 1983, Long-wavelength magnetic and gravity anomaly correlations of Africa and Europe, IAGA Bulletin, v. 47, p. 140.

von Frese, R.R.B., Hinze, W.J., Olivier, R., and Bentley, C.R., 1986, Regional magnetic anomaly constraints on continental breakup, Geology, v. 14, p. 68-71.

Wiggins, R., 1972, The general linear inverse problem: implications of surface waves and free oscillations on earth structure, Rev. Geophys. Space Phys., v. 10, p. 251-285.

Figure Captions

Figure 1 Numerical experiments showing how stabilities of lithospheric inversions of the magnetic anomalies in (A) are affected by various singularity parameters given in panels (B), (C), (D) and (E). These effects are considered in terms of (K) which estimates the relative loss of significant figures in the least-squares solution (ΔX).

Figure 2 Analysis of the ill-conditioned inverse problem for differentially reducing the MAGSAT magnetic anomalies of India to the radial pole.

Figure 3 EV-spectra derived from solutions of the MAGSAT anomalies over India produced by equivalent point source inversion.

Figure 4 Strategy of grid manipulations used to obtain a bootstrap solution for the MAGSAT anomalies of India. This solution is for a 3° source grid which was produced from four successive inversions on a 6° source function, where the dashed arrows show how the southwestern origin of the grid was shifted for each iteration.

Figure 5 Reducing the MAGSAT magnetic anomalies of India differentially to the radial pole by bootstrap inversion.

TABLE I

Magnetic properties of the lithospheric prisms in Figure 2-D used to model MAGSAT anomaly observations over the region of the Indian subcontinent

Prism (#)	Magnetic Susceptibility (*4π SI)
A	0.0027
B	0.0022
C (2)	0.0020
D	0.0016
E	0.0012
F	0.0010
G (3)	-0.0014
H	-0.0015
I	-0.0018
J	-0.0021
K	-0.0051

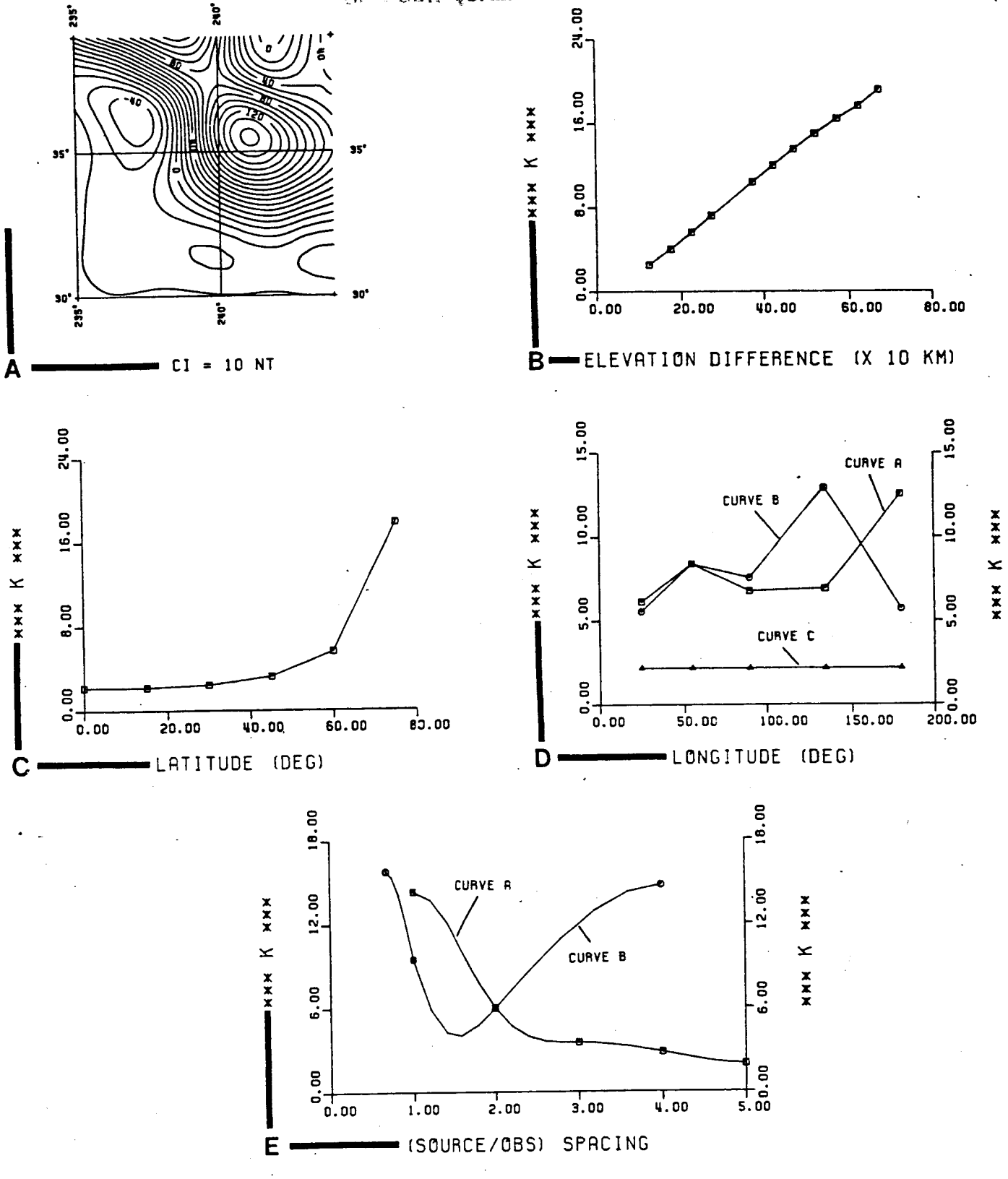

FIGURE 1

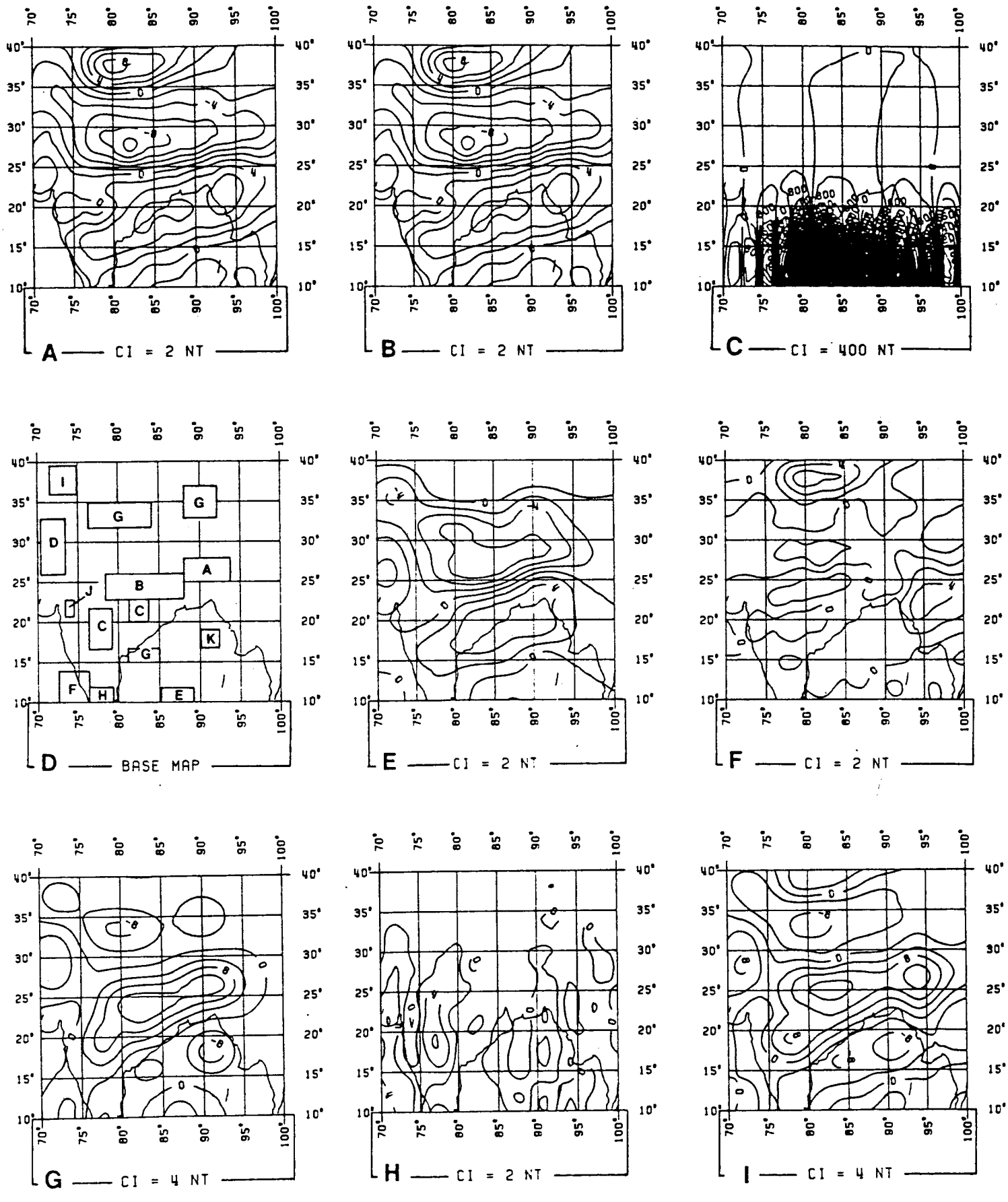
A — CI = 2 NT
B — CI = 2 NT
C — CI = 400 NT
D — BASE MAP
E — CI = 2 NT
F — CI = 2 NT
G — CI = 4 NT
H — CI = 2 NT
I — CI = 4 NT

FIGURE 2

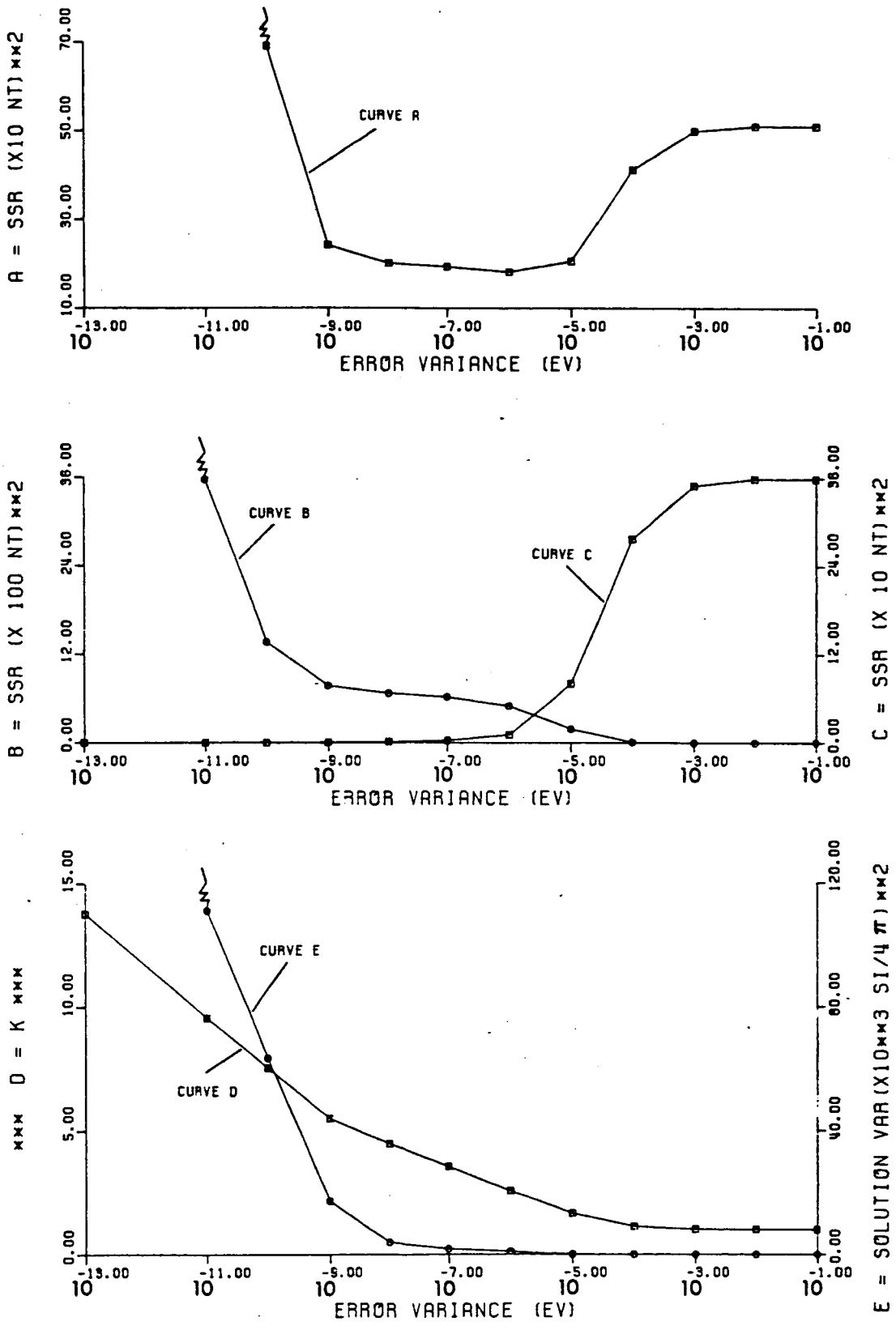
A = SSR (X10 NT)**2
70.00
50.00
30.00
10.00
CURVE A
-13.00
-11.00
-9.00
-7.00
-5.00
-3.00
-1.00
10
ERROR VARIANCE (EV)
B = SSR (X 100 NT)**2
36.00
24.00
12.00
0.00
CURVE B
CURVE C
C = SSR (X 10 NT)**2
ERROR VARIANCE (EV)
*** D = K ***
15.00
10.00
5.00
0.00
CURVE E
CURVE D
E = SOLUTION VAR(X10**3 SI/4 π)**2
120.00
80.00
40.00
ERROR VARIANCE (EV)

FIGURE 3

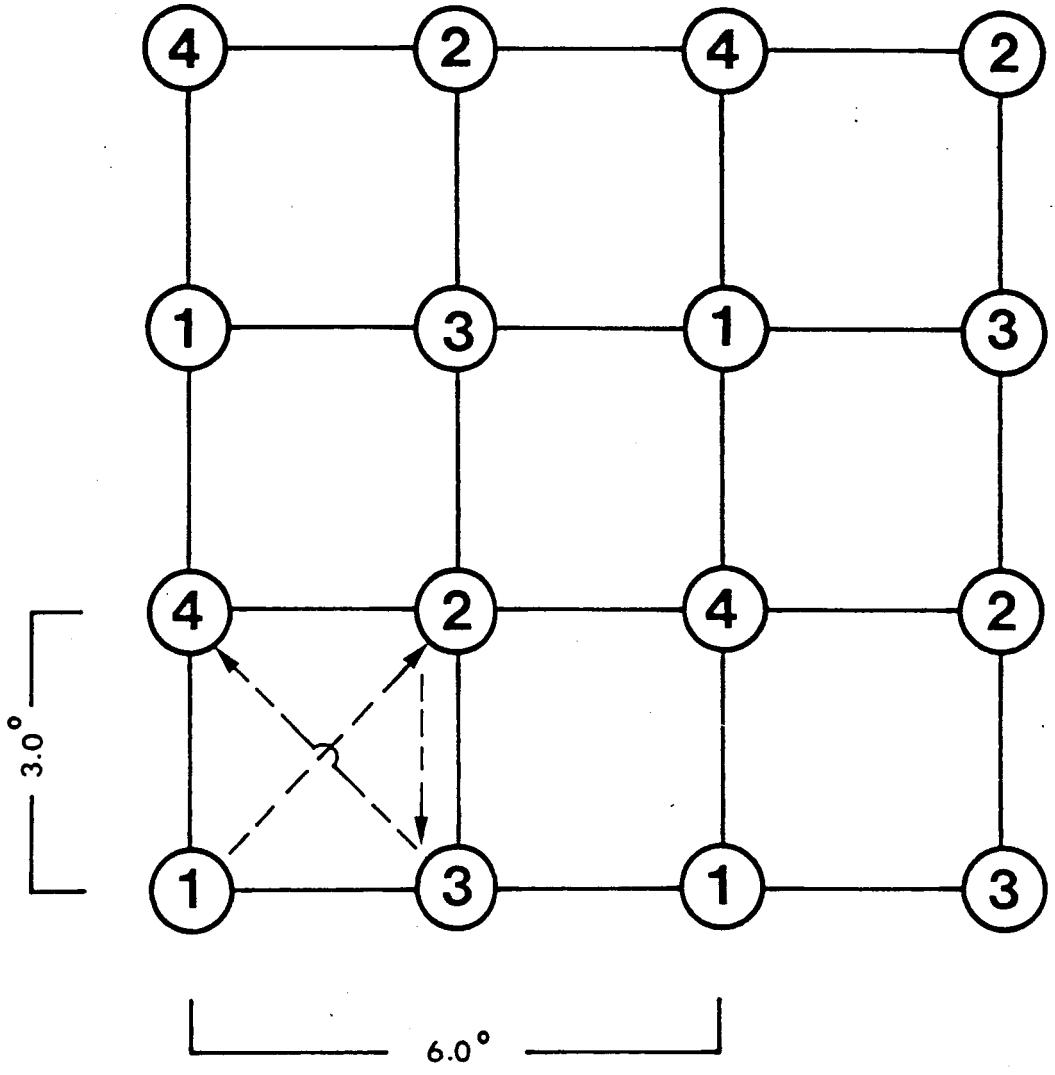

FIGURE 4

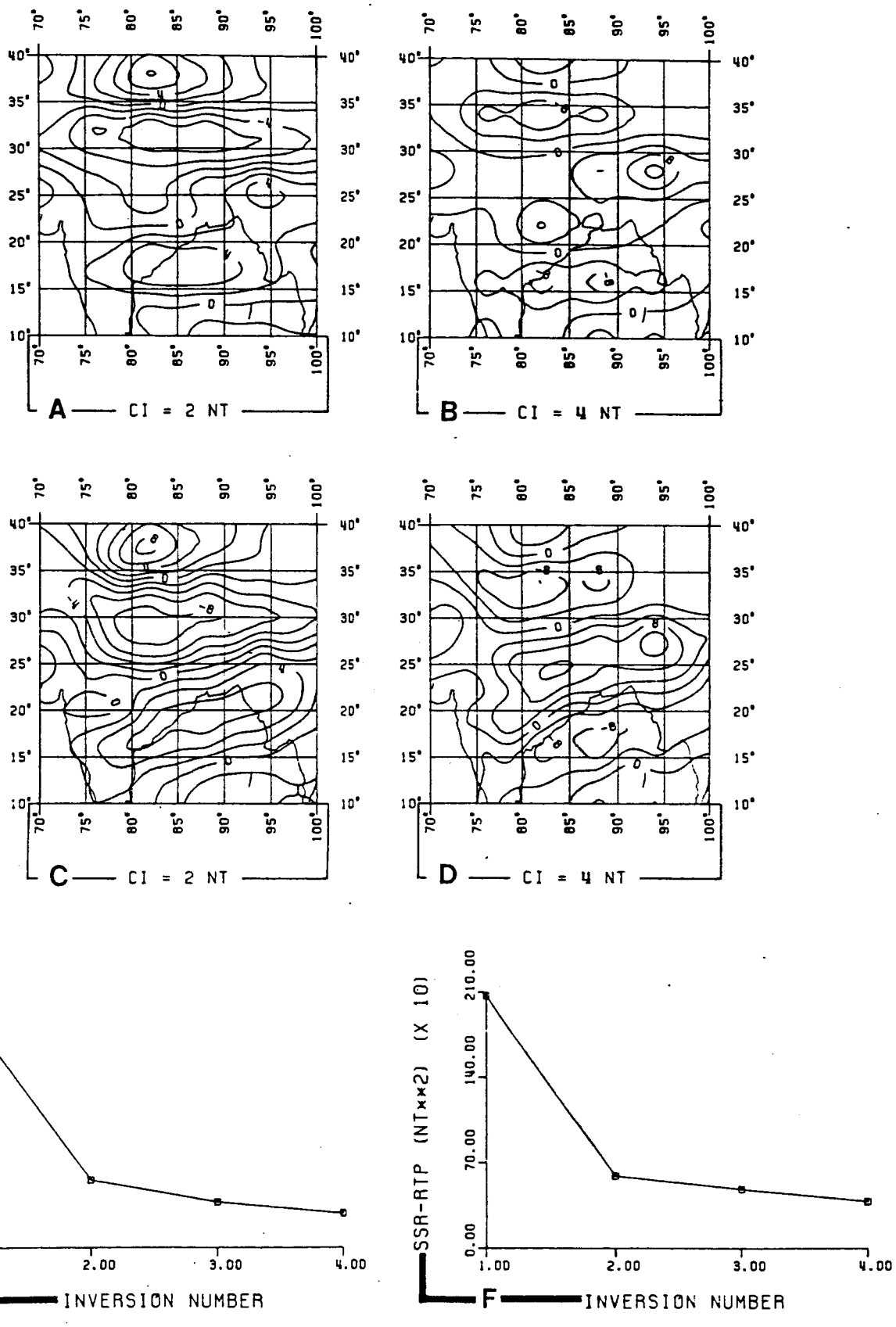
A — CI = 2 NT
B — CI = 4 NT
C — CI = 2 NT
D — CI = 4 NT
SSR-TFLD (NT**2) (X 10)
105.00
70.00
35.00
0.00
1.00
2.00
3.00
4.00
E — INVERSION NUMBER
SSR-RTP (NT**2) (X 10)
210.00
140.00
70.00
0.00
1.00
2.00
3.00
4.00
F — INVERSION NUMBER

FIGURE 5

PREPRINT*

SATELLITE MAGNETIC ANOMALIES OF GONDWANA

by

R. R. B. von Frese[1], W. J. Hinze[2], R. Olivier[3], and C. R. Bentley[4]

[1] Dept. of Geology & Mineralogy
The Ohio State University
Columbus, OH 43210

[2] Dept. of Geosciences
Purdue University
W. Lafayette, IN 47907

[3] Institut de Geophysique
Universite de Lausanne
Rue de l'Universite 5
1005 LAUSANNE, Switzerland

[4] Dept.of Geology & Geophysics
University of Wisconsin-Madison
Madison, WI 53706

Abstract

Regional magnetic anomalies observed by NASA's magnetic satellite mission (MAGSAT) over the eastern Pacific Ocean, North and South America, the Atlantic Ocean, Europe, Africa, India, Australia, and Antarctica are adjusted to a fixed elevation of 400 km and differentially reduced to the radial pole of intensity 60,000 nT. Having been normalized for differential inclination, declination and intensity effects of the core field, these radially polarized anomalies in principle directly map the geometric and magnetic property variations of sources within the lithosphere. Continental satellite magnetic data show a sharp truncation and even parallelism of anomalies along the active edges of the North and South American Plates, whereas across passive plate continental margins the truncation of anomalies is less distinct, possibly reflecting subsided continental crust or the tracks of hotspots in the ocean basins. When plotted on an early Cambrian reconstruction of Gondwanaland, many of the radially polarized anomalies of the continents demonstrate detailed correlation across the continental boundaries to verify the pre-rift origin of their sources. Accordingly, these anomalies provide fundamental constraints on the geologic evolution of the continents and their reconstructions.

*accepted for publication in Am. Geophys. Union Monograph Series #39.

Introduction

Magnetic measurements collected by NASA's POGO and MAGSAT satellite missions have yielded fundamental and unique information concerning not only the core field, but also anomalies derived from the lithosphere. Quantitative geologic analyses of these anomalies are limited due to several factors including anomaly distortion introduced by the variable attitude and intensity attributes of the core field. This distortion, which is severe when dealing with tectonic analyses on global or regional scales, is demonstrated by the regional magnetic anomalies mapped by the MAGSAT mission in Figure 1-A. Satellite magnetic anomalies for the eastern Pacific Ocean, North and South America, the Atlantic Ocean, Europe, Africa, India, Australia, and Antarctica are differentially reduced to the pole by an equivalent point dipole inversion procedure to minimize their contamination by the core field. Finally, the geological significance of these adjusted anomalies is considered for studying the evolution and dynamics of the continents and oceans.

Enhancement of Satellite Magnetic Anomalies for Geologic Analysis

Satellite magnetic anomalies implemented in this study are based on areal averages of MAGSAT scalar observations obtained during periods of low temporal magnetic activity. A model developed by NASA-GSFC was used to remove the geomagnetic core field from the observations. Quadratic functions were then fitted by least-squares and subtracted from the orbital magnetic profiles to account for external field effects and to enhance data consistency. Removal of these quadratic functions tends to enhance E/W anomaly components over the N/S components as MAGSAT was essentially a polar-orbiting satellite (Langel et al., 1982). The resulting data were

then averaged within 2°-bins to produce the anomalies plotted in Figure 1-A.

The 2°-averaged MAGSAT scalar magnetic anomalies cannot be readily compared in terms of the magnetic properties and geometries of lithospheric sources because the data are registered at altitudes that range 120 km about a mean elevation of 400 km over the study area. Furthermore, the anomalies are contaminated by differential inclination, declination and intensity variations of the geomagnetic field. The attributes of the IGS'75 geomagnetic reference field updated to 1980 over the surface of the study area are plotted in Figure 2 to illustrate their variability. Inclinations of the reference field in this region vary from 0° at the magnetic equator to ±90° at the poles, whereas declinations vary between about 51° and -66°. These attitudinal characteristics operate over the geometries of the lithospheric sources and at the observation points to vary the attributes of magnetic anomalies continuously from the poles to the equator where inversion of the anomaly signs occurs. Assuming induced magnetization, the anomaly amplitudes are a function of the susceptibility of the sources, and the ambient field strength which varies as shown in Figure 2 from roughly 23,000 nT to 62,000 nT. Thus, an inductively magnetized source located in central southeastern South America produces an anomaly which is only about a third to one-half as strong as the anomaly produced by the same source at high magnetic latitudes. In general, the sign, shape and strength of the anomalies over the study area in Figure 1-A are not simple functions of the magnetic and geometric properties of the lithospheric sources.

An equivalent point dipole inversion scheme (von Frese et al., 1981) was used to adjust the regional satellite magnetic anomalies for variable

elevation effects and differential inclination, declination and intensity variations of the core field. Application of the procedure involved least-squares matrix inversion of the magnetic anomalies of Figure 1-A, using the IGS'75 reference field updated to 1980, to determine magnetic susceptibilities for an array of point dipoles constrained to a spherical surface and spaced on a 4° grid. This produced stable point sources which model the observed anomalies with negligible error. The adjusted magnetic anomalies were then obtained as shown in Figure 1-B by computing the anomalies at a fixed elevation (400 km) from the equivalent point dipoles assuming a radial field of constant strength (60,000 nT).

The effects of differential reduction to the radial pole are readily appreciated by comparing Figures 1-A and 1-B. Note the marked shift of the radially polarized anomalies relative to their total field counterparts along isogonic lines towards the poles. At low geomagnetic latitudes this shift is as great as several degrees, whereas along the geomagnetic equator the radially polarized anomalies are reversed in sign relative to corresponding total field anomalies. These effects have a major impact on relating satellite elevation magnetic anomalies to regional lithospheric features. Also, the radially polarized anomalies indicate the presence of relatively strong lithospheric magnetic sources, particularly in east-central and southern South America, which are not readily apparent in the total field anomaly data due to the weak polarization characteristics of the core field in this region.

Geologic Implications of Radially Polarized MAGSAT Anomalies

The lithospheric sources of the regional satellite magnetic anomalies are varied and complex, and only a few have been investigated quantitatively using constraining geological and geophysical data. However, as

reviewed by Mayhew et al. (1985), limited analyses of continental magnetic anomalies suggest sources which include regional petrologic variations of the crust and upper mantle and crustal thickness and thermal perturbations. These anomaly sources behave predominately as inductively magnetized features and they include sources whose magnetization may be dominated by visco-remanence. Accordingly, the radially polarized anomalies of the continents are in principle centered over their sources and source geometric and magnetic property variations are mapped directly by these anomaly variations. This has important implications for tectonic analyses on a continental or global basis, as geologic source regions may be compared directly in terms of their radially polarized magnetic anomaly signatures.

For example, previous investigators have noted, using predominantly total field POGO (Frey et al., 1983) and MAGSAT (Galdeano, 1983) anomalies, the existence of magnetically disturbed regions on the rifted margins of continents which match except for the sign, shape, and amplitude of the anomalies on pre-drift reconstructions. However, when differentially adjusted to the radial pole as in Figure 1-B, the anomalies are sufficiently consistent in these attributes that they may be contoured across or along the rifted continental margins. In fact, the continuity of lithospheric source regions across the rifted margins is suggested in remarkable detail as shown in Figure 3, where radially polarized MAGSAT data are plotted on an early Cambrian reconstruction of Gondwanaland (after Smith et al., 1981). Included in Figure 3 are 2°-averaged anomalies reduced to an elevation of 400 km and to a radial pole strength of 60,000 nT for South America, Africa, Madagascar, India and Australia. For

Antarctica, 3°-averaged scalar anomalies, derived by Ritzwoller & Bentley (1983) from MAGSAT vector component measurements, have also been adjusted to these parameters of fixed elevation and radial pole strength for inclusion in Figure 3. The adjacent (rifted) margins of the present continents as illustrated in this Cambrian reconstruction consist primarily of Precambrian age rocks with only spatially restricted, superimposed intrusive and extrusive igneous rocks and essentially non-magnetic Phanerozoic sedimentary rocks which presumably overly Precambrian basement crystalline rocks. Phanerozoic crust or crust strongly modified by orogenic related tectonic and thermal processes occur primarily along the margins of the Gondwanaland supercontinent shown in Figure 3.

The correlation of magnetic source regions indicated by the radially polarized anomalies in Figure 3 is particularly striking along the rifted margins between South America and Africa and between Australia and Antarctica. The most intense positive anomaly of Figure 1-B is the Bangui anomaly of westcentral Africa which has been related to a major intra-crustal feature by Regan & Marsh (1982). In Figure 3, the Bangui anomaly correlates across the Atlantic rift margin with a positive anomaly of the Sao Luiz Craton which projects further northeastwards (in the grid coordinates of the cylindrical equidistant projection) as an extensive positive anomaly overlying the Central Brazilian Shield. This positive feature extends northwestwards back to the rift margin where it ties into a broad positive African anomaly overlying the Cubango Basin and an extensive region of Precambrian rocks. The details of the last correlation are better illustrated in Figure 1-B where the data are contoured at a finer interval than was used in Figure 3.

Adjacent to the Bangui anomaly on the north is an intense magnetic low (Figure 3) which reaches a minimum at its westernmost limit in Africa over the Zaire Basin. This feature correlates across the Atlantic rift margin with a comparable low overlying the Sao Franciso Craton of southern Brazil. Additional striking associations include the positive anomaly overlying Archean-Proterozoic cratonic blocks in southcentral and western Australia which correlates with a pronounced high over Wilkes Land in Antarctica. Also, the magnetic low flanking the large Australian positive anomaly on the north and overlying the Alelaide and Tasman Orogens correlates with an Antarctic minimum over the Ross Sea Embayment and Transantarctic Mountains.

In contrast to these associations is the overall poor correlation of magnetic anomalies for the Africa-Madagascar-India-Antarctica fit in Figure 3. The anomaly data suggest problems with the adopted reconstruction if it can be assumed that the anomaly sources actually predate rifting. Verifying this proviso is clearly difficult for regional-scale, deep-seated magnetic features of the lithosphere which are not well-understood in terms of conventional surface geologic and geophysical evidence.

The interpretational complexities are demonstrated by considering the prominent mismatch of anomalies in Figure 3 which involves the juxtaposition of the large magnetic positive of Madagascar with the well-defined minimum at the African margin. If the sources of the radially polarized anomaly of Madagascar and the continental anomalies along the Indian Ocean margin of Africa were formed prior to breakup, then it appears feasible to suggest that the pre-rift attachment of Madagascar to Africa was close to its present position in Figure 1-B as a possible continuation of the broad

positive anomaly of southern Africa. However, recent analysis of seafloor spreading and fracture zone magnetic anomalies of the region supports the Gondwanaland position of Madagascar which is indicated in the reconstruction of Figure 3 (Martin & Hartnady, 1986). Accordingly, it is possible that one or both of these anomaly sources may have been formed during or subsequent to the opening of the Indian Ocean. The pronounced magnetic minimum of the mismatched anomaly pair, for example, may reflect the failed arm of a triple junction extending into the African continent from the ocean margin. This interpretation is suggested only because negative radially polarized MAGSAT anomalies have been observed to overly other rift features such as the Amazon River and Takatu rift systems (Ridgway & Hinze, 1986), and the Rio Grande rift (Mayhew, 1985) and the rift structure of the Mississippi River embayment (von Frese et al., 1982). However, no other geophysical or geological evidence appears available to support or further constrain this hypothesis.

Other interesting features of the radially polarized data (Figure 1-B) include an apparent sharp truncation and even parallelism of continental anomalies along the western edges of the North and South American Plates, whereas across the passive continental margins of the South Atlantic Ocean many prominent anomalies are not distinctly truncated. In contrast, in the North Atlantic Ocean a good correlation exists between the age of the oceanic crust and satellite magnetic anomalies (LaBrecque & Raymond, 1985). A quite different relationship appears to hold for the South Atlantic where the radially polarized anomalies transect the central ridge.

The source of passive continental margin anomalies, which for the South Atlantic Ocean can be traced into the South American continent and Africa for considerable distances, is not immediately obvious. They may be

related to external geomagnetic electrojet effects, especially in the region between ± 30° inclination of Figure 2. However, they are replicated in hundreds of orbits (Ridgway & Hinze, 1986) to yield the temporally-static signatures which typify anomalies of magnetic sources within the lithosphere. In their geologic context, on the other hand, passive continental margin anomalies may be associated with oceanic rises which have continental affinities. A possible example involves the area of the southern tip of Africa where seismic refraction and dredging results indicate continental crust beneath the Agulhas Plateau in the southwestern Indian Ocean (Tucholke et al., 1981). This area is characterized in Figure 1-B by a pronounced positive magnetic anomaly which is consistent with the anomalously positive magnetic source regions geographically associated with the West Antarctic Peninsula and the Patagonian Platform of southern South America as reconstructed in Figure 3.

In the central South Atlantic Ocean, the anomalies trend NE, but closer to the African shoreline they turn generally to a N/NE trend. Many of these anomalies show a striking parallelism with the tracks of hotspots in the South Atlantic (Duncan, 1981; Morgan, 1983) and their extensions into the sub-African upper mantle (Morgan, 1983). There is no consistent magnetic anomaly sign with these tracks which complicates their interpretation. However, it seems plausible that the hotspots may indeed leave a magnetic signature imprint by virtue of their related thermal aureoles and magmatic activity. The origin of these anomalies and why they are prominent in the South Atlantic Ocean is not understood, but their analysis is a potentially important area of inquiry for further clues on the history of the continents and oceans.

Conclusions

The utility of MAGSAT magnetometer observations for regional geologic analysis is significantly enhanced by normalizing magnetic anomalies for global attitude and intensity variations of the magnetic field of the core. The resulting radially polarized anomalies of a reconstructed Gondwanaland show remarkable correlation across present continental boundaries. This strongly suggests that a principal source of these anomalies are pre-rift terranes which have acquired their magnetic characteristics during Precambrian tectonic and thermal events. Discrepancies in correlation across rifted margins reflect rift or post-rift modification of the magnetic characteristics of the crust or problems in continental reconstruction. In general, the resolution of satellite magnetic anomalies and the capacity to analyze them for lithospheric information is reaching the stage where these data can provide significant input for studies of continental reconstructions.

Acknowledgements

Financial support for this investigation was provided by the Goddard Space Flight Center under NASA contract NAG5-304, and by grant DPP-8313071 from the National Science Foundation. This is contribution number 567 of the Institute of Polar Studies, The Ohio State University, Columbus, Ohio.

References Cited

Duncan, R. A., 1981, Hotspots of the southern oceans-an absolute frame of reference for motion of the Gondwana continents, Tectonophysics, v. 74, p. 29-42.

Frey, H., R. A. Langel, G. Mead and K. Brown, 1983, POGO and Pangea, Tectonophysics, v. 95, p. 181-189.

Galdeano, A., 1983, Acquisition of long wavelength magnetic anomalies predates continental drift, Phys. of Earth & Planet. Interiors, v. 32, p. 289-292.

LaBrecque, J.L., and C.A. Raymond, 1985, Seafloor spreading anomalies in the Magsat field of the North Atlantic, J. Geophys. Res., V. 90, p. 2565-2575.

Langel, R. A., J. D. Phillips and R. J. Horner, 1982, Initial scalar magnetic anomaly map from MAGSAT, Geophys. Res. Lett., v. 9, p. 269-272.

Martin, A.K., and C.J.H. Hartnady, 1986, Plate tectonic development of the Southwest Indian Ocean: A revised reconstruction of East Antarctica and Africa, J. Geophys. Res., V. 91, p. 4767-4786.

Mayhew, M. A., 1985, Curie isotherm surfaces inferred from high-altitude magnetic anomaly data, J. Geophys. Res., V. 90, p. 2647-2654.

Mayhew, M. A., B. D. Johnson, and P. J. Wasilewski, 1985, A review of problems and progress in studies of satellite magnetic anomalies, J. Geophys. Res., v. 90, p. 2511-2522.

Morgan, W. J., 1983, Hotspot tracks and the early rifting of the Atlantic, Tectonophysics, v. 94, p. 123-139.

Regan, R. D., and B. D. Marsh, 1982, The Bangui magnetic anomaly: Its geological origin, J. Geophys. Res., v. 87, p. 1107-1120.

Ridgway, J. R., and W. J. Hinze, 1986, MAGSAT scalar anomaly map of South America, Geophysics, V. 51, p. 1472-1479.

Ritzwoller, M. H., and C. R. Bentley, 1983, Magnetic anomalies over Antarctica measured from MAGSAT, in (Olivier, R. L., P. R. James and J. B. Jago, eds.) Antarctic Earth Science-Fourth International Symposium, Cambridge Univ. Press, N. Y., p. 504-507.

Smith, A. G., A. M. Hurley and J. C. Briden, 1981, Phanerozoic Paleocontinental World Maps, Cambridge Univ. Press, N. Y., 102 p.

Tucholke, B. E., R. E. Houtz and D. M. Barrett, 1981, Continental crust beneath the Agulhas Plateau, Southwest Indian Ocean, J. Geophys. Res., v. 86, p. 3791-3806.

von Frese, R. R. B., W. J. Hinze and L. W. Braile, 1981, Spherical earth gravity and magnetic anomaly analysis by equivalent point source inversion, Earth Planet. Sci. Lett., v. 53, p. 69-83.

von Frese, R. R. B., W. J. Hinze and L. W. Braile, 1982, Regional North American gravity and magnetic anomaly correlations, Geophys. J. R. astr. Soc., v. 69, p. 745-761.

Figure Captions

Figure 1. A) MAGSAT scalar 2°-averaged magnetic anomalies for the eastern Pacific Ocean, North and South America, the Atlantic Ocean, and Euro-Africa. These total field anomalies are contoured at 2 nT intervals.

B) MAGSAT scalar magnetic anomalies adjusted to a fixed elevation of 400 km and differentially reduced to the pole of 60,000 nT intensity. The radially polarized anomalies are contoured at 4 nT intervals.

Figure 2. Attributes of the core field over the surface of the region considered in Figure 1.

Figure 3. Radially polarized MAGSAT anomalies plotted on an Aldanian reconstruction of Gondwanaland. The coast lines of Antarctica and Africa are high-lighted to facilitate identifying the continental components of Gondwana.

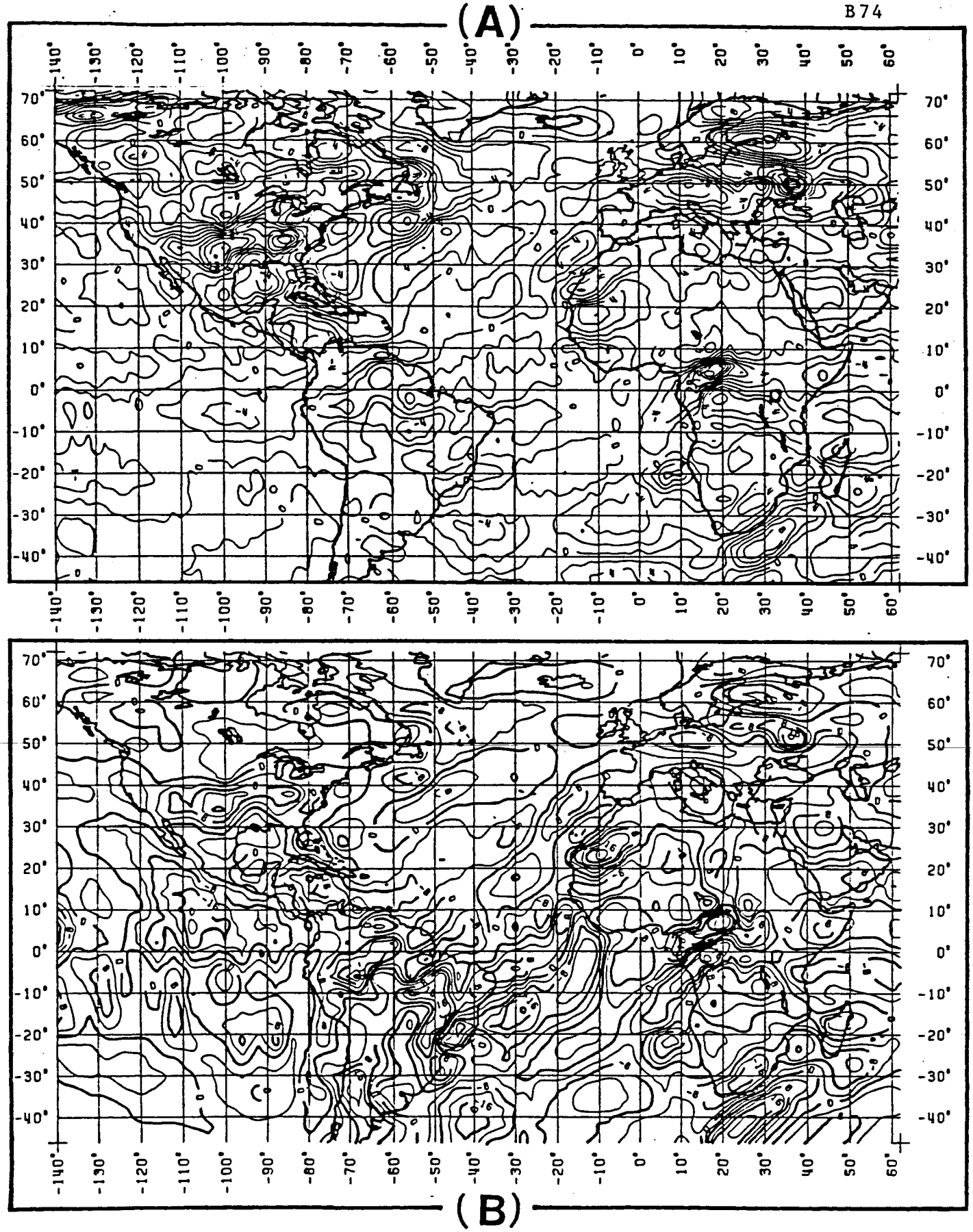

FIGURE 1

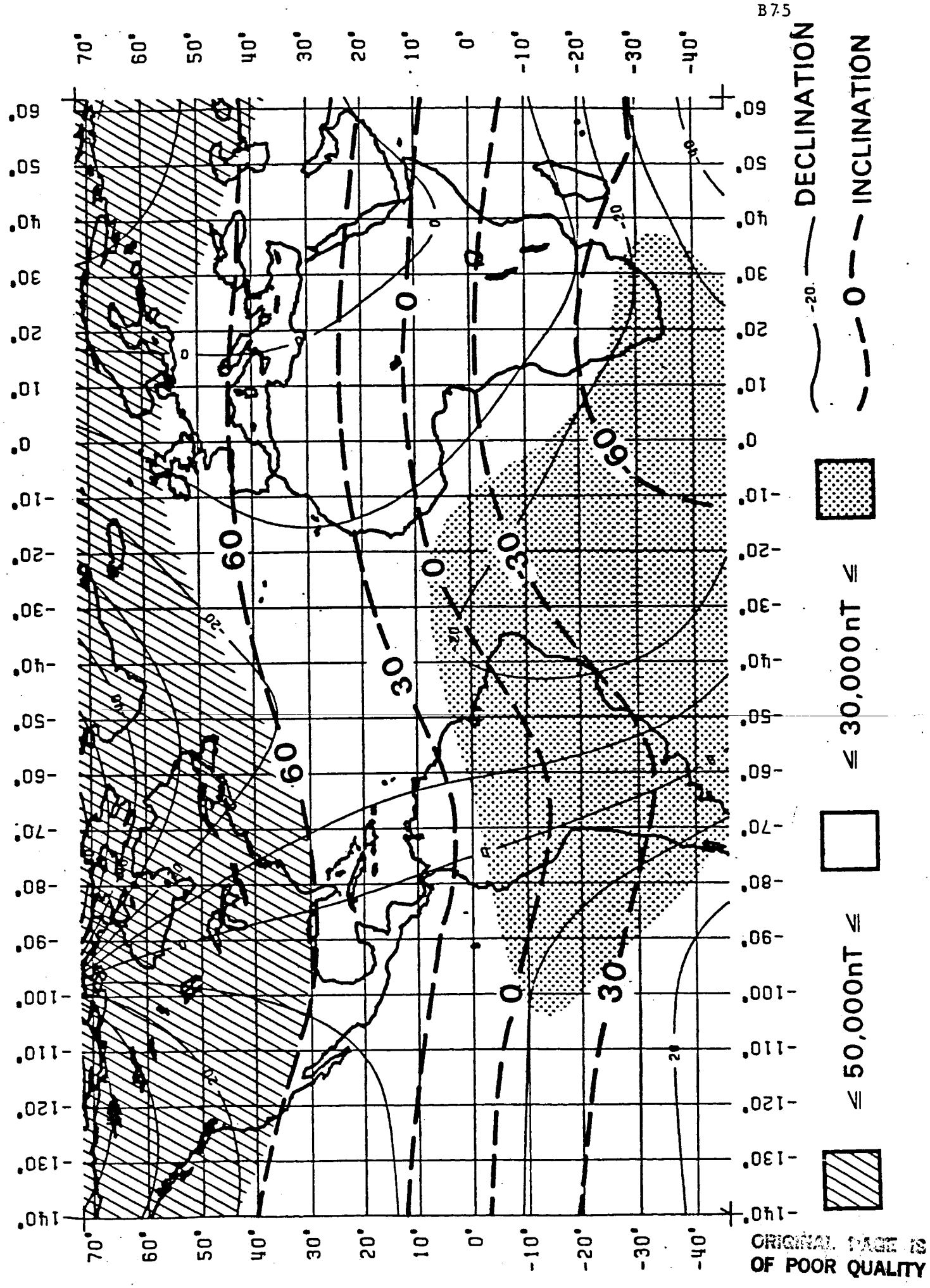

FIGURE 2

GONDWANALAND AND RADIALLY POLARIZED MAGSAT MAGNETIC ANOMALIES

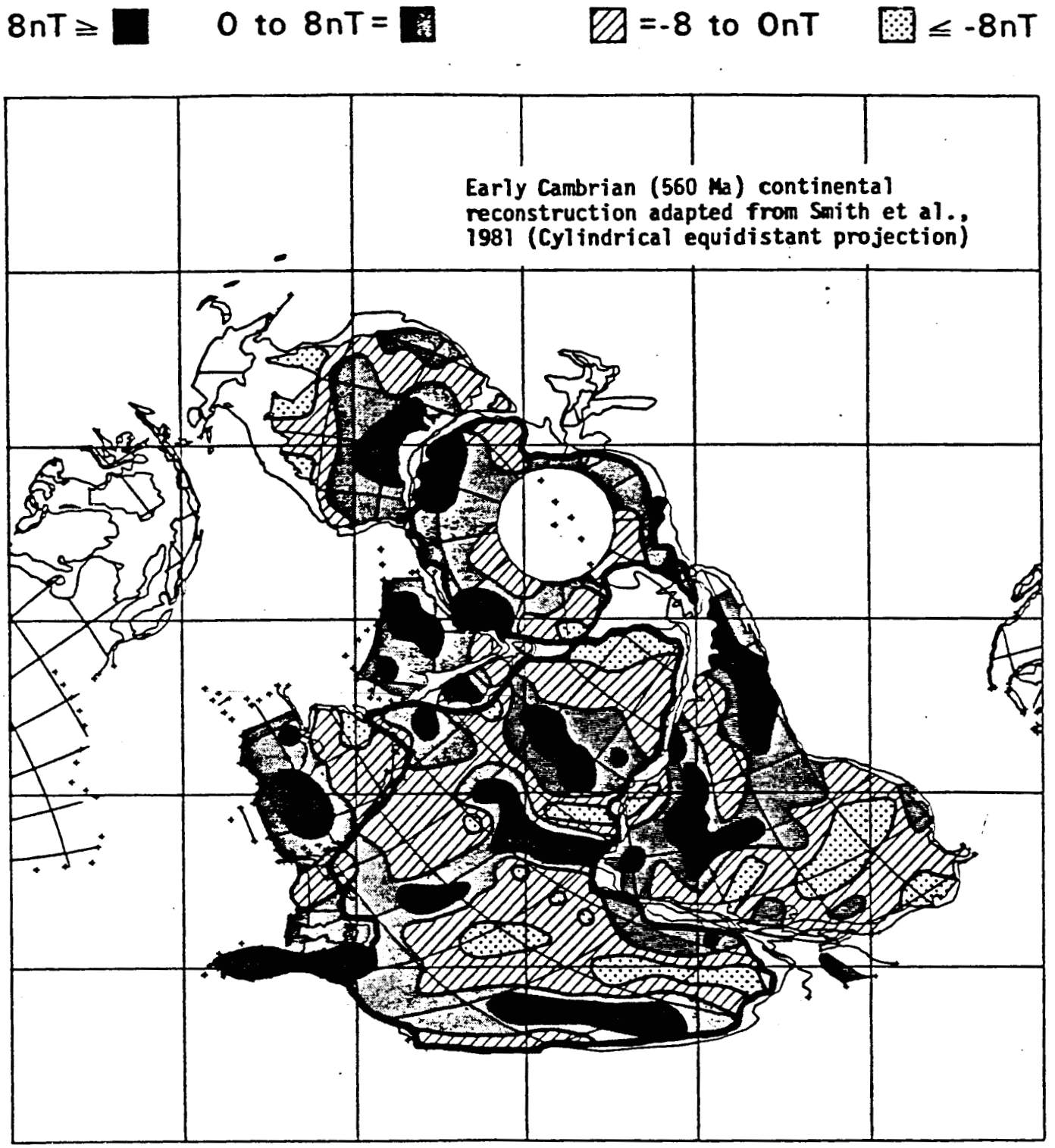

FIGURE 3